UNIVERSITÀ DEGLI STUDI DI NAPOLI FEDERICO II

DIPARTIMENTO DI INGEGNERIA CHIMICA, DEI MATERIALI E DELLA PRODUZIONE INDUSTRIALE

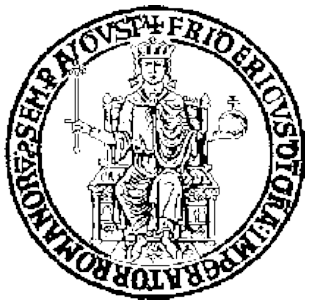

Dottorato di ricerca in ingegneria chimica

(XXVI ciclo)

Advances in short contact time catalytic partial oxidation systems for syngas and olefins production

Scientific committee:

Prof. Gennaro Russo

Prof. Roberto Andreozzi

Dr. Stefano Cimino

Dr. Luciana Lisi

Candidate:

Gabriella Mancino

March 2014

"Volli, sempre volli, fortissimamente volli"

In loving memory of my beloved father

Acknowledgements

This PhD thesis is the result of three years of work during which I have been supported and accompanied by many people. It is now my great pleasure to take this opportunity to thank them.

First af all, I would like to thank Prof. Gennaro Russo, for his guidance, support and motivation during the course of my PhD. I would like also to acknowledge Prof. Roberto Andreozzi, for introducing me towards the passion for the scientific research.

I am deeply grateful to Dr. Luciana Lisi, for giving me the appropriate tools to critically undertstand the results obtained during these last three years. She was always ready to listen and support my ideas, continuously giving me encouragement and making me feel always up to the journey I have undertaken three years ago.

I express my profound sense of gratitude to Dr. Stefano Cimino, constantly present in my PhD work, transmitting me, day by day, every kind of knowledge. He has injected enthusiasm into this research, helping me to realize the power of critical reasoning and inciting to accomplish the objectives of this thesis.

I would like also to thank Prof. Johannes Lercher, who gave me the possibility to spend an amazing period a TUM university in his laboratories and Prof. Andreas Jentys for our interesting talks about science. Special thanks must go to Dr. Oliver Gutierrez, for his time spent together to think about the results achieved and the future directions of the project carried out. I am also really grateful to Dr. Eszter Barath, for her complete scientific and organizational helpfulness, making me feel as integral part of Biomass Team.

My sincere thanks must also go to Prof. Christian Hulteberg who generously gave his time to read my preliminary work and offered me valuable comments toward improving my thesis.

I would like to thank people who accompanied me during these experience: Miriam, colleague and friend, I shared with her worries and happy moments, sure I could always count on her during these three years; Giovanna and Ilaria, always ready to offer me their support and unconditional friendship; Gianluca e Paola, rich in suggestions and gifted with a sensitive ability to listen.

My heartfelt thank goes to my bestfriend Gemma: since the beginning of our university career we have shared a lot, anxieties, laughs and we enjoyed our reciprocal success. In this time of the final sprint, very stressful for both, our friendship was strengthened even more, willing to be present one for each other, at any time. I could not be more proud and pleased to share with her even this accomplishment.

I thank with strong love Nicola, he has given me strength and courage in the darkest moments, listening to every outburst, even those inappropriate, trying to make me see the right sense of things. Nobody more than him was able to keep me calm when I needed. But most of all I thank him for the loving way he has always demonstrated his admiration towards me and my efforts to achieve my goal.

The greatest thank goes to my mum and my sisters, everyone, in her own way, has helped me during these three years, simply listening to me and providing unconditional love and care. Without them and their advices, very often I would have done or said the wrong thing. I thank them especially for the patience they had with me even when I was really unbearable.

I would like to dedicate this thesis to my dad, who has supported my choice three years ago, but unfortunately he cannot enjoy with me the ultimate goal. His teachings have guided me day after day, in perseverance and determination that I put in all the things I have done, and in the tenacity with which I approached my work.

Abstract

The catalytic partial oxidation (CPO) of natural gas over noble metal catalysts is an attractive way to obtain syngas (CO and H_2) which can be employed for downstream processes to produce synthetic fuels. The preliminary conversion of methane to syngas is also interesting in the context of advanced combustion systems with reduced NO_x emissions. Several catalysts have been studied for CPO of methane, but Rh-based systems have established as the best performing catalysts in terms of both activity and selectivity.

Sulphur poisoning is a tricky issue for industrial processes, leading to catalysts loss of activity. Recently, the presence of sulphur containing compounds naturally occurring in natural gas or added as odorants necessary for safety reasons, was recognized as a serious drawback for the costly Rh catalysts. Indeed, sulphur adversely affects the catalytic performance during catalytic partial oxidation adsorbing onto Rh active sites, causing a (reversible) suppression of their steam reforming activity, with an associated risk of catalyst overheating during CPO autothermal operation. Therefore the development of catalysts that are intrinsically sulphur tolerant and are not readily poisoned by the amounts of sulphur commonly found in natural gas is desirable.

On the basis of recent works that have shown that metal phosphide catalysts have promising hydrodesulphurization (HDS) properties due to a higher sulphur tolerance than the correspondent metal based catalysts, in this work, a novel structured Rh catalyst doped with phosphorous and supported on alumina, has been prepared and investigated during the CPO of methane under self-sustained conditions at short contact time in the presence of sulphur. Results were compared with the reference undoped $Rh/\gamma Al_2O_3$, showing a significant enhancement of the specific steam reforming reaction rate of P-doped catalyst, and a higher sulphur tolerance. Both the findings were correlated to the presence of phosphorous, whose interaction with Rh improved the metal dispersion on the support and inhibited the strong sulphur adsorption lowering the resulting surface S coverage.

Since natural gas may comprise significant amounts of ethane beside methane, the CPO of ethane is also object of study, in the view of a direct use of natural gas as feed at the on-site gas field without separating respective components. The importance of the role of the gas phase chemistry, which was found negligible in the case of CH_4 CPO over Rh and Pt catalysts, increases for higher alkanes

following the progressive lower stability of the C-H bond, as in the case of CPO of ethane or propane, when large quantities of ethylene can be formed with Pt based catalysts (but not with Rh). However, the literature data available in the field of sulphur poisoning during CPO of higher hydrocarbon is so far scarce and somehow contradictory.

Therefore, in the second part of this PhD thesis, the effect of sulphur addition to the feed during the CPO of ethane for syngas production (C_2H_6/O_2=1) has been investigated over more conventional Rh and Pt catalysts supported on a γ-alumina washcoat anchored to honeycomb monoliths. The findings obtained confirmed the previous results on CPO of methane on Rh: sulphur addition resulted in a rapid and reversible poisoning, depending on its concentration. However the adverse impact of sulphur is much larger on Rh than on Pt. Due to the more complex chemistry of ethane, two main effects related to the presence of sulphur during its CPO have been identified: i) the strong inhibition of the hydrogenolysis of ethane to methane occurring on Rh but not on Pt; ii) the progressive inhibition of steam reforming of both the reactant (ethane) and one of the products, ethylene, whose formation in turn increases after the introduction of sulphur. The latter result was also observed for Pt catalyst. Since ethylene is thought to be mainly formed by the homogeneous oxidative dehydrogenation of ethane, this result suggested the possibility to take advantage of selective sulphur poisoning in order to maximize the formation of ethylene.

The oxidative catalytic conversion of light alkanes (in particular ethane) to olefins is an attractive solution to obtain ethylene and propylene, the most important building blocks for the polymers industry. The CPO of ethane to ethylene (stoichiometric feed ratio C_2H_6/O_2=2) is characterized by a complicated chemistry which involves both heterogeneous and homogeneous reaction paths, whose contribution and synergy may be strongly alterated by S-poisoning.

In the final part of this PhD work, S-poisoning of catalytic steam reforming of C_2H_6 and C_2H_4 has been investigated as a strategy to increase the process selectivity and yield to ethylene during the CPO of ethane to ethylene (C_2H_6/O_2=2) over Rh and Pt catalysts. In other words, the possibility to use sulphur as an intentional selective poison of undesired heterogeneous reactions to boost the production of ethylene has been exploited. At the same time, taking advantage of the selective poisoning of sulphur on catalytic reforming paths, an attempt has been done to shed light on the complex interaction of hetero-homogeneous chemistry available in a C_2H_6 CPO reactor, to understand the contribution of heterogeneous reforming reactions to the overall performance of the reactor.

Contents

1	**Introduction**	**1**
1.1	**Syngas from Methane**	**5**
1.1.1	**Steam Reforming**	**5**
1.1.2	**Autothermal Reforming**	**7**
1.1.3	**Non Catalytic Partial Oxidation**	**8**
1.1.4	**Dry reforming**	**8**
1.1.5	**Catalytic Partial oxidation**	**9**
1.2	**Catalysts for catalytic partial oxidation**	**13**
1.2.1	**A brief historical summary**	**13**
1.2.2	**Structured catalysts for CPO**	**13**
1.2.3	**Noble metal based structured catalysts for CPO**	**14**
1.3	**Mechanism of catalytic partial oxidation of methane**	**16**
1.4	**The catalytic oxidative conversion of light alkanes to syngas and olefins**	**19**
1.5	**An issue for Catalytic Partial Oxidation: Sulphur poisoning**	**24**
1.5.1	**Sulphur poisoning in catalytic partial oxidation**	**25**
1.6	**A novel class of sulphur tolerant catalysts : metal phosphides**	**30**
1.7	**Summary**	**34**
1.7.1	**The effect of Phosphorous doping on Rh catalysts during Catalytic Partial Oxidation and Dry Reforming of methane**	**35**
1.7.2	**The effect of sulphur during the CPO of ethane to syngas**	**37**
1.7.3	**Ethane CPO to ethylene with sulphur and H_2 addition**	**37**
	References	**39**
2	**Experimental and Characterization Techniques**	**44**
2.1	**Catalyst Preparation**	**44**
2.1.1	**Powder Catalysts**	**44**
2.1.2	**Monolith catalysts**	**45**
2.2	**Catalytic testing**	**47**
2.2.1	**Catalytic Partial Oxidation of methane**	**47**
2.2.2	**Catalytic Partial Oxidation of ethane**	**48**
2.2.3	**Dry reforming of methane**	**49**
2.3	**Catalyst characterization techniques**	**51**
	References	**56**
3	**Effect of Phosphorous doping on Rh catalysts during the Catalytic Partial Oxidation and Dry Reforming of methane**	**57**
3.1	**Introduction**	**57**
3.1.1	**Sulphur tolerance of a P-doped $Rh/\gamma Al_2O_3$ catalyst during the partial oxidation of methane to syngas**	**57**
3.1.2	**Dry reforming of methane over a P-doped Rhodium catalyst**	**57**
3.2	**Experimental Procedure**	**59**
3.3	**Results and Discussion**	**59**
3.3.1	**Characterization of Rh catalysts for CPO of methane**	**59**
3.3.2	**DRIFT and volumetric study of adsorbed CO**	**64**
3.3.3	**Catalytic partial oxidation performance testing**	**72**
3.3.4	**Equilibrium considerations**	**77**
3.3.5	**Dry reforming tests**	**82**
3.3.5.1	**Catalysts characterization**	**82**
3.3.5.2	**Dry reforming catalytic tests**	**84**

3.4	**Conclusions**	**87**
	References	**88**
4	**Effect of sulphur during the catalytic partial oxidation of ethane to syngas over Rh and Pt honeycomb catalysts**	**91**
4.1	**Introduction**	**91**
4.2	**Experimental Procedure**	**92**
4.3	**Results and Discussion**	**92**
4.3.1	**Rh catalyst**	**92**
4.3.2	**Pt catalyst**	**100**
4.4	**Conclusions**	**103**
	References	**105**
5	**Ethane Catalytic Partial Oxidation to Ethylene with Sulphur and Hydrogen Addition over Rh and Pt Honeycombs**	**107**
5.1	**Introduction**	**107**
5.2	**Experimental Procedure**	**107**
5.3	**Results and Discussion**	**108**
5.3.1	**CPO operation at $C_2H_6/O_2 = 2$**	**108**
5.3.2	**Sulphur addition**	**112**
5.3.3	**Sulphur addition with sacrificial H_2**	**114**
5.4	**Conclusions**	**117**
	References	**119**
	Overall conclusions	**120**

1. Introduction

The demand for energy is continuously increasing as the world population keeps growing and economies develop. Moreover, the increased demand is enhanced by the requirement for cleaner sources of energy to minimize impact on the environment [1].

Currently, gasoline and petroleum based energy is being replaced worldwide, as its price is revealing a rising trend [2], indeed the demand for natural gas is likely to overtake other fossil fuels due to its availability, accessibility, versatility and smaller environmental footprint [1].

Natural gas is a gas mixture consisting mainly of methane (CH_4), some higher alkanes and low percentage of carbon dioxide and nitrogen [3].

Component	**% mol**
Methane (CH_4)	83.0-97.0
Ethane (C_2H_6)	1.5-7.0
Propane (C_3H_8)	0.1-1.5
Butane (C_4H_{10})	0.02-0.6
Pentane (C_5H_{12})	≤0.08
Hexanes plus (C_6+)	≤0.06
Nitrogen (N_2)	0.2-5.5
Carbon dioxide (CO_2)	0.1-1.0
Oxygen (O_2)	0.01-0.1
Hydrogen (H_2)	≤0.02

Table 1: Composition of natural gas [3].

The International Energy Agency (IEA) proposed in May 2012 (IEA, 2012) that global demand for natural gas could rise more than 50% by 2035, from 2010 levels [1].

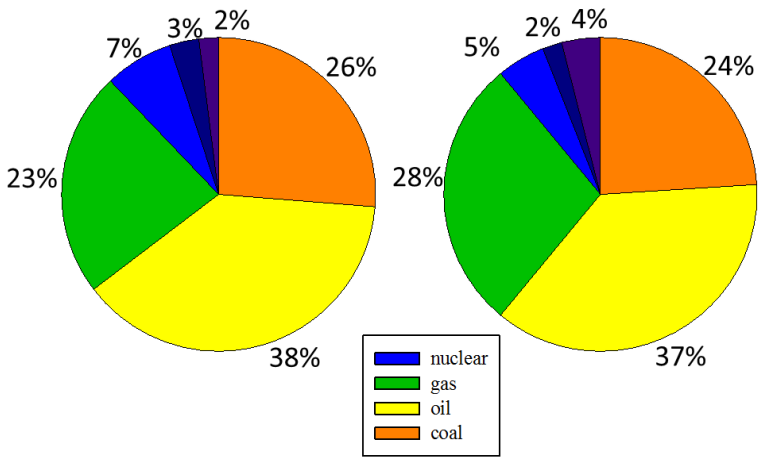

Figure 1: Portfolio Energy demand 2000-2030 [4].

Nowadays, global natural gas reserves are increasing as the rate of new discovery is greater than the rate of consumption [1]. Indeed, a substantial amount of the global natural gas resources remains in remote locations, as it has done for several decades. Monetization of these gas reserves commonly requires large amounts of capital investment to build processing and export infrastructure [1]. The physical nature of natural gas, very different from that of oil, needs elevated costs for its transport from "remote" areas to the markets of consumption, primarily Europe and the United States. Accordingly, only 20% of the gas produced is object of transportation on long distances, 5% via LNG (liquefied natural gas) and 15% via pipeline [4].

Industry is currently facing the challenge of reducing this geographical imbalance by developing technologies and processes to market remote natural gas reserves. Conversion of methane to more useful and easily transportable chemicals (liquids) has therefore been given high priority by scientists in the chemistry society. At this time, the only economically available route for the conversion of methane into more valuable chemicals is via *synthesis gas*. Methods to enhance the value of natural gas, either by synthesising more valuable chemicals or more readily transportable products, have been investigated, particularly in the last 20 years [5]. The conversion of methane into value-added products is a challenging task and the main reason for this is the high CH_3–H(g) bond dissociation energy (439.3 kJ/mol). Heterogeneous catalysts have therefore been a key to the successful conversion of methane. The reason for this is that once methane is adsorbed on a metal surface, the bond dissociation energies CH_x–H depends on the hosting surface metal, and the total bond dissociation energy appears to be useful for identifying promising catalysts.

The relevance of the via-synthesis gas processes is recognized and further developments will occur in forthcoming years [6]. Synthesis gas is now produced for obtaining: i) the H_2 required by the

refining processes and by the NH_3 and Urea synthesis, ii) the MeOH and its derivatives, iii) synthetic oils and fuels through the Gas To Liquid (GTL) processes and iv) electric energy with the Integrated Gasification Combined Cycles (IGCC) [7].

Gas to Liquid (GTL) processes have received great attention as an effective technology for converting natural gas to ultra clean liquid fuels. Evolution in Fisher-Tropsch reactor brought the growth in the capacity of FT process to tens of thousands of barrels per day. In order to improve the total energy efficiency of GTL process, the syngas production reactor has been also developed because, in GTL process, the capital cost of syngas production section is considered the largest portion of the total capital cost. Therefore, reduction in syngas generation costs would have a large and direct influence on the overall economics of these downstream processes. Furthermore, the reduction of greenhouse gas, such as CO_2 emission, is strongly required for the suppression of the global warming. Therefore the development of more compact synthesis gas production processes with high energy efficiency is desired [8].

In addition, reforming natural gas or liquid hydrocarbons into syngas is the initial step in all fuel reforming systems being developed to power the *hydrogen economy* of the future. In hydrogen production systems syngas generation is generally followed by a water gas shift (WGS) and a CO clean up reactor or a hydrogen separation device to yield fuel cell quality hydrogen.

In combustion systems operating on natural gas, such as power turbines and utility burners, preliminary conversion of methane into syngas can help in stabilizing lower temperature flames reducing NO_x emissions [9]. In such systems, the hydrocarbon fuel is mixed with a first air stream to form a fuel/air mixture having an equivalence ratio greater than one and it is partially oxidized by contacting with an oxidation catalyst to generate a heat of reaction and a partial oxidation product stream comprising hydrogen, carbon oxides, primarly CO, and unreacted hydrocarbon fuel. Catalytic oxidation in this context means a flameless, rapid oxidation reaction carried out at a temperature below that required to support thermal combustion, that is, conventional combustion with a flame, and below which thermal NO_x are formed in appreciable amounts. Partial oxidation means that there is insufficient oxygen available to completely convert the fuel to CO_2 and H_2O and to fully liberate the chemical energy stored in the fuel. The partial oxidation product stream is then mixed with a second air stream and completely combusted in a main combustor in which the adiabatic flame temperature and flame stability characteristics depend on the temperature and composition of the partial oxidation product stream and the equivalence ratio in the combustor. In

general, the H_2 in the partial oxidation product stream enhances flame stability because H_2 is lighter and more reactive than the original fuel and mixes better with the second air stream. A more stable flame permits the main combustor to be operated at a lower equivalence ratio, which produces a lower adiabatic flame temperature and less thermal NO_x [10].

1.1 Syngas from methane

The current worldwide production capacity of H_2 through syngas amounts to ca. 80 MTPY and it is mainly devoted to NH_3 synthesis, refining operations and MeOH synthesis.

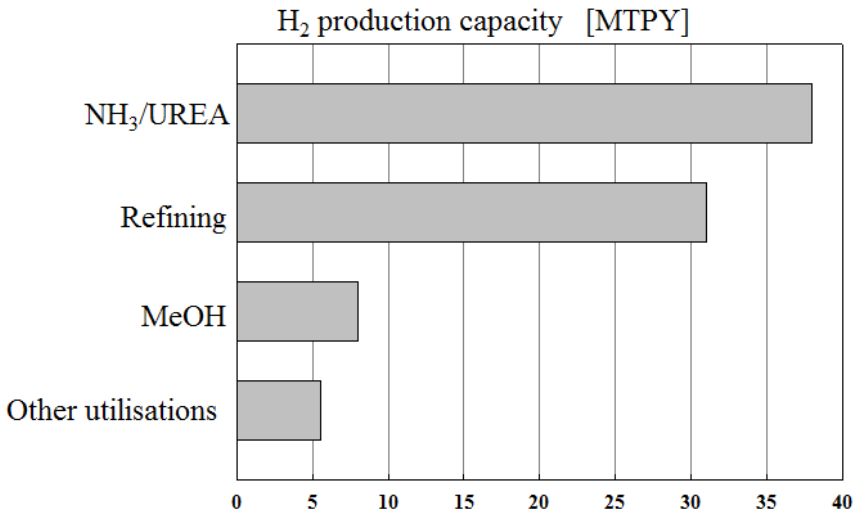

Figure 2: Estimated H_2 production capacities (2012) devoted to the main via-synthesis gas processes [6].

The corresponding invested capital in the synthesis gas production plants is around 180 BEu and it is estimated to grow in the following 5 years for approximately 3,000 MEuPY [6]. Three main technologies are commercialized by engineering and gas producing companies: the Steam Reforming (SR) [11-12], the non-catalytic Partial Oxidation (PO_x) [13] and the AutoThermal reforming (ATR)[14-15] even if they remain energy and capital intensive processes.

Although not yet commercialized and fully applied in industry, dry reforming of methane has recently attracted significant attention from both industrial and environmental sectors.

Short Contact Time – Catalytic Partial Oxidation (SCT-CPO) is among the new technologies that has reached the industrial level of development [6]. In the next section, a brief description of all these processes is given, focusing on pro and cons of each technology.

1.1.1 Steam reforming

Currently most syngas is produced on large scale by steam reforming (SR). In this endothermic reaction, generally represented by equation (1.1), methane reacts with steam over a heated catalyst at high pressures and temperatures to produce syngas with high hydrogen content [8].

$CH_4 + H_2O \rightarrow CO + 3H_2$, $\Delta H_r^{298K} = +206$ KJ/mol (1.1)

Steam reforming has been used for many decades since first developed in the late 1920s and over the years there have been many advances in reforming technology. The reaction is highly endothermic and it takes place in tubes located inside a furnace. Heat for the endothermic reformer reactions is provided by direct burning of natural gas and the tail gas from the synthesis loop. Consequently, the reformer tubes are subject to very high thermal stress. In most cases the outlet temperature from the reformer is in the interval of 700–950 °C, the outlet pressure between 15 and 40 bar. A major drawback is that the residence time in steam reforming reactions are of the order of seconds. Therefore, large reactors are required for a large output of hydrogen. The rate of syngas production is typically limited by the rate at which heat can be transferred from the furnace to the catalyst inside the reactor tubes, since the reaction takes place at such a high temperature and the heat transfer is mainly via radiation to the tubes. In order to increase the effluent temperature and the methane conversion, it is necessary to increase that heat transfer capability. Producing hydrogen at the large quantities required by the industrial processes has therefore led to very large reactors with hundreds of tubes having small diameters in order to achieve the highest possible flux to the catalyst [16].

The current industrial catalysts for steam reforming are usually based on nickel, however, Ni promotes carbon formation, which leads to catalyst deactivation resulting in blockage of reformer tubes and increased pressure drops, therefore a periodic shutdown of the reactor is required. To overcome this problem, and render carbon formation thermodynamically unfavorable, excess quantities of steam to the feedstock are added into industrial steam reformers. However, while suppressing carbon formation, this practice creates a new problem, namely an increase in the H_2/CO and/or CO_2/CO ratios, where low ratios are desirable for optimal downstream processes. A big disadvantage of the steam reforming processes is that the production of syngas is accompanied by the emission of large quantities of CO_2 into the atmosphere.

A possible reaction enhancement can be obtained by removing either H_2 or CO_2, resulting in a lower temperature of operation, which in turn may alleviate the problems associated with catalyst fouling, and high process energy requirements. The standard steam reforming process can be transformed into a cleaner technology moving to a sorption–enhanced steam reforming of natural gas which is an innovative concept of precombustion decarbonization technology to convert fuel with in situ CO_2 capture. The modified process involves CO_2 emissions almost equal to those produced from renewable based processes [17]. The reaction is performed over catalytic bed mixed to a proper sorbent: in this way the equilibrium is shifted toward the H_2 product direction via selectively adsorbing the co-generated CO_2 [18-19]. Several advantages can be gained from this concept such as (1) lower operational temperatures (400–500 °C) than those in conventional steam

reformers, (2) the process is presumed to achieve a conversion higher than 95% even at relatively lower temperatures, (3) lower capital costs, (4) minimization of unfavourable side reactions, (5) reduction of excess steam used in conventional steam reformers.

1.1.2 Non Catalytic Partial Oxidation

Partial oxidation is a process in which the quantity of oxidizer is less than that stoichiometric requested for the complete combustion of a hydrocarbon fuel. The overall reaction describing the partial oxidation of methane is:

$CH_4 + ½O_2 \rightarrow CO + 2H_2$, ΔH_r^{298K} = -36 KJ/mol (1.2)

Typically, preheated natural gas and oxygen are fed to the reactor. They are mixed by a burner and react with flame temperatures of 1300–1500 °C to ensure complete conversion [20]. The reactor is refractory lined to sustain the high temperatures of the produced syngas. The outlet temperature is in the order of 1000–1100 C, and the gas at this stage is near thermodynamic equilibrium with a narrow range of H_2/CO = 1.7–1.8.

The efficiency of the partial oxidation process depends on the conversion efficiency of natural gas to hydrogen and carbon monoxide and the efficiency of the produced syngas sensible heat recovery. Partial oxidation of natural gas from gaseous or liquid hydrocarbons is a commercialized technology, for example, by Texaco and Shell [21]. These processes use a waste-heat boiler configuration for heat recovery: superheated steam is produced for utilization in steam turbines for power generation

POX process provides a simplified system due to absence of external water supply, therefore, it is potentially less expensive. Moreover it has the capability to process a variety of gaseous and liquid hydrocarbon fuels including methane, LPG, gasoline, diesel fuel, methanol, etc.

The main drawback of partial oxidation is the requirement of oxygen, thus an expensive cryogenic air separation unit has to be provided, typically amounting to 30-40% of the investment of the syngas unit. [22]. POX process suffers also from other disadvantages: reformate gas, in the case of air as oxidant instead of pure oxygen is heavily diluted with nitrogen leading to a lower calorific value; in addition, some soot is normally formed and it has to be removed in a separate soot scrubber system downstream of the partial oxidation reactor. [22].

1.1.3 Autothermal reforming

Another process for synthesis gas production is the autothermal reforming: a combination of homogeneous partial oxidation (1.2) and steam reforming (1.1) which was first developed in the late 1970s with the aim of carrying out reforming in a single reactor.

$CH_4 + ½ O_2 \rightarrow CO + 2H_2$, ΔH_r^{298K} = -36 KJ/mol (1.2)

$CH_4 + H_2O \leftrightarrow CO + 3H_2$, ΔH_r^{298K} = +206 KJ/mol (1.1)

The preheated feed streams ($H_2O + CH_4$ and $H_2O + O_2$) are mixed in a burner located at the top where the partial oxidation reactions take place. H_2O is added to the feed streams to prevent carbon formation and allow premixing of CH_4 and O_2. The final steam reforming and equilibration take place in the catalyst bed below the burner. At normal operation, the autothermal reforming operates at high temperatures around 1500°C in the combustion zone and l000-1200°C in the catalytic zone. An undesired side reaction in the combustion zone is the formation of carbon or soot which leads to solid carbon deposition on the catalysts and subsequent deactivation. Gas phase carbon forms soot on downstream surfaces thereby causing equipment damage and heat transfer problems. Excessive local temperatures also lead to burner damage. This also calls for a catalyst of high thermal stability and mechanical strength. Moreover, the Air Separation Unit (ASU) for production of pure oxygen accounts also in this case for a large part of the investment of the production of synthesis gas.

1.1.4 Dry reforming

In recent years, the carbon dioxide reforming of methane (DRM) to syngas (1.3) has gained renewed interest from academic and industrial point of views [23-25].

$CH_4 + CO_2 \leftrightarrow 2\ CO + H_2$, ΔH_r^{298K} = +247 kJ/mol (1.3)

It provides a low H_2/CO ratio (≤1) which is suitable for processes in hydrocarbon formation and the synthesis of valuable oxygenated chemicals. Moreover this reaction offers an environmental benefit since it allows the conversion of two greenhouse gases, namely CH_4 and CO_2, into valuable products [23,26-30]. At last, due to its high reaction enthalpy, it is an attractive as a choice of media in solar–chemical energy transmission system [27-28]. Carbon dioxide is also a significant component of natural gas at many locations, which may be an incentive to apply in part CO_2 reforming rather than separating methane and CO_2 [31].

Biogas is renewable energy carrier with a potential for diverse end-use applications such as heating, combined heat and power (CHP) generation, transportation fuel (after being upgraded to biomethane) or upgraded to natural gas quality for diverse applications [32]. Biogas is a mixture of

methane and carbon dioxide produced from the anaerobic microbial digestion of biomass. Thus, dry reforming reaction is an useful option that has the potential to fully utilize the energy contained in the biogas [33].

However, large scale dry reforming remains a significant challenge since the process is strongly endothermic, it requires high temperatures (typically, 800-900°C) and, under such severe conditions, deactivation of the catalyst due to carbon deposition and/or sintering of the metal often occurs [26,29]. Among the catalysts developed, supported Ni catalysts have been extensively investigated due to their relatively high activity and low cost with the results generally showing that despite high initial activity, these catalysts are often prone to deactivation due to carbon formation [34-38]. Recent literature also indicated that Rh based catalysts, although their relatively high cost, provide high selectivities with carbon-free operations and high activities [39]. Potential use of dry reforming of methane in the production of synthesis gas strongly depends upon the development of active and stable catalysts which do not deactivate quickly [30].

One way to overcome the drawback of high energy requirement could be the introduction of an exothermic reaction, such as partial oxidation of methane. This combined reaction system is named as Oxy-CO_2 Reforming of Methane (OCRM). This kind of reaction system can reduce not only the total energy requirement, but also the amount of carbon deposition since the oxygen available in the reaction system can easily oxidize the deposited carbon on the catalyst. Another distinct advantage is that the OCRM reaction enables production of syngas with various ratios of H_2/CO via manipulation of the feed composition.

1.1.5 Catalytic Partial Oxidation

Over the years the emphasis has been on minimizing the use of expensive steam moving steadily from steam reforming to partial oxidation of CH_4/O_2 mixtures:

$CH_4 + ½O_2 \rightarrow CO + 2H_2$, ΔH_r^{298K} = -36 KJ/mol (1.2)

Even if the hydrogen yield is lower than in the case of steam reforming, the catalytic partial oxidation route offers different advantages. First of all, partial oxidation is mildly exothermic, thus, the adiabatic reactor avoids the use of external burners to provide the heat required when endothermic reforming reactions are involved. The exothermic behavior simplifies the design, operation and costs of this process as compared with the conventional reforming technologies for low to medium size facilities. . An estimated 10-15% reduction in the energy requirement and 25-30% lower capital investment is expected for catalytic partial oxidation compared to the typical

steam reforming processes. In addition it can be combined with endothermic reactions, such as dry reforming, as stated above, to make these processes more energy efficient. Moreover the H_2/CO ratio produced in stoichiometric partial oxidation is around 2, and this ratio is ideal for downstream processes, in particular for Fischer-Tropsch process or high value chemicals synthesis, such as methanol [40]. This avoids the need to remove valuable hydrogen, which is produced in excess in steam reforming. In addition, control over a CPO reactor is simple if compared to the control over a SR reactor. In the SR process it is necessary to assure balance between heat generation on the combustion side and heat consumption on the reforming side along the entire length of the reactor and this requires intensive control over the flow rates and flow distribution. In the CPO process, performance is essentially determined by the methane to oxygen ratio in the inlet mixture, such that only this parameter should be controlled. Furthermore the product gases from methane partial oxidation can be extremely low in carbon dioxide content, which must often be removed before synthesis gas can be used downstream. Since this process operates at temperatures below 1000 ºC there is no significant production of NOx unlike from steam reforming, in fact, for the latter, flames inside the furnace can reach temperatures of 1500 – 2000 °C, high enough to produce significant quantities of harmful pollutants like NOx. The absence of homogeneous reactions prevents the formation of undesired soot which can not be avoided during non-catalytic partial oxidation. Although CPO has never been used commercially, it is most promising because it offers the advantages above mentioned**.** However, a challenge to take in account for the commercialization of CPO is the use of pure oxygen that seems to be a requirement in cases where nitrogen (from air) is undesirable in high-pressure downstream processes. This means that an oxygen separation plant may be necessary, increasing the investment costs of the production of synthesis gas.

Nevertheless, if CPO is performed under adiabatic conditions, the overall exothermic nature of catalytic partial oxidation of methane could lead to the formation of hot spots. However, if the catalytic material has a high thermal conductivity this may help to distribute the excess heat through the catalyst bed or monolith, reducing the presence of small local hot spots. On the other hand, the exothermicity of this reaction could be convenient recovering the generated heat operating the CPO reactor under non adiabatic conditions, as it happens in advanced combustion systems. Indeed, CPO of various hydrocarbons has been proposed as a preliminary conversion stage for advanced combustion systems such as hybrid gas turbine catalytic burners [10,41]: in this case a fuel-rich/air mixture is first catalytically converted to partial oxidation products which are subsequently burnt with excess air to complete the combustion in a relatively cold and very stable homogeneous flame, allowing strong reduction of NO_x emissions [10,41]. Recently, a novel staged hybrid catalytic gas burner, schematized in Fig.3, with integrated interstage heat removal by IR radiation from the hot

catalytic partial oxidation reactor/radiator has been proposed [42]. This represents a solution to take advantage of the exothermicity of the reaction. Moreover, the recent advent of H_2 as a potential alternative for fossil fuel, and increasing availability of hydrogen-containing fuels, i.e. from biomass/coal conversion processes, have generated interest in the possible use of hydrogen-hydrocarbon blends in combustion devices.

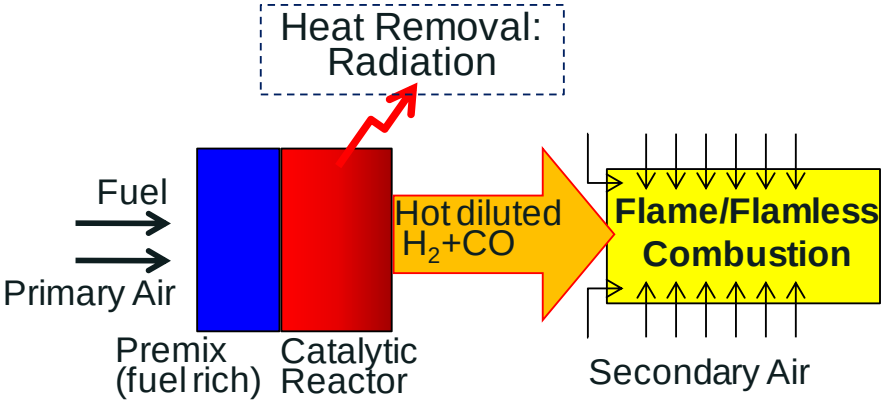

Figure 3: Schematization of hybrid catalytic gas burner.

Hybrid gas turbine catalytic burners can be considered as a promising candidate also for hydrogen-hydrocarbon blends. The fuel-air mixture fed to the burner is generally above its upper flammability limit, therefore this technology is intrinsically safe even for fuel with a larger range of flammability as H_2-CH_4 mixtures.

The term *short-contact time* (SCT) typically refers to conditions where the residence time is within the range of a few milliseconds [43]; in the CPO process, the short contact time enables the design of compact reactors for fuel conversion with extremely high power density. The short contact time guarantees a very high throughput using a small amount of catalyst and low energy and capital costs. Indeed, the SCT-CPO of methane to syngas provides close to 100% methane conversion and >90% syngas yields in millisecond contact times in small reactors ideal for decentralized applications in a remote gas field. Furthermore, at the extremely high power density for the CPO process small, simple and inexpensive bench scale reactors can be directly used to produce syngas for industrial scale applications. This will promote utilization of natural gas in a broad range of efficient and environmentally friendly energy generation processes. On such basis, CPO at short contact time technology is intrinsically suited for process intensification and therefore it has emerged as a favourable approach for onboard reforming of gaseous or liquid fuels for automotive and residential fuel cell systems.

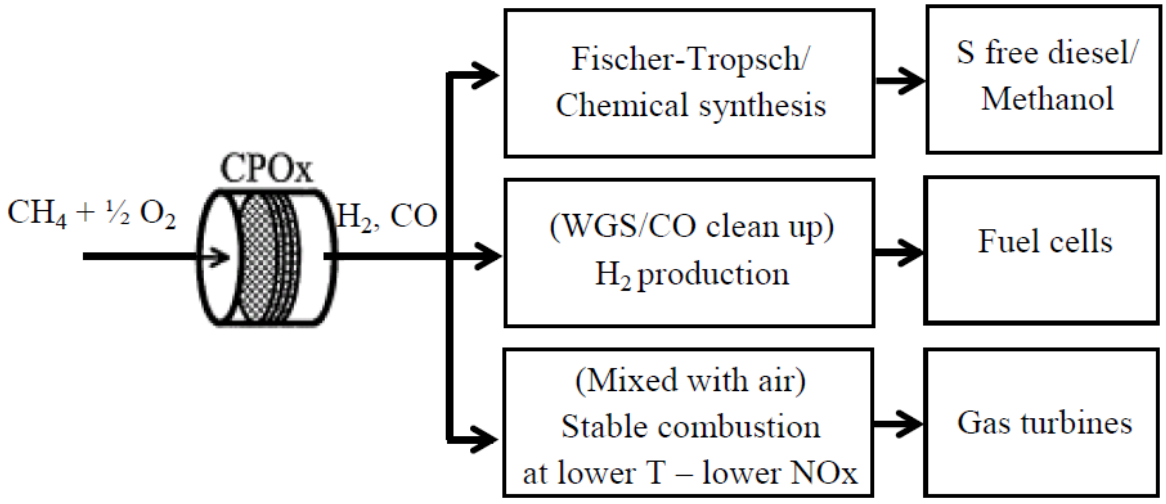

Figure 4: Scheme of the most important methane applications via syngas as an intermediate.

1.2 Catalysts for catalytic partial oxidation

1.2.1 A brief historical summary

The first papers detailing the catalytic partial oxidation of methane to synthesis gas were published in 1929 by Liander, in 1933 by Padovani and Franchetti and in 1946 by Prettre et al. [44-48]. However, high yields of synthesis gas were only obtained at temperatures in excess of 850°C. The latter studies showed that below this temperature non-equilibrium product distributions were observed. In 1970, studying a single grain of Ni/mullite, Huszar et al. reported limitations on the overall process caused by O_2 diffusion through the gas film surrounding the catalyst [47]. Catalyst deactivation was observed in the temperature range 750-900°C, explained by $NiAl_2O_4$ formation. Because of these factors, as well as the success of the steam reforming process, partial oxidation was left alone for decades. In the late 1980s Green and co-workers began a renaissance in the study of methane partial oxidation. While investigating trends in the behavior of the lanthanides for oxidative coupling using pyrochlores containing noble metals and rare earth metals, they observed high yields of synthesis gas [48]. Studies revealed that reduction of the noble metal ruthenium in a lanthanum pyrochlore $Ln_2Ru_2O_7$ resulted in a lanthanide oxide-supported ruthenium catalyst which had excellent activity for methane partial oxidation. This time no carbon could be detected. This observation prompted a detailed investigation of stoichiometric methane partial oxidation over noble metals, and other catalysts, by a very substantial number of research groups. As a consequence, the publications appearing in the 1990s were for the most part concerned with catalyst screening, although the effects of principal system properties such as operating temperature and pressure were also studied. By the end of 1993-1994 the focus began to shift towards improving catalyst stability and performance.

1.2.2 Structured catalysts for CPO

In recent years there has been interest in the possibility of using *structured catalysts*, including microreactors, gauzes, monoliths and foams for partial oxidation reactions and most of previous studies on them involved noble metals, but nickel has also been tested. Structured catalysts are very compact and easy to handle and they offer the benefit of a reduced pressure drop over the bed. This makes operation at higher linear gas velocities possible, which increase the overall throughput, an aspect which may be important when upscaling the process [43].

Although Hohn, Schmidt, Maestri et al. [49-50] have shown that lower heat and mass transfer coefficients enhance the resistance of packed beds to extinction even at high flow rates, the better heat transfer properties and lower heat capacity of honeycomb monoliths lead to shorter start-up time. Moreover at flow rates of practical interest, honeycombs perform better than packed beds in terms of conversion, selectivity, and pressure drop. These features make honeycomb monoliths a suitable choice for miniaturized applications, including on-board fuel reforming and distributed power generation. Additionally, honeycomb monoliths offer several advantages for experimental investigation and its quantitative analysis; among them (i) representativeness of the laboratory-scale data; (ii) availability in the open literature of well-established methodologies for catalyst deposition in uniform, compact and thin layers (a controlling factor for reproducibility of experimental results); (iii) ability to monitor the axial temperature profiles along the channels by means of multiple sliding thermocouples; (iv) reliability of correlations for heat and mass transfer coefficients even at very low Reynolds numbers. Most of these aspects make honeycombs also preferable to foams for kinetic investigation.

Among structured carriers for such a fast, diffusion-limited, highly exothermic process, metallic foams represent a suitable choice to reduce hot spot formation and the size of the reactor needed to reach high conversions for their outstanding gas-to-solid heat- and mass-transfer characteristics and high specific geometric surface areas [51-54]. Furthermore, due to their very open and reticulated cell structure consisting of a network of thin solid struts, they retain some mechanical strength and allow to design lightweight reactors pre-shaped in almost any geometry, with low thermal inertia and fast transient response during start-ups and load variations [51-53].

1.2.3 Noble metal based structured catalysts for CPO

The production of CO and H_2 by the catalytic partial oxidation of CH_4, in air at atmospheric pressure was examined by Schmidt and his group over Pt-coated and Rh-coated monolith catalysts in autothermal reactors at residence times between 10^{-4} and 10^{-2} s [55]. They contrasted the performance of these two catalysts (Pt and Rh) at conditions approaching adiabatic reactor operation. Rh was found to be a much better catalyst than Pt. Using O_2, CO selectivities above 95% and H_2 selectivities above 90% with > 90% CH_4 conversion were reported for Rh catalysts. An interesting observation was the increase in conversion and selectivities observed with a decrease in contact time. Torniainen and Schmidt studied methane oxidation also on other metals supported on monoliths [56]. Ni was found to give similar conversions and selectivities as Rh but exhibited deactivation via oxide and aluminate formation. Other metals were tested showing lower

conversions and selectivities as Pt and Ir, or even complete inactivity for the syngas production as Ru and Fe. Problems related to the deactivation were found with Re through volatilization, and Pd that deactivated due to coke formation. It is possible conclude that a large number of catalysts have been tested for the CPO of hydrocarbons from methane up to diesel and jet-fuels and Rh-based catalysts have shown the highest activity and selectivity to syngas, for this reason they are the most suitable for syngas production through catalytic partial oxidation.

1.3 Mechanism of catalytic partial oxidation of methane

An important and open question in methane CPO research is the reaction mechanism and product development in the catalyst bed under autothermal conditions. Direct and indirect mechanisms are proposed [55]. The direct mechanism assumes that H_2 and CO are primary reaction products formed by partial oxidation in the presence of gas-phase O_2. Equation (1.4) ($0 \leq x \leq 2$, $0 \leq y \leq 1$) shows the direct mechanism including the competitive formation of H_2O and CO_2.

$$CH_4 + (2 - x/2 - y/2)O_2 \rightarrow xH_2 + yCO + (2-x)\,H_2O + (1-y)\,CO_2 \quad (1.4)$$

The indirect mechanism postulates a two-zone model with strongly exothermic CH_4 combustion to H_2O and CO_2 at the catalyst entrance (1.5), followed by strongly endothermic steam and CO_2 reforming, (1.1) and (1.3) respectively, downstream.

$$CH_4 + 2O_2 \rightarrow CO_2 + 2H_2O, \qquad \Delta H_r^{298K} = -803 \text{ kJ/mol} \quad (1.5)$$

$$CH_4 + H_2O \leftrightarrow CO + 3H_2, \qquad \Delta H_r^{298K} = +206 \text{ kJ/mol} \quad (1.1)$$

$$CH_4 + CO_2 \rightarrow 2CO + 2H_2, \qquad \Delta H_r^{298K} = +247 \text{ kJ/mol} \quad (1.3)$$

Recently, Horn et al. compared Rh and Pt foam catalysts perfomances in the partial oxidation of methane to syngas at millisecond contact times to give an insight to the mechanism. Firstly they analyzed conventional conversion and selectivity data at the reactor exit [55]. They obtained syngas yields generally higher on Rh than on Pt, O_2 conversion equal to 100% on both metals regardless the feed ratio, and an exit CH_4 conversion always higher on Rh than on Pt. Lower H_2 and CO selectivities on Pt and the higher exit temperatures on Pt clearly show that Pt favored the strongly exothermic total oxidation of CH_4 to CO_2 and H_2O, whereas Rh was the better partial oxidation catalyst, favoring the less endothermic H_2 and CO formation. However, the reactor exit data are not suited to explain how these different conversion, selectivity, and temperature values are achieved inside the catalyst. For these reason, they analyzed high resolution species and temperature profiles to deeply understand the reaction mechanism under technically relevant conditions.

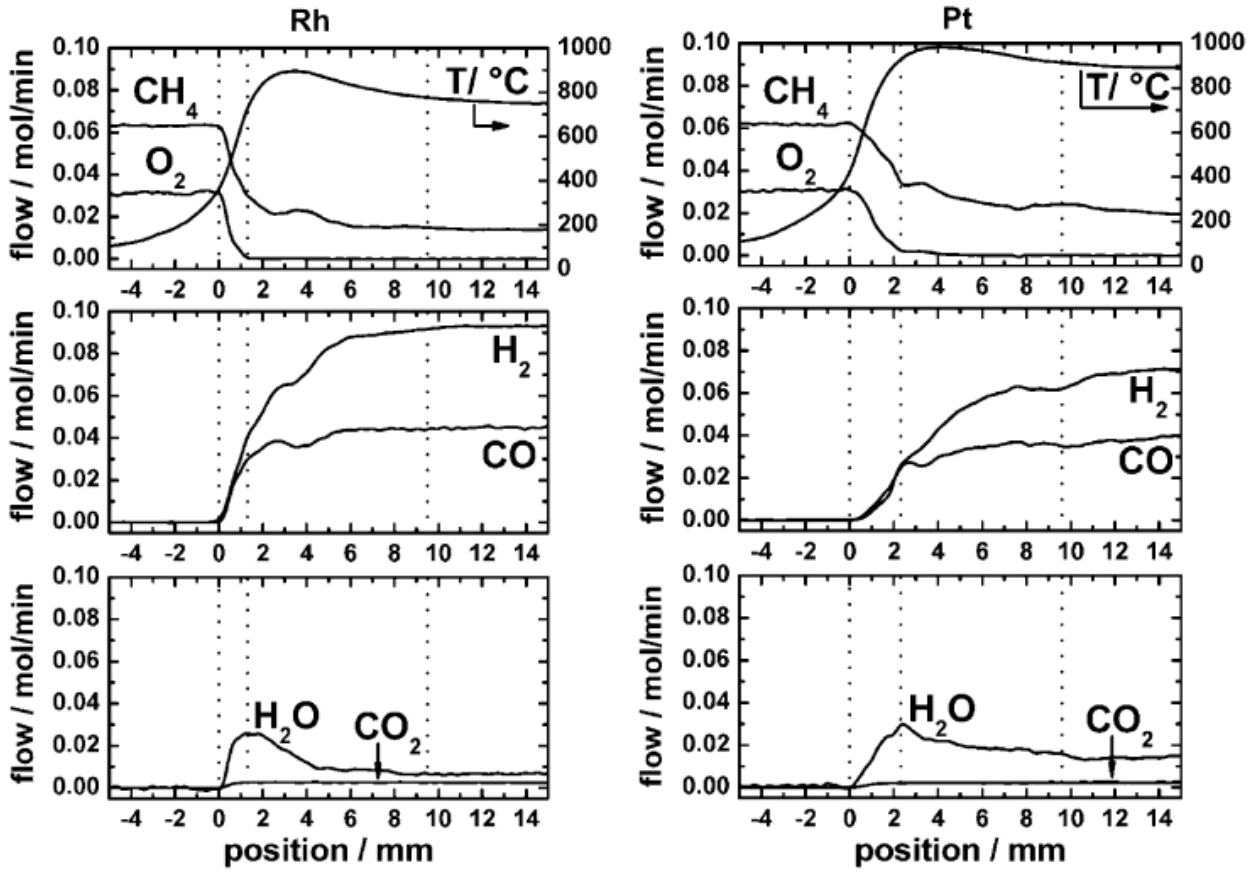

Figure 5: Spatially resolved species and temperature profiles for syngas stoichiometry (C/O = 1.0) in CPO of methane on Rh and Pt foam catalysts [55].

The reactant profiles presented in fig.5 show a zone at the catalyst entrance in which O_2 and CH_4 are rapidly consumed until O_2 is fully converted. This zone is called the "oxidation zone" and is generally longer on Pt than on Rh. The predominant oxidation products on both metals are H_2, CO, and H_2O whereas CO_2 is formed only in small amounts in the oxidation zone. Behind the point of total conversion of gas phase O_2 methane conversion continues on both metals, but the conversion rate slows significantly with a drop in H_2 and CO formation rates. H_2O now becomes the co-reactant to CH_4; therefore this second zone is designated the "steam reforming zone" where the developing profiles clearly reflect the H_2/CO molar ratio of 3/1 predicted by Eq. (1.1). The CO_2 molar flow rate remains constant after gas phase O_2 has been fully consumed, thus CO_2 reforming (1.3) is not observed. As in the oxidation zone, Rh converts more CH_4 than Pt in the steam-reforming zone. The temperature profiles shown in Fig.5 reflect the heat production by the strongly exothermic oxidation reactions in the oxidation zone followed by heat consumption due to the strongly endothermic steam reforming. The Pt catalyst operates at higher temperatures than the Rh catalyst because more heat is generated in the oxidation zone and less heat is consumed, because endothermic steam reforming is slower on Pt than on Rh. In the end, from the high-resolution

spatial profiles, it can be concluded that the mechanism of the methane CPO is a combination of partial oxidation and steam reforming. The overall yields of H_2 and CO are higher on Rh than on Pt for three reasons: (1) Rh activates CH_4 more efficiently in the presence of O_2 than Pt, (2) Rh forms H_2 more selectively in the presence of O_2 than Pt, (3) Rh is the more active steam-reforming catalyst. The O_2 profiles on Rh and Pt show that the reaction is largely mass transport-controlled in the oxidation zone on Rh but kinetically controlled on Pt and O_2 mass transport limitations are another reason for the better performance of Rh as catalyst for the partial oxidation of methane.

1.4 The catalytic oxidative conversion of light alkanes to syngas and olefins

In addition to methane, other fuel feedstocks, such as light hydrocarbons heavier than CH_4, could be considered to feed a CPO reactor to obtain syngas. Since the natural gas is typically composed of methane (90%) and ethane (6%), the objective of carrying out the partial oxidation of ethane to syngas (C_2H_6/O_2=1, eq.1.6) is a direct use of natural gas as feed at the on-site gas field without separating respective components.

$C_2H_6 + O_2 \rightarrow 2CO + 3H_2$, ΔH_r^{298K}= -136 kJ/mol (1.6)

For this reason methods for syngas production must be demonstrated to be effective for ethane as well as methane [57]. In the early 1990's, Huff and Schmidt [58] noticed that Rh produced primarily syngas with no carbon buildup in short contact times (~ 5 ms) by adding O_2 to the ethane feed. Since in the last 20 years Rh has been shown to be an excellent catalyst for CH_4 conversion to synthesis gas, the results from Huff et al. suggested that the presence of ethane should not be an interference [58]. In other words, the already described processes for partial oxidation of methane to syngas over Rh based catalysts are suitable for natural gas feed containing also ethane.

Moreover, CPO of other light alkanes as propane and butane could be attractive as a suitable reaction path for onboard reforming of these liquefied fuels easy to transport and storage together to the application of CPO as a preliminary conversion stage for hybrid gas turbine catalytic burners.

Light olefins are the most important building blocks for the polymers industry and the world demand for ethylene and propylene is expected to increase significantly in the next decade [59-60]. Worldwide Ethylene and Propylene production capacities amount respectively to ca. 130-140 MTPY and ca. 85-90 MTPY and these molecules are obtained primarily through Steam Cracking (SC producing the 98% of the Ethylene and 56% of Propylene) starting from feedstock as naphtha, ethane and gasoil. The steam cracking (SC) is carried out in large, gas-fired furnaces and it is the most energy-consuming process in the chemical industry and globally uses approximately 8% of the sector's total primary energy use, excluding energy content of final products excluded releasing ca. 200 MTPY of CO_2 [6].

The primary reaction to produce ethylene is the homogeneous pyrolysis of ethane:

$C_2H_6 \leftrightarrow C_2H_4 + H_2$, ΔH_r^{298K}= +136 kJ/mol (1.7)

which is endothermic and for this reason the reactors are placed in large furnaces to supply the necessary heat for reaction. Steam cracking requires long residence times and produces significant amounts of emissions such as NO_x because of flames in the furnace [61]. Under the severe pyrolysis

conditions (~ 800 °C), the formation of coke is thermodynamically predicted: to avoid this situation the feed is mixed with steam, but still periodic shutdown of the reactor is required [60].

Progress in this area may crucially affect the modern petrochemistry: the selective oxidative dehydrogenation (ODH) of ethane to ethylene (1.8) has attracted some interest as a possible alternative technology to steam cracking with potentially low capital investment, improved energy efficiency and reduced NO_x and CO_2 emissions [62-63].

$C_2H_6 + ½\ O_2 \rightarrow C_2H_4 + H_2O, \qquad \Delta H_r^{298K} = -105$ kJ/mol (1.8)

Oxidative dehydrogenation of ethane ($C_2H_6/O_2=2$) is a partial oxidation reaction and it has been demonstrated that Pt and Pt-Sn catalysts, through this reaction, can provide selectivity to ethylene up to 70 % [61] and yields comparable to those of commercial cracking units. The overall reaction is exothermic, which avoids the complications associated with external heating, and can be operated autothermally without any externally applied heat at very short residence time (5 ms) [61].

Due to a simpler reactor system and fewer fractionation columns, estimated investment cost for the ethane CPO process is about 20–25% lower than for the corresponding ethane steam cracker. On the other hand, estimated production costs are somewhat higher (10–15%), mainly due to the additional cost of making or purchasing oxygen [64].

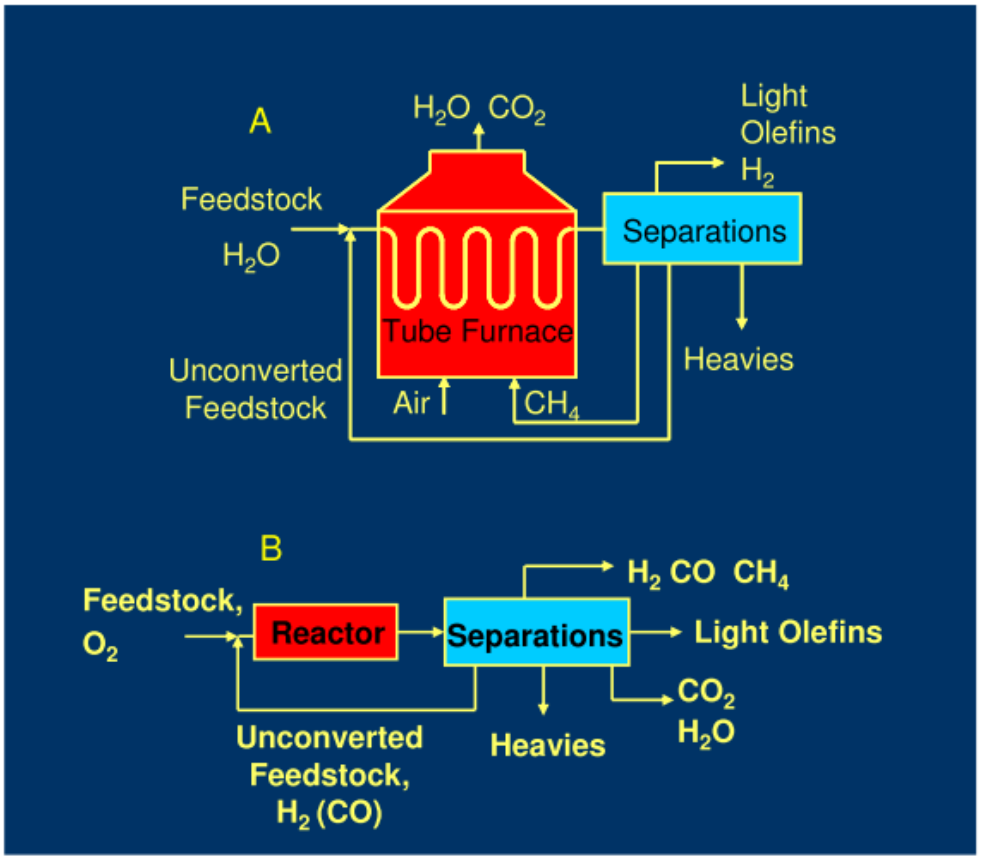

Figure 6: Simplified block scheme of the Steam Cracking (SC) A, and of the Short Contact Time – Oxidative Dehydrogenation (SCT-ODH) B, processes for the production of olefins [6].

For the oxidative dehydrogenation of ethane to ethylene, several different theories about the process have been proposed based on extensive experiments and kinetic modelling. The performance of ethane can be summarized as heterogeneous production of CO-H_2, and/or preferably CO_2-H_2O, by oxidation of surface carbon and hydrogen, coupled to homogeneous dehydrogenation of ethane to produce ethylene [65-67]. Many investigations report that production of C_2H_4 occurs in the gas phase [62-65,68], though it is very low in the presence of Rh catalysts, whereas molar yields in excess of 60% can be attained on Pt based systems [62,64-65,68-69]. Recently it was shown by detailed spatial and temperature profiles, reported in Fig. 7, that a definite correlation can be made between C_2H_4 production and reactor temperature, since more than 750°C are required for the onset of homogeneous dehydrogenation reaction [57].

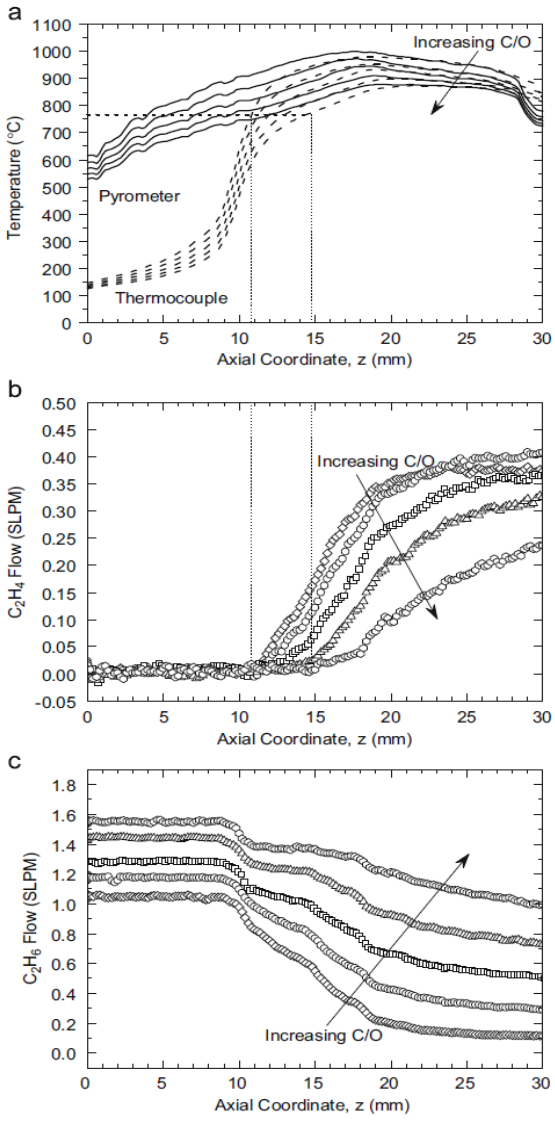

Figure 7: Comparison of reactor temperature profiles(a), measured by pyrometer (solid lines) and thermocouple (dashed lines), with C_2H_4 formation (b) and C_2H_6 consumption (c) for multiple C/O over the 4.7 wt % Pt/45PPI a-Al_2O_3 catalyst [57].

The final olefin yield and selectivity are strongly affected by the way heterogeneous and homogeneous reaction paths are coupled together in the short contact time catalytic reactor, which, in turn, is highly dependent on catalyst formulation and morphology, reactor configuration and operating conditions. The enhancement of ethylene yield and selectivity can be obtained with proper catalyst formulation leading to a more favourable product distribution in the first oxidation zone of the reactor, where a sacrificial co-fed fuel (H_2 or CO) has to be oxidized selectively with respect to ethane while oxygen has to be consumed to form total rather than partial oxidation products in order to minimize its consumption, required to sustain the optimal surface temperature level slightly below 1000 °C. Indeed, it has been shown that for Pt systems the addition of H_2 to the inlet feed of this reactor results in surface hydrogen oxidation at the expense of surface carbon oxidation. Coincident with this oxidation is the release of a great amount of heat that is transferred to the gas phase, resulting from the overall exothermicity of the reaction $H_2 + 1/2\ O_2 \rightarrow H_2O$ (ΔH_r^{298K} = -241.8 kJ/mol). Importantly, since C_2H_6 is not consumed for heat, the yield of C_2H_4 increases dramatically since homogeneous ethane dehydrogenation is enhanced; moreover, the selectivity to ethylene increases because selectivity to CO and CO_2 is decreased [67]. Donsì et al. [68] described an analogous process involving preferential CO oxidation over perovskites, giving similar yields as H_2 co-feed over Pt, thus suggesting that C_2H_4 enhancement is not unique to H_2/Pt, but rather heat generation in general.

Despite homogeneous reactions play the most important role in the conversion of ethane, catalytic processes for C_2H_4 consumption are also important in determining C_2H_4 selectivity since both contribute to the net production [57]. The role of side heterogeneous and homogeneous reactions consuming both the reactant and the desired product is still debated [57,63,68,70-74]: their contribution appears to depend on the type of reactor [64,72-73] and catalyst [57,63-64,71,73,75]. In effect, lower selectivity to ethylene is observed with Rh than with Pt. It is likely that the high reforming activity of Rh compared to Pt [76-77] competes with the pyrolysis reaction that occurs in the gas phase. The competition can occur in two ways according to scheme reported in fig. 8: the C_2H_6 consumption via reforming (r_2) maybe is higher than pyrolysis (r_1), or the C_2H_4 consumption by reforming (r_3) may compete with its production by pyrolysis. For any net C_2H_4 production to occur, the average reforming rates r_2 and r_3 must be lower than the pyrolysis rate r_1[57].

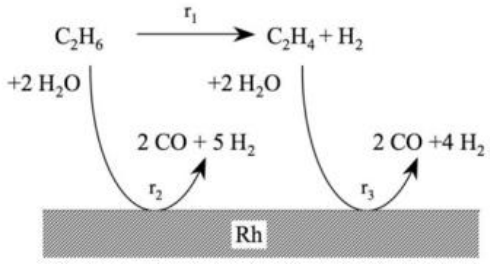

Figure 7: Ethane to ethylene and syngas[57].

Taking in account the different behaviour of Pt and Rh, it seems that Rh would act as a sort of catalytic filter, since it converts both the feed and the gas-phase products into CO and H_2 [76]. This circumstance is ascribed to their relative activity in reforming. A comparative study of methane, ethane and ethylene steam reforming on Pt and Rh on YSZ reported from Graf et al. has shown large differences between them. The order of activity of Pt/YSZ was $CH_4>C_2H_6>C_2H_4$ while on Rh/YSZ the order of activity was completely different: $C_2H_6\approx C_2H_4>CH_4$ [78]. They reported that reforming of C_2H_4 and C_2H_6 proceeds at similar rates on Rh/YSZ [78], with slight differences that can be attributed to the activation of hydrogenolysis in the case of ethane feed. Importantly, the authors noticed that the rate of C_2H_4 reforming on Pt is lower than on Rh, supporting the hypothesis that reforming activity plays an important role in the selectivity to C_2H_4 with the two different catalysts.

1.5 An issue for Catalytic Partial Oxidation: Sulphur poisoning

The presence of sulphur containing compounds naturally occurring in natural gas or added as odorants necessary for safety reasons can result in a sulphur concentration approximately 10 ppm, which can adversely affect the catalytic performance during catalytic partial oxidation [40,79-80]. Although desulphurisation units can be used to significantly reduce the sulphur content in the feed, its inclusion increases the complexity, size and cost of the fuel processing system. Moreover, the present catalytic hydrodesulphurisation (HDS) technology can not completely remove all the sulphur from the fuel. Thus, "sulphur-free" fuels in fact still contain up to 10 ppm of S after HDS treatment which can significantly reduce the catalytic activity. Therefore it will be more desirable to develop catalysts that are intrinsically sulphur tolerant and are not readily poisoned by the amounts of sulphur commonly found in fuels such as natural gas and commercial low sulphur fuels.

Catalyst deactivation, the loss over time of catalytic activity and/or selectivity, is a problem of great and continuing concern in the practice of industrial catalytic processes. Catalyst replacement and process shutdown cost to industry total billions of dollars per year. Time scales for catalyst deactivation vary considerably but it is inevitable that all catalysts will decay. While catalyst deactivation is inevitable for most processes, some of its immediate, drastic consequences may be avoided, postponed, or even reversed. Thus, deactivation issues (i.e. extent, rate and reactivation) greatly impact research, development, design, and operation of commercial processes.

Poisoning is the strong chemisorption of reactants, products or impurities on sites otherwise available for catalysis. Thus, poisoning has operational meaning; that is, whether a species acts as a poison depends upon its adsorption strength relative to the other species competing for catalytic sites. In addition to physically blocking of adsorption sites, adsorbed poisons may induce changes in the electronic or geometric structure of the surface [81].

Sulfur poisoning of metallic catalysts is a difficult problem in many important catalytic processes and it is due to the presence of unshared electrons in sulfur, through which strong sulfur metal interaction forms. Previous studies have revealed that the chemisorptive sulfur adsorption on metals is very detrimental because the direct metal–sulfur interaction can adversely affect multiple metal sites in the proximity of sulfur. For example, Erley and Wagner pointed out that a sulfur atom is capable of blocking about nine CO adsorption sites on Ni [82]. Feibelman's calculation further confirmed that the strong poisoning effect of a sulfur atom on the electronic structure of metals

exceeds its nearest metal neighbors [83]. According to Joyner and Pendry [84], the poisoning range for a sulfur atom is 5–7A˚, meaning that it can negatively affect at least ten close-packed metal surface atoms. Due to such a long-range adverse electronic impact, the direct chemisorptive metal–sulfur interaction reduces the availability of metal d-electrons and suppresses the sticking probability and coverage of other reactants on metals [85]. Previous work have shown some evidence that sulfur preferentially adsorbs on sites of lowest coordination, such as corner and edge sites, on stepped single-crystal surfaces, and, by implication, on equivalent sites of small metal crystallite surfaces [86].

It can be expected that the poisoning effect of sulfur on metals would be attenuated if it is shielded by other elements such that no unshared electrons of sulfur are available for the direct sulfur–metal interaction [85].

1.5.1 Sulphur poisoning in catalytic partial oxidation

Even if sulphur poisoning is a difficult problem in many catalytic processes, studies on the effect of sulphur during the CPO have so far remained scarce. Recently, Bitsch-Larsen, Degenstein, and Schmidt studied the addition of CH_3SH during CPO experiments of methane over Rh–Ce coated foam monoliths [80].

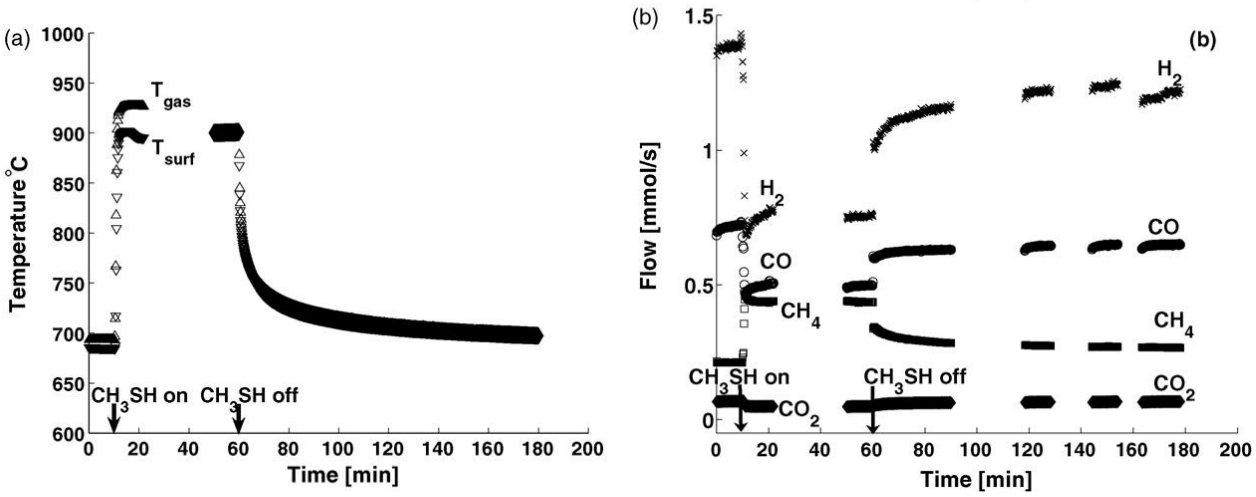

Figure 9: Effect of CH_3SH addition in CPO of methane over Rh-Ce foam monoliths [80].

As shown in fig.9, the temperatures increased by 200°C, and at the new steady state reached upon the addition of CH_3SH, the production of H_2 decreased by 45% from the non-sulfur level. This was accompanied by an increase in the flow of methane of 20% due to lower conversions. It is possible to see that sulfur poisoning is reversible as the catalyst slowly regains its activity when sulfur is

removed from the feed. The authors suggested that the rise in temperature, the drop in methane conversion and the increased amount of water indicated that the endothermic SR was strongly affected by the presence of sulfur on the surface. The addition of sulfur increased the amount of water significantly, due to the inhibition of water consuming paths. Through the spatial profiles of temperatures and compositions, they observed that the rates of O_2 conversion and the initial CH_4 conversion were independent of the sulfur level.

Similar results were found in the last works by Cimino et al. who investigated the impact of sulphur adding H_2S or SO_2 during the CPO of methane at high temperatures (>800°C) and short contact times over Rh structured catalysts [87-89]. Accordingly to Bitsch-Larsen, they demonstrated that the addition of sulphur resulted in a rapid decrease in CH_4 conversion and H_2 selectivity with a corresponding sharp increase in the catalyst temperature; moreover the extent of catalyst deactivation was depending on sulphur concentration in the feed. As well in this study, the complete reversibility of the S-poisoning effect under the studied reaction condition was confirmed by the regaining of the initial performance in terms of activity/selectivity and temperature after the removal of sulphur from the feed. Furthermore, the rapid response upon the introduction and removal of sulphur suggested that direct adsorption onto the active Rh sites is responsible for the adverse effects of sulphur. However, the catalyst performance continued stable in the presence of sulphur indicating the occurrence of a steady state between S adsorbing on the surface of the active sites and S desorbing into the gas phase, which is governed by the catalyst temperature and sulphur concentration [89]. The decrease in methane conversion measured in the presence of sulphur was accompanied by a corresponding increase in water production of the same magnitude and at the same time less CO and H_2 were produced. These results confirmed, in agreement to Schmidt and his group's work above mentioned, that the poisoning effect is related to the ability of S to inhibit the endothermic steam reforming reaction. The slight increase in CO_2 yield was related to the shift in the equilibrium of the slightly exothermic water gas shift reaction, due to significant reduction of H_2 and rise of H_2O partial pressures. In order to investigate if the extent of catalyst poisoning was affected by different sulphur bearing compounds, the experiments were repeated by substituting H_2S with SO_2 into the reaction feed. The CPO results were completely reproducible in terms of catalyst temperatures and methane conversions as well as H_2 and CO yields being only affected by the total S concentration in the feed and not by the type of sulphur precursor. This is in good agreement with the results reported by Fisher: in the presence of thiophene, sulphur dioxide, benzothiophene, dibenzothiophene, the predominant sulfur species is H_2S and the impact on catalytic performance scaled with sulfur content, not with sulfur compound. This is most probably due to the rapid and complete conversion of all the S-species into H_2S, which is the

thermodynamically stable specie under the typical CPO operating conditions, i.e. high H_2 partial pressure and high temperatures (>800 C).

As regards the impact of sulphur poisoning of Rh based catalysts on the performance of CPO to syngas of higher hydrocarbons, only few publications are available also in this field and some of these show surprising results. It was reported that increasing both the molecular weight and the aromaticity makes the fuel more sulphur tolerant for H_2 generation.

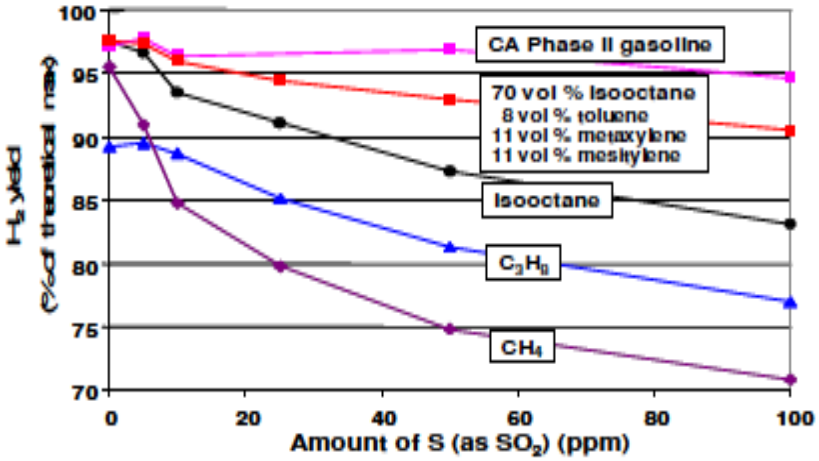

Figure 10: Effect of S on H_2 yield during CPO of different fuels [90].

In contrast to the findings obtained in the CPO of methane, during which even a low amount of sulphur leads to a decrease in H_2 yield, in a previous work of Fisher et al. [90], as it is possible to see in fig.10, it was reported a trend of H_2 yield at different sulphur concentration with a maximum at low ppm of sulphur. This promoting effect of low concentrations of sulphur on the hydrogen production was identified during the CPO of propane over Rh but was not discussed further [90].

On the other hand, it has been reported that sulphur inhibits the reforming reactions, which in the case of CPO of ethane to ethylene seem to be competitive with the production of the desired product, consuming both C_2H_6 and C_2H_4 to form syngas instead of the olefin. It can be argued that sulphur added to the feed might inhibit simultaneously those reforming reactions, thus favouring the homogeneous ethylene formation chemistry, since also the temperature level increases, due to the lack of endothermic heterogeneous chemistry [78].

There are a number of industrial processes in which one intentionally poisons the catalyst in order to improve its selectivity. For example, Pt-containing naphtha reforming catalysts are often pre-sulfided to minimize unwanted cracking reactions [82]. Therefore, selective S-poisoning of catalytic

sites can be used as a strategy to alter the balance and synergy between homogeneous and heterogeneous chemistry in the CPO of highly reactive feeds.

In the search for sulfur-tolerant catalysts, it could be useful to refer to the equilibrium diagram relative to the formation of metal sulphides depending on the temperature.

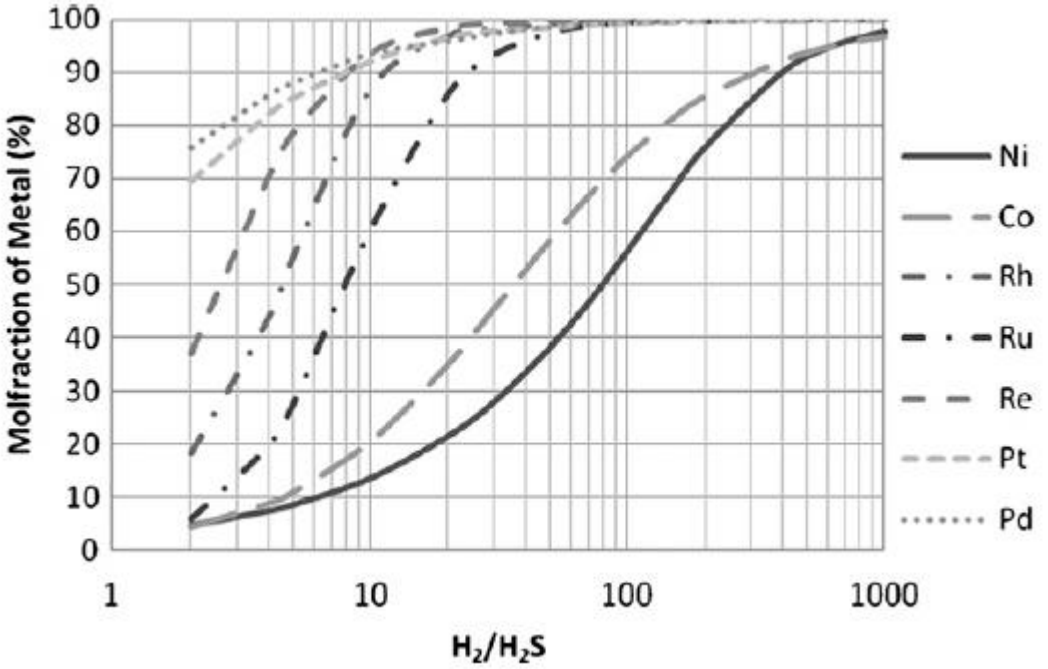

Figure 11: The equilibrium distribution of the metal and metal sulphide phase as a function of the hydrogen-to-hydrogen sulphide ratio at 900 °C [91]

From the fig. 11 it is possible to see that the base-metals (Ni and Co) are more prone to form metal sulphides than the other metals considered. On such basis, noble metals should be preferred to the other metals for operations in sulphur laden environment. However, this type of equilibrium diagram represents only a guideline, as behind thermodynamics, also kinetics and surface cover phenomena play a role into the formation of sulphides species [91]. Some attempts have been tried into the research for sulphur tolerant materials during the catalytic partial oxidation of different feedstocks in the presence of sulphur. Haynes and his coworkers tested the activity of Ni hexaaluminate during the partial oxidation of liquid hydrocarbons in the presence of sulphur: they found a faster deactivation of Ni hexaaluminate than a Ni reference catalyst [92]. On the other hand, they showed that by dispersing the Ni-hexaaluminate onto a gadolinium doped ceria (GDC), during CPO of n-tetradecane containing sulphur compounds, these catalysts demonstrated greatly reduced deactivation compared to 3 wt% Ni/alumina and 3 wt% Ni/GDC [93].

In the partial oxidation of tar derived from the pyrolysis of wood biomass (cedar wood), Tomishige et al. [94-95] investigated the effect of H_2S addition over Ni catalyst and Rh/CeO_2-SiO_2 using a

fluidized bed reactor. Steam reforming Ni catalyst was effective for the tar removal without H_2S addition, however, the addition of H_2S (168 ppm) drastically deactivated the catalyst. In contrast, Rh/CeO_2-SiO_2 exhibited higher and more stable activity than the Ni catalyst even under the presence of high concentration of H_2S (280 ppm).

Since it was reported that the addition of Pt [96] or Pd [97] to Rh improved the activity of the catalyst during the steam reforming of sulphur containing fuels, Cimino et al. investigated the enhancement in sulphur tolerance of Rh-based catalyst by partially substituting Rh with either Pt or Pd [89]. The substitution of half of the Rh loading with same weight amount of Pt, and even more with Pd, entailed a reduction in fuel conversion and yield to syngas. These findings confirmed that Rh is the most active and selective metal for methane CPO, however, among bimetallic catalysts, Rh-Pt performed better than Rh-Pd. Indeed, the bimetallic Rh-Pt catalyst showed a significantly enhanced specific tolerance to sulphur inhibition with respect to Rh and Rh-Pd counterparts. The higher sulphur tolerance of the Rh-Pt bimetallic catalyst appeared to be strictly connected to the higher catalyst temperature, which reduced the impact of S on Rh sites favouring surface sulphide decomposition, and to the simultaneous presence of Pt sites, which activity is almost unaffected by S-poisoning [89,98].

With these premises in mind, it is possible to conclude that Rh is the most suitable catalyst for CPO, also in presence of sulphur. However, since Rh is not immune from sulphur poisoning, it is still desirable to develop Rh based catalysts that are intrinsically sulphur tolerant and are not readily poisoned by the amounts of sulphur commonly found in fuels such as natural gas and commercial low sulphur fuels.

1.6 A novel class of sulphur tolerant catalysts : metal phosphides

Phosphorus reacts with most elements of the periodic table to form a diverse class of compounds known as phosphides. The bonding in these materials ranges from ionic for the alkali and alkaline earth metals, metallic or covalent for the transition elements, and covalent for the main group elements. They combine the properties of metals and ceramics, and thus are good conductors of heat and electricity, are hard and strong, and have high thermal and chemical stability [99].

Transition metal phosphides have recently been reported in literature as a new class of high activity hydrotreating catalysts that have substantial promise as next-generation catalysts. They are regarded as a group of stable, sulfur-resistant, metallic compounds that have exceptional hydroprocessing properties [100].

A number of methods have been employed for the preparation of phosphide catalysts, and the development of new methods facilitating the control of phase composition, structure, dispersion and morphology is an active area of current interest [101-102]. The most widespread method involves reduction of phosphate at elevated temperature [103]. The relative ease of preparing supported phosphate materials (via incipient wetness technique) has made this method the most suitable for the preparation of these catalysts, and the product formed is dependent on both the reduction temperature as well as the chemical nature of the precursor [104]. Generally phosphorus is added to a metal nitrate salt in the form of a thermally decomposable precursor such as $(NH_4)_2HPO_4$. Following drying and calcination to decompose the precursors salts, temperature programmed reduction is then performed to obtain the desired phase. Surplus phosphorus is often added to counteract subsequent losses that occur during preparation [103]. Regarding the effect of P-loading, for example it is claimed that the synthesis of Ni_2P requires excess P; this is because there are several intermediate phosphides, and phosphorus compounds (PH_3 and reduced P) are volatile at high temperatures.

The role of the support has proven to be complex as it affects both the dispersion and the geometric and electronic properties of the active phase as a consequence of the metal-support interaction [105]. Thus the optimization of P content depends also on the support. The use of alumina as a support for phosphide catalysts has been reported by many authors [106-107]. An increase in the dispersion of phosphide based phases in HDS reactions by using γ-Al_2O_3 instead of SiO_2 as a material support has been fully reported [108] and is mainly due to the high acidity of the former. However, the main drawback of alumina as a carrier for metal phosphide catalysts is its interaction with phosphorus [105]. Indeed, a large difference was found for the optimal P/Ni ratio of Ni_2P/SiO_2 ((P/Ni) = 0.8) and Ni_2P/Al_2O_3 ((P/Ni) = 2) [107]. In this respect, it is well-known that, upon

calcination, phosphorus strongly interacts with γ-Al_2O_3, thus, for P-rich catalysts, one might expect the formation of a strongly bound amorphous phosphate ($AlPO_4$) surface layer on the alumina support [109-112]. As a consequence, a stronger phosphorus-alumina support interaction requires higher temperatures to form the desired phase [105,111].

Transition metal phosphides such as MoP, CoP and Ni_2P were prepared by temperature-programmed reduction and tested in hydrodesulfurization [112]. The HDS activities of metal phosphides vary substantially depending upon the metal and the phosphorus-to-metal (P/Me) molar ratio [113]: phosphides prepared with lower metal loading exhibited higher HDS activity whereas higher loadings resulted in sintering of particles during reduction and lower activities. Lower loadings are also beneficial for practical cost reasons [99]. It was demonstrated that highly dispersed Ni_2P is particularly active for HDS and resistant to sulphur [99], exhibiting excellent stability in activity tests extending over 100 h. In developing an understanding of the HDS properties of metal phosphide catalysts, the resistance of these catalysts to S incorporation plays a critical role, in fact it seems that P blocks S incorporation into the catalysts [113]. Moreover it was shown that a H_2 reduction of the sulfided MoP/SiO_2 partially restores the phosphide nature of the catalyst: for the catalyst sulfided by H_2S/H_2 at 573 K, the sulfided surface can be converted mostly to phosphide by an H_2 activation at 923 K. This indicates that there exist both reversibly and irreversibly bonded sulfur species on the sulfide catalyst and most sulfur species is reversibly bonded on the surface. The full regeneration of the phosphide nature of the sulfided catalyst indicates that most P atoms in molybdenum phosphide may not be exchanged or removed by sulfur species under reaction conditions [112].

Besides the transition metal, under the conditions of low hydrogen sulfide partial pressure, noble metals (including Rh) have been shown to be highly active for deep HDS applications. On this basis, Kanda et al. expected that noble metal phosphides (NM_xP_y) show high catalytic activities for HDS reaction [114]. A number of metal phosphides of Ru, Rh and Pd have been prepared on high surface area silica by optimization of the precursor composition (P/Me molar ratio) and TPR parameters. The order of the HDS activities of NM-P/SiO_2 catalysts was Rh-P>Pd-P>Ru-P>Pt-P. Especially, P addition remarkably enhanced the HDS activity of the Rh/SiO_2 catalyst.

Rh_2P adopts the anti-fluorite structure in which the Rh atoms occupy tetrahedral positions and the P atoms occupy cubic positions in the lattice.

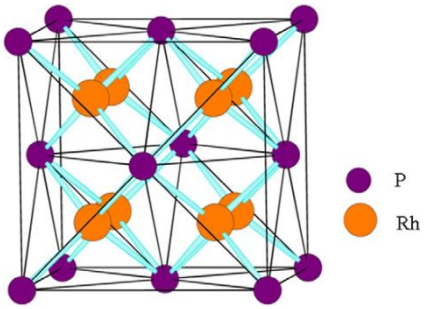

Figure 12: Rh_2P structure [115].

The lattice constant for Rh_2P was determined to be 0.5498 nm with Rh-Rh and Rh-P distances of 0.2749 and 0.2381 nm, respectively. By comparison, a Rh-Rh distance of 0.269 nm for bulk Rh metal can be calculated: consistent with these Rh-Rh distances for Rh_2P and Rh metal, electronic structure calculations for Rh_2P indicate that the bonding is dominated by Rh-P interactions, with Rh-Rh and P-P interactions being substantially weaker [115].

Hayes et al. prepared a silica-supported Rh_2P by TPR in H_2 flow of a Rh phosphate-like precursor, obtained by impregnation of silica with an aqueous solution of rhodium chloride and ammonium dihydrogen phosphate followed by calcination. The Rh_2P/SiO_2 catalyst exhibited a higher dibenzothiophene hydrodesulfurization activity than did the reference catalyst Rh/SiO_2 and it was also more active than a commercial Ni-Mo/Al_2O_3 catalyst. Moreover the Rh_2P/SiO_2 catalyst showed excellent stability over a 100 h DBT HDS activity measurement and was more S tolerant than the Rh/SiO_2 catalyst [115].

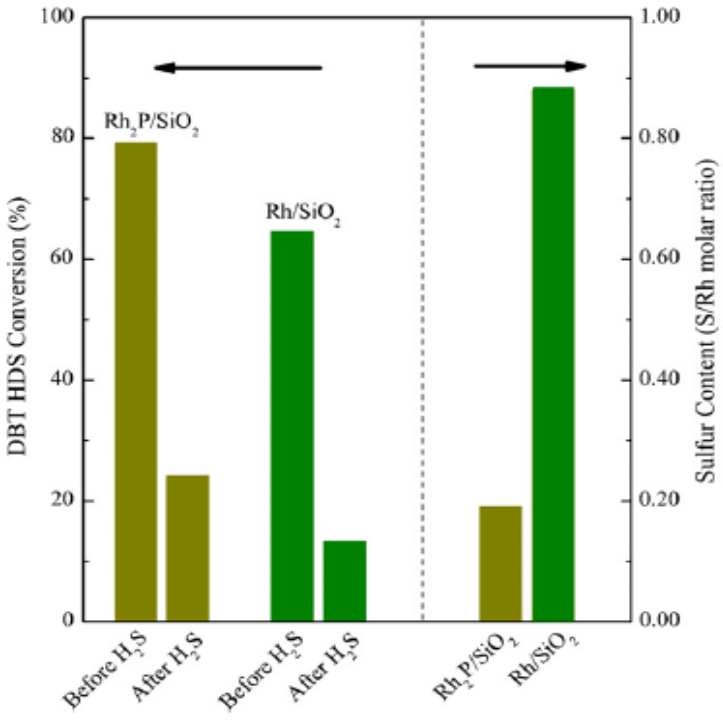

Figure 13: DBT HD S conversion and sulphur content of Rh_2P/SiO_2 and Rh/SiO_2 catalysts [115].

Indeed, as it is shown in fig.13, the results of S content analyses of the catalysts subjected to the H_2 then H_2S/H_2 pretreatment indicate that the site blockage is due to strongly bonded S species, with the Rh/SiO_2 catalyst (S/Rh = 0.88) having an S content over 4.5 times higher than that of the Rh_2P/SiO_2 catalyst (S/Rh = 0.19). The authors attributed the excellent properties of the Rh_2P/SiO_2 catalyst to the metallic nature of the Rh_2P and its strong resistance to sulphur incorporation. The resistance to S incorporation of the Rh_2P/SiO_2 catalyst is attributed to the P in the Rh_2P particles, which inhibits the irreversible adsorption of sulphur at the particle surface as well as the incorporation of sulphur into the bulk (i.e. to form Rh sulfide) [115]. At the same time the surface P does not appear to suppress CO adsorption on Rh, preserving it even in the presence of S, which is the reason for the high catalytic activity [114-115].

1.7 Summary

Rhodium catalysts are the most active and selective for CPO of methane to syngas under high temperature at short contact time conditions. However Rh is also very expensive due the increasing request for automotive catalytic converters to meet more stringent legislation limits [116-117]. Moreover Rh catalysts are affected by sulphur poisoning already at very low concentration levels [40,79-80].

The objective of this thesis has been to study the effect of sulphur poisoning during the catalytic partial oxidation of methane and ethane (the main components of natural gas) at high temperatures and short contact times over noble metal based structured catalysts.
Some recent studies have focused on the negative effect of sulphur during CPO of different hydrocarbon feedstocks and showed that also Rh is not immune from sulphur poisoning. However, it can be expected that the poisoning effect of sulfur on Rh metal can be attenuated if it is shielded by other elements such that no unshared electrons of sulfur are available for the direct sulfur–metal interaction.

The first objective of this PhD work, reported in Chapter 3, has been to investigate the possible beneficial effect of Phosphorous doping of Rhodium catalysts with regards to catalytic activity and S-tolerance during the self-sustained methane CPO at short contact time. To the best of knowledge, this kind of catalyst has never been evaluated as active phase for CPO while recent literature demonstrates the superior performance of phosphides in terms of activity and sulphur tolerance during deep HDS .
During a six-month period spent as a visiting scientist at the Chemistry Department of Technical University in Munich (TUM- Technische Universität München), the effect of phosphorous addition has been investigated in dry reforming reaction. This reaction is attractive as it consumes two greenhouse gas emissions, CH_4 and CO_2, but strongly affected by coke deposition issue. For this reason it requires an active and stable catalysts which do not deactivate quickly to obtain good perfomances in terms of syngas production. Recent studies reported the detrimental effect of phosphorous added ex-situ to Rh causing a lower dispersion in comparison to the undoped sample, lower methane conversion during steam reforming reaction, and attitude to form coke [118]. With these premises, in the final part of Chapter 3, dry reforming has been exploited as a model reaction, in order to further probe the beneficial effect of phosphorous addition to Rh catalysts previously demonstrated during CPO of methane, focusing on deactivation problems caused by carbon deposition through a reaction more prone to this issue than steam reforming.

In second part of the work, the impact of sulphur has been studied during the CPO of ethane to produce syngas and ethylene performed on conventional Rh and Pt catalysts supported on γ-Al_2O_3. Up to now, methods for syngas production have been demonstrated to be effective also for ethane, the main component of natural gas beside methane; however, the studies concerning the sulphur poisoning effect on higher hydrocarbons are so far scarce and somehow contradictory. In Chapter 4, the characterization of sulphur impact during the CPO of ethane to syngas has been investigated in order to estimate the effect of S poisoning with respect to practical issues for industrial implementation such as catalyst activity and durability and multi-fuel operability of a CPO reactor.

From the literature it turned out that the higher reactivity of ethane and the higher number of possible reactions and products, determines a much more complicated chemistry during CPO of ethane in comparison to methane, involving interacting hetero-homogeneous reaction paths, whose contribution and synergy may be strongly alterated by S-poisoning. In this context the final aim of this work can be placed: sulphur has been explored, in Chapter 5, as an intentional selective poison of undesired heterogeneous reactions to improve the production of ethylene by altering the balance and synergy between homogeneous and heterogeneous chemistry. At the same time, taking advantage of the selective poisoning of sulphur of reforming paths, an attempt has been done to shed light on the complex interaction of hetero-homogeneous chemistry available in a C_2H_6 CPO reactor, to understand the contribution of heterogeneous reforming ractions to the overall performance of the reactor.

1.7.1 The effect of Phosphorous doping on Rh catalysts during Catalytic Partial Oxidation and Dry Reforming of methane

A novel monolith catalyst with Rh supported on γ/Al_2O_3 and doped with phosphorous was prepared by temperature-programmed reduction of oxidic precursors and tested for the first time in the CPO of methane at short contact time and high temperature in the presence of sulphur.
The catalyst was characterized by N_2-Physisorption and CO-Chemisorption to obtain informations about the surface area of catalysts, porosity and metal dispersion, before and after exposure to S-laden atmosphere; ICP-MS: elemental analysis; SEM-EDAX to obtain a morphological characterization and distribution of active elements; XRD: crystallographic analysis; H_2-TPR to get details about redox behavior; in situ DRIFT on freshly reduced samples or after exposures to sulphur , to investigate the state and nature of active surface metal sites. Results were compared with the reference undoped $Rh/\gamma Al_2O_3$ catalyst and the $P/\gamma Al_2O_3$ support. Methane CPO

experiments were performed under autothermal conditions at high temperatures and short contact times under self-sustained pseudo-adiabatic conditions at an overall reactor pressure of P=1.2 bar. Both transient and steady state operation were investigated particularly with regards to the effect of the addition/removal of variable S quantities in the feed on catalyst temperature, on the formation of main reaction products, on the approach to equilibrium and on the apparent reaction rate.
The interaction of phosphorous with Rh resulted in a metallic surface capable to strongly adsorb CO, moreover it improved the metal dispersion on the alumina support and significantly inhibited the strong sulphur adsorption. As result of these beneficial effects, a direct comparison of CPO performance data with the reference undoped Rh catalysts showed a significant enhancement of the sulphur tolerance of the novel phase developed, providing a higher methane conversion and H_2 selectivity at any S level in the feed, at the same time reducing the risk of excessive catalyst overheating due to the S-inhibition of the endothermic steam reforming reaction path. The higher residual steam reforming activity of the Rh-P catalyst during the CPO of methane in the presence of sulphur appears to be correlated to the larger exposed active metal surface capable to strongly bond CO (as gem-dicarbonyl species) at room temperature.

In the final part of Chapter 3, P doped Rh samples ri-prepared at TUM following a similar procedure to that utilized to synthesize the catalysts devoted to the CPO of methane, were tested during dry reforming of methane ($CH_4/CO_2/N_2$=1/1/2) at 850°C and atmospheric pressure, focusing on the role of phosphorous on the noble metal activity and stability. The catalyst was characterized by N_2-Physisorption, H_2 and CO Chemisorption in order to confirm that this catalysts, prepared in second place at TUM, was similar to the previous system utilized during CPO. The addition of phosphorous resulted in a higher dispersion of the catalyst in comparison to the result obtained with a reference sample without phosphorous, as already pointed out for the Rh based systems earlier prepared and tested in CPO. This finding, together to a good interaction achieved between noble metal and dopant during the preparation routine, resulted in a higher activity of P doped sample in terms of methane and CO_2 conversion. Moreover, both catalysts showed a an excellent stability for the whole period of investigation, and no coke formation was observed which is particularly relevant for doped catalyst in the view of previous findings on coke formation tendency after phosphorous addition [118].

1.7.2 The effect of sulphur during the CPO of ethane to syngas

The impact of Sulphur addition (2-58 ppm) during the CPO of ethane to syngas (C_2H_6/O_2=1) was carried out on Rh- and Pt-based honeycomb catalysts tested under self-sustained high temperature conditions. Both steady state and transient operation of the CPO reactor were investigated particularly with regards to poisoning/regeneration cycles. Sulphur addition resulted in a rapid and reversible poisoning effect, leading to a new steady state characterised by a higher surface temperature of the catalyst and a corrispondent drop in fuel conversion and yield to syngas. The adverse impact of sulphur addition was larger on Rh catalyst than on Pt, although Rh is more active with S-free feed, mainly due to its higher activity for steam reforming and hydrogenolysis of ethane Two main effects of sulphur poisoning on Rh performance were indicated through a detailed examination of the variation in the flows of the main products and a simplified heat balance of the CPO reactor: sulphur selectively inhibits ethane hydrogenolysis and, to a lower extent, steam reforming of ethane and ethylene. Moreover, only for operation with Rh at temperatures below 750°C, reverse water gas shift reaction was inhibited, preventing the WGS equilibrium to be reached. The increase in the H_2 yield obtained in correspondence of few ppm of sulphur added to the feed, was associated to the combined poisoning effect of hydrogenolysis and r-WGS.

1.7.3 Ethane CPO to ethylene with sulphur and H_2 addition

The catalytic partial oxidation of ethane to ethylene was investigated over Rh and Pt based honeycomb reactors with the addition of sulphur to the feed (up to 51 ppmv as SO_2). Transient and steady state ethane CPO tests were run at C_2H_6/O_2= 2 under self-sustained high temperature and short contact time conditions. To further probe the differences between Pt and Rh the effect of sulphur addition with H_2 co-fed as sacrificial fuel was also studied, as H_2 addition was proved to significantly enhance ethylene yield. The two catalyst showed a different behaviour after the addition of SO_2 which only marginally impacted on the product distribution and temperature of the Pt catalyst. On the contrary, ethylene formation increased by as much as five times on Rh in presence of sulphur, which was accompanied by a significant temperature increase on the catalyst, whereas ethane conversion was unaltered. The effect of sulphur was compatible with the selective inhibition of the undesired steam reforming of ethane/ethylene. Even when the ethylene production on Rh was increased due to sulphur addition, markedly larger amounts of ethylene and water were obtained with the Pt catalyst, thus confirming a faster production of C_2H_4 in the gas phase.

When H_2 was co-fed as a sacrificial fuel in presence of sulphur, both the catalysts showed a larger increase in ethylene formation and temperature, suggesting that sulphur poisoning enhanced the selectivity of the catalytic oxidation of the sacrificial H_2 rather than ethane feed. The direct inhibition of the catalytic partial oxidation and steam reforming of ethane and ethylene due to the suphur presence, and the increase in the temperature, enhanced ethylene yield particularly for Pt catalyst.

References

1) Wood D. A., Nwaoh C., Towler B. F., Journal of Natural Gas Science and Engineering 9 (2012) 196-208
2) Khana M.I., Yasmin T., Journal of Natural Gas Science and Engineering Volume 17 (2014) 99-109
3) Hajbabaei M., Karavalakis G., Johnson K. C., Lee L., Durbin T. D., Energy 62 (2013) 425-434
4) Eni Corporate University (2005) Available at: (2005) http://www.eni.com/en_IT/attachments/lavora-con-noi/pdf/GTL-technology.pdf
5) York A.P.E., Xiao T., Green M.L.H., Topics in catalysis 22 (2003) 345-358
6) Basini L.E., Guarinoni A., Ind. Eng. Chem. Res., 52 (2013) 17023-17037
7) Rostrup-Nielsen J.R., Proceedings of the NATO ASI Springer, Dortrecht (2005), p.3
8) Kado S., Imagawa K., Kiryu A., Yagi F., Minami T., Kawai H., Kawazuishi K., Tomishige K., Nakamura A., Suehiro Y.; Catal. Today 171 (2011) 97-103
9) Lyubovsky M., Roychoudhury S., LaPierre R.; Catal. Lett. 99 (2005)
10) Colket M.B., Keaten A.S., Sangiovanni J.J., Zabielaki M.F., Pandy D.R.,seery D.J. Patent number 5235804 (1993)
11) Rostrup-Nielsen J.R. Springer-Verlag, Berlin, Heidelberg, New York, 5 (1984) 1-117
12) Rostrup-Nielsen J.R. Cat. Today 145 (2009) 72-75
13) Higman C., Topsoe Catalysis Forum (1996) www.topsoe.com/sitecore/shell/Applications/~/media/PDF%20files/Topsoe_Catalysis_Forum/2006/Higman.ashx
14) Bakkerud P.K., Cat. Today 106 (2005) 30-33
15) Stitt E.H. Proceedings of the NATO ASI, Springer, Dortrecht (2005) p. 185
16) GF Froment, KB Bischoff, J De Wilde (1990).
17) Ewan, B.C.R., Allen, R.W.K., Int. J. Hydrogen Energy 30 (2005) 809 - 819.
18) Bromberg, L., Cohn, D.R., Rabinovich, A., Alexeev, N., Int. J.Hydrogen Energ. 24 (1999) 1131-1137.
19) O'Brien, C.J., Hochgreb, S., Rabinovich, A., Bromberg, L., Cohn, D.R., Proceedings of the Intersociety Energy Conversion Engineering Conference, USA, (1996) 1747-1752.
20) Holladay J.D., Hu J., King D.L., Wang Y., Catal. Today 139 (2009) 244-260.
21) Ullman's Encyclopedia of Industrial Chemistry, Gas production, Wiley-VCH, Verlag Gmbh £ Co., 2002.
22) Rostrup-Nielsen J. R., Phys. Chem. Chem. Phys., 3 (2001) 283-288.
23) Barroso-Quiroga M. M., Castro-Luna A. E., Int. J. Hydrogen Energ. 35 (2010) 6052-6056

24) Energy Information Administration, Annual Energy Review 2006 (2007)
25) Mark, M.F., Maier, W. F. J. Catal. 164 (1996) 122-130.
26) Wang H.Y., Ruckenstein E., Appl. Catal. A, 204 (2000) 143-152
27) Hou Z., Chen P., Fang H., Zheng X., Yashima T., Int. J. Hydrogen Energ. 31 (2006) 555-561
28) Ferreira-Aparicio P., Fernandez-Garcia M., Guerrero-Ruiz A., Rodriguez-Ramos I., J. Catal. 190 (2000) 296-308
29) Pelletier L., D.S. Liu, Appl. Catal. A 317 (2000) 293-298
30) Arbag H., Yasyerli S., Yasyerli N., Dogu G., Int. J. Hydrogen Energ. 35 (2010) 2296-2304
31) Nagaoka K., Seshan K., Aika K., Lercher J. A., J. Catal. 197 (2001) 34-42
32) Surendra K.C., Takara D., Hashimoto A. G., Khanal S. K., Renew. Sust. Energ. Rev. 31 (2014) 846-859.
33) Kohn M.P., Castaldi M.J., Farrauto R.J., Appl. Catal. B. 144 (2014) 353-361
34) Brungs A. J., York A. P.E., Claridge J. B., Márquez-Alvarez C., Green M. L.H., Catal. Lett. 70 (2000) 117-122
35) Araujo G. C., Lima S. M., Assaf J. M., Peña M. A., García Fierro J. L., Rangel M., Catal. Today 133-135 (2008) 129-135
36) Sierra Gallego G., Batiot-Dupeyrat C., Barrault J., Florez E., Mondragon F., Appl. Catal. A 334 (2008) 251-258
37) Daza C. E., J. Gallego, F. Mondragon, S. Moreno, R. Molina, 89 (2010) 592-603
38) García-Diéguez M., Pieta I.S., Herrera M.C., Larrubia M.A., Alemany L.J. , J. Catal. 170 (2010) 136-145
39) Rostrup-Nielsen J. R.; Catal. Rev. 46 (2004) 247-270
40) Hong J., Zhang L., Thompson M., Wei W., Liu K.; Ind. Eng. Chem. Res. 50 (2011) 4373-4380
41) Bairda B., Etemad S., Karim H., Alavandi S., Pfefferle Catal Today 155 (2010) 13-17
42) Cimino S., Russo G. , Accordini C., Toniato G., Combust. Sci. Technol., 182 (2010) 380-391
43) Enger B.C. , Lødeng R., Holmen A.; Appl. Catal. A, 346 (2008) 1-27
44) Liander H.; Trans. Faraday Soc. 25 (1929) 462
45) Padovani C., Franchetti P.; Giorn. Chem. Ind. Appl. Catal. 15 (1933) 429
46) Prettre M., Eichner Ch., Perrin M., Trans. Faraday Soc. 42 (1946) 335
47) Huszar K., Racz G., Szekely G., Acta Chim. Acad. Sci. Hung. 70 (1971) 287
48) Ashcroft A.T., Cheetam A.K., Green M.L.H, Grey C.P., Vernon P.D.F., J. Chem. Soc. (1989) 1667-1669
49) Hohn K.L., Schmidt L. D.; . Appl. Catal., A 211 (2001) 53–68.

50) Maestri, M.; Beretta, A.; Groppi, G.; Tronconi, E.; Forzatti, P.; Catal. Today 105 (2005) 709-717.
51) Giani L, Groppi G, Tronconi E., Ind. Eng. Chem. Res. 44 (2005) 4993-5002.
52) Giani L, Cristiani C, Groppi G, Tronconi E., ApplCatal B Environ 62 (2006) 121-131
53) Coleman L, Croiset E, Epling W, Fowler M, Hudgins R., Catal Lett (2009) 128-144
54) BasileF., BenitoP., FornasariG., Rosetti V., Scavetta E., Tonelli D. et al., Appl Catal B Environ 91 (2009) 563-572
55) Horn R., Williams K.A., Degenstein N.J., Bitsch-Larsen A., Dalle Nogare D.,Tupy S.A., Schmidt L.D. J. of Catal. 249 (2007) 380-393
56) Torniainen, P., Chu, X. ,Schmidt, L.D., J. Catal. 146 (1994) l-10
57) Michael BC, Nare DN, Schmidt LD. Chem. Eng. Sci. 65 (2010) 3893-3902
58) Huff M., Schmidt L. D., J. Phys. Chem. 97 (1993) 11815-11822
59) Eng C., Tallman M., Hydrocarbon Processing 87 (2008) 95-101
60) F. Cavani, N. Ballarini, A. Cericola, Catal. Today 127 (2007) 113-131
61) Bodke A, Olschki D, Schmidt LD, Ranzi E.; Science 285 (1999) 285 712-715
62) Bodke A, Henning D., Schmidt L., Bharadwaj S., Maj J., Siddall J., J. Catal. 191(2000) 62-74
63) Lange JP, Schoonebeek RJ, Mercera PDL, Van Breukelen FW.; Appl. Catal. A 253 (2005) 243-253
64) Cimino S., Donsì F., Russo G., Sanfilippo D.; Catal. Today 157 (2010) 310-314
65) Beretta A, Ranzi E, Forzatti P.; Chem Eng Sci 56 (2001) 779-787
66) R. Vincent, R. Lindstedt, N. Malik, I. Reid, B. Messenger, J. Catal. 260 (2008) 37-64
67) D. K. Zerkle, M. D. Allendorf, M.Wolf, O. Deutschmann, J. Catal. 196 (2000) 18-39
68) Donsì F, Cimino S, Di Benedetto A, Pirone R, Russo G.; Catal. Today 105 (2005) 551-559
69) Cimino S, Donsì F, Russo G, Sanfilippo D.; Catal. Lett. 122 (2008) 228-237
70) Vincent R.S., Lindstedt R.P., Malik N.A., Reid I.A.B., Messenger B.E., Proc. Com-bust. Inst. 33 (2011) 1809-1817
71) Henning D.A., Schmidt L.D., Chem. Eng. Sci. 57 (2002) 2615-2625
72) Yang B., Yuschak T., Mazanec T., Tonkovich A., Perry S., Chem. Eng. J. 135 (2008)147-152.
73) Donazzi A., Livio D., Maestri M., Beretta A., Groppi G., Tronconi E., Forzatti P., Angew. Chem. Int. Ed. 50 (2011) 3943-3946
74) Basini L., Cimino S., Guarinoni A., Russo G., Arca V., Chem. Eng. J 207-208 (2012) 473-480.
75) Hakonsen S., Walmsley J., Holmen A., Appl. Catal., A 378 (2010) 1-10
76) Beretta A., Forzatti P., Chem. Eng. J. 99 (2004) 219-226

77) Jones G., Jakobsen J. G., Shim S. S., Kleis J., Andersson M. P., Rossmeisl J., Abild-Pedersen F., Bligaard T., Helveg S., Hinnemann B., Rostrup-Nielsen J. R., Chorkendor I., Sehested J., Norskov J. K., J. Catal. 259 (2008) 147-160
78) Graf P, Mojet B, Van Ommen J., Lefferts L.; Appl. Catal. A 332 (2007) 310-317
79) Cimino S., Lisi L., Russo G., Int. J. Hydrog. Energ. 37 (2012) 10680-1689
80) Bitsch-Larsen A., Degenstein N.J., Schmidt L.D.; Appl. Catal. B. 78 (2008) 364-370
81) Bartholomew C.H.; Appl. Catal. A. 212 (2001) 17-60
82) Erley W., Wagner H., J. of Catal. 53 (1978) 287
83) Feibelman P.J., Hamann D.R.; Phys. Rev. Lett. 52 (1984) 61-64
84) Joyner R.W., Pendry J.B., Catal. Lett. 1 (1988) 1-6
85) Xie C., Chen Y., Li Y., Wang X., Song C., Appl. Catal. A 390 (2010) 210-218
86) Barbier J., Lamy-Pitara E., Marecot P.; Adv. Catal. volume 37
87) Cimino S. , Torbati R., Lisi L., Russo G.; Appl. Catal. A. 360 (2009) 43-49
88) Torbati R. , Cimino S., Lisi L., Russo G.; Catal Lett 127 (2009) 260-269
89) Cimino S., Lisi L., Russo G., Torbati R.; Catal. Today 154 (2010) 283-292
90) Fisher G. B., Rahmoeller K. M., DiMaggio C. L., Wadu-Mesthrige K., Weissman J. G., Tan E. C., Chen L., Kirwan J.E.; NAM Meeting, 2007
91) Hulteberg C. Int J Hydrog Energ 37 (2012) 3978-3992
92) Haynes DJ, Campos A, Smith MW, Berry DA, Shekahawat D,Spivey JJ. Catal Today 154 (2010) 210-216.
93) Smith MW, Berry DA, Shekhawat D, Haynes DJ, Spivey JJ. ; Fuel 89 (2010) 1193-1201.
94) Tomishige K., Miyazawa T., Kimura T., Kunimori K., Koizumi N., Yamada M., Appl. Catal. B. 60 (2005) 299
95) Tomishige K., Miyazawa T., Kimura T., Kunimori K., Catal. Commun. 6 (2005) 37
96) Kaila R.K., Gutiérrez A., Krause A.I., Appl. Catal. B 84 (2008) 324.
97) McCoy A.C., Duran M.J., Azad A.M., Chattopadhyay S., Abraham M.A., Energ. Fuel 21 (2007) 3513
98) Mundschau M.V. , Burk C. G., Gribble D. A.; Jr. Catalysis Today 136 (2008) 190-205
99) Oyama S. T., Gott T., Zhao H., Lee Y. Catal.Today 143 (2009) 94-107
100) Sun F., Wu W., Wu Z., Guo J., Wei Z., Yang Y., Jiang Z., Tian F., Li C.; Journal of Catalysis 228 (2004) 298-310
101) J. W. Wang, A. C. Johnston-Peck and J. B. Tracy, Chem. Mater., 21 (2009) 4462-4467
102) Ma D., Xiao T. C.,. Xie S. H, Zhou W. Z., Gonzalez-Cortes S. K., Green M. L. H., Chem. Mater., 16 (2004) 2697-2699

103) Alexander A., Hargreaves J. S. J., Chem. Soc. Rev. 39 (2010) 4388-4401

104) Sweeney C. M., Stamm K. L., Brock S. L. J. Alloys Compd. 448 (2008) 122-127

105) Cecilia J.A., Infantes-Molina A., Rodríguez-Castellón E., Jiménez-López A., J. Catal. 163 (2009) 4-15

106) Clark P., Oyama S.T., J. Catal. 218 (2003) 78-87

107) Sawhill S. J., Layman K. A., Van Wyk D. R., Engelhard M. H., Wang C., Bussell M. E., J. Catal. 231(2005) 300-313

108) Sawhill S. J., Phillips D. C., Bussell M.E., J. Catal. 215 (2003) 208-219

109) Montesinos-Castellanos A., Zepeda T. A., Pawelec B., Fierro J. L. G., De Los Reyes J. A. Chem. Mater. 19 (2007) 5627-5636

110) Mangnus, P. J.; Van Veen, J. A. R.; Eijsbouts, S.; de Beer, V. H. R.; Moulijn, J. A. Appl. Catal. 61 (1990) 99

111) Infantes-Molina A., Cecilia J.A., Pawelec B., Fierro J.L.G., Rodríguez-Castellón E., Jiménez-López A., Appl. Cata. A 390 (2010) 253-263

112) Wu Z., Sun F., Wu W., Feng Z., Liang C.,Wei Z., Li C., Journal of Catalysis 222 (2004) 41-52

113) Burns A. W., Layman K. A.,. Bale D. H, Bussell M. E.; Appl. Catal. A. 343 (2008) 68-76

114) Kanda Y. ,Temma C., Nakata K., Kobayashi T., Sugioka M., Uemichi Y.; Appl. Catal. A. 386 (2010) 171-178

115) Hayes J.R., Bowker J. R., Gaudette A. F., Smith M. C., Moak C. E., Nam C. Y., Pratum T. K., Bussell M. E. J. of Catal. 276 (2010) 249-258

116) Tanaka H., Uenishi M., Taniguchi M., Tan I., Narita K., Kimura M., Kaneko K., Nishihata Y., Mizuki J., Catal. Today 117 (2006) 321-328

117) Machida M., Murakami K., Hinokuma S., Uemura K., Ikeue K., Matsuda M., Chai M., Nakahara Y., Sato T., Chem. Mater. 21 (2009) 1796-1798

118) Chakrabarti R, Colby JL, Schmidt LD. Appl Catal B 107 (2011) 188-94

2. Experimental and Characterization Techniques

2.1 Catalyst Preparation

2.1.1 Powder Catalysts

Rh catalysts doped with phosphorous and supported on a 3% w./w. La_2O_3-stabilised γ-Al_2O_3 (SCFa140-L3 Sasol) were prepared in powder form by the incipient wetness co-impregnation procedure using an aqueous acid solution of $Rh(NO_3)_3$ (Aldrich) and $(NH_4)H_2PO_4$ (Aldrich). The incipient wetness impregnation method is the simplest and most direct method of deposition of the active components and was used to prepare all the powder catalysts. The object is to fill the pores with a solution of metal salt of sufficient concentration to give the correct metal loading. Drying is necessary to crystallize the salt on the pore surface, then calcination converts the salt to an oxide or metal.

Precursors were dosed at a P/Rh atomic ratio of 0.7 in order to obtain a target loading of 1.0% wt of Rh in the catalyst through 2 impregnation cycles. Following drying in stove at 120°C and calcination in air at 550°C for 2h after each impregnation step, the catalysts were finally reduced in a 2% H_2/Ar mix by heating at 10 °C min^{-1} between room temperature and 900 °C, and holding for 1h at this temperature. The excess of P with respect to the formation of Rh_2P (P/Rh = 0.5) was selected in order to maximize phosphide formation during TPR as suggested in [1]. Two reference powder samples were also prepared with the same nominal content of Rh or P by excluding either phosphorous or rhodium precursors from the impregnating solution while keeping all the rest the same.

According to their elemental composition, samples were labelled as Rh-P/LA, Rh/LA and P/LA, where LA represents the lanthanum stabilized γ-Al_2O_3. When desired, the reduced catalysts were subjected to controlled *sulphurization* in a fixed bed quartz reactor at 800°C for 1h under a flow of H_2S/H_2 (20ppm/1.8%, balance N_2) at atmospheric pressure, and then exposed to air at room temperature.

Catalysts in powder form, fresh, reduced and sulphurized, were prepared to be used in the characterization experiments.

During the period spent as a visiting scientist at the Chemistry Department of Technical University in Munich (TUM- Technische Universität München), a Rh catalyst (1% wt.) doped with phosphorous and supported on a 3% w/w La_2O_3-stabilised-Al_2O_3 (SCFa140-L3 Sasol) labeled Rh-P/LA_T, with identical nominal composition as the sample above described (Rh-P/LA), was ri-prepared via an incipient wetness co-impregnation procedure using an aqueous acid solution of

$Rh(NO_3)_3$ (Aldrich) and $(NH_4)_2HPO_4$ (Aldrich). Following drying overnight at 110 °C and calcination in air at 550 °C for 2 h, the catalyst was finally reduced in H_2 by heating at 10 °C/min between room temperature and 900 °C, and holding for 1 h at this temperature. A reference powder sample was also prepared with the same nominal content of Rh by excluding phosphorous precursor from the impregnating solution (Rh/LA_T). A few differences can be noted in the preparation methods followed for the synthesis of the Rh-P/LA_T and Rh-P/LA catalysts with identical nominal composition: i) precursor of phosphorous, using $(NH_4)_2HPO_4$ for Rh-P/LA_T instead of NH_4H2PO_4 as described for Rh-P/LA, ii) number of impregnation cycles, limited to 1 for the catalysts prepared at TUM and 2 for the others, iii) reduction step at high temperature carried out in pure H_2 for TUM samples while in a 2%H_2/Ar mixture in the other case (keeping the same flow rate (i.e. 50 cm^3/min)). However, the main discrepancy between the two preparation routine lies into the phosphorous precursor, which perhaps affected the dispersion of metal particles on the support, as it will be shown later.
Both Rh-P/LA_T and Rh-P/LA were devoted to Dry reforming reaction of methane.

2.1.2 Monolith catalysts

Commercial cordierite monoliths (NGK) with a cell density of 600 cpsi were cut in the shape of disks (L=10 mm, D=17mm) and washcoated with La_2O_3-stabilised γ-Al_2O_3 (S_{BET}=140 m^2/g) using a modified dip-coating procedure [2]. The high surface area washcoat was selected in order to improve the noble metal dispersion and stabilize metal particles against sintering and migration during high temperature operation The samples were dipped in a slurry (20% wt of solid) of finely grounded La_2O_3 stabilised γ-Al_2O_3 powder, diluted nitric acid solution and Disperal (Condea). Following each coating the excess slurry was removed by blowing air through the channels, after which the samples were dried at 120 °C and then calcined in air at 550 °C for 2 h. The process was repeated nine times in order to achieve a washcoat loading of approximately 30% (w/w) with respect to the initial weight of the monolith sample, after which the samples were finally calcined in air at 800 °C for 3 h.
Phosphorous doped Rh based monoliths were prepared to test them during CPO of methane, while standard Rh and Pt structured catalysts were exploited for CPO of ethane.

Rhodium with a target loading of ~1% (w/w) and phosphorous with a loading of 0.2% (w/w) (atomic ratio P/Rh= 0.7) with respect to the active washcoat layer were dispersed onto the coated monoliths by co-impregnation cycles using an aqueous solution of $Rh(NO_3)_3$ (Aldrich) and

$NH_4H_2PO_4$ (Aldrich). After each cycle the excess solution was removed by gently blowing with compressed air, the monolith samples were dried at 120 °C and then calcined in air at 550 °C for 2 h. Finally, monoliths were reduced in 20% H_2/N_2 flow up to 900°C. The final loading of active phase (Rh-P/LA) applied on the honeycombs was 0.11 g/cm^3, corresponding to a nominal average thickness of the washcoat of ca. 20 µm.

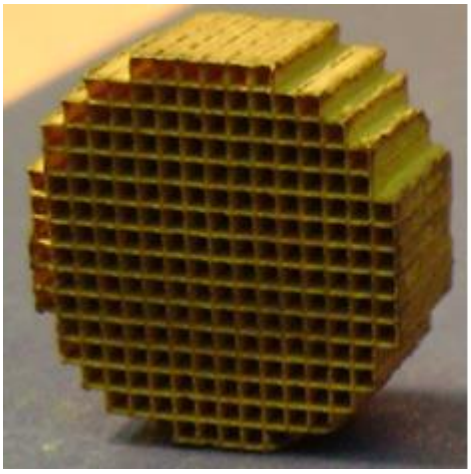

a)

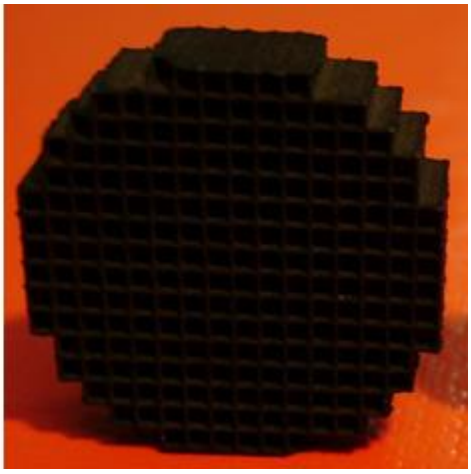

b)

Figure 1: Monoliths after calcination at 550°C (a) and reduction at 900°C (b).

Standard supported Rh and Pt catalysts (respectively 1 and 2% by weight of the alumina, in order to obtain similar atomic concentrations) were prepared via repeated incipient wetness impregnations onto washcoated monoliths using an aqueous solution of $Rh(NO_3)_3$ or H_2PtCl_6(Aldrich). The catalysts were dried at 120 °C and calcined in air at 550 °C for 3 h after each impregnation (4 cycles). Finally they were conditioned directly under CPO reacting atmosphere until stabilisation of catalytic performance.

2.2 Catalytic testing

2.2.1 Catalytic Partial Oxidation of methane

P-doped Rh/La-Al_2O_3 honeycomb catalysts were tested for the CPO of methane to syngas in a lab scale reactor operated at nearly atmospheric pressure under self-sustained short contact time conditions using (simulated) air as oxidant. The catalytic honeycomb was stacked between two mullite foam monoliths (45 ppi, L=12 mm) as heat shields and placed in a quartz tube inserted in an electric furnace that was used for pre-heating (fixed at 235°C). High-purity gases (CH_4, O_2, N_2, SO_2 208 ppm in N_2) calibrated via Brooks 5850-MFCs, were pre-mixed and fed to the reactor at a total flow 135 Sl/h, corresponding to a gas hourly space velocity GHSV = 8*104 h^{-1} (based on the empty volume of the honeycomb). The impact of sulphur addition (2-58 ppmv SO_2) was investigated at fixed CH_4/O_2 feed ratio = 2 (stoichiometric for syngas production), under both transient and steady state conditions, by partially substituting the N_2 flow in the feed with an equal flow of the SO_2 in N_2 mix. Reactor temperatures were measured by means of K-type thermocouples (d=0.5mm) placed in the middle and at the exit of the central channel of the catalytic honeycomb (Tcat and Tout), as well as in the gas downstream of heat shield.

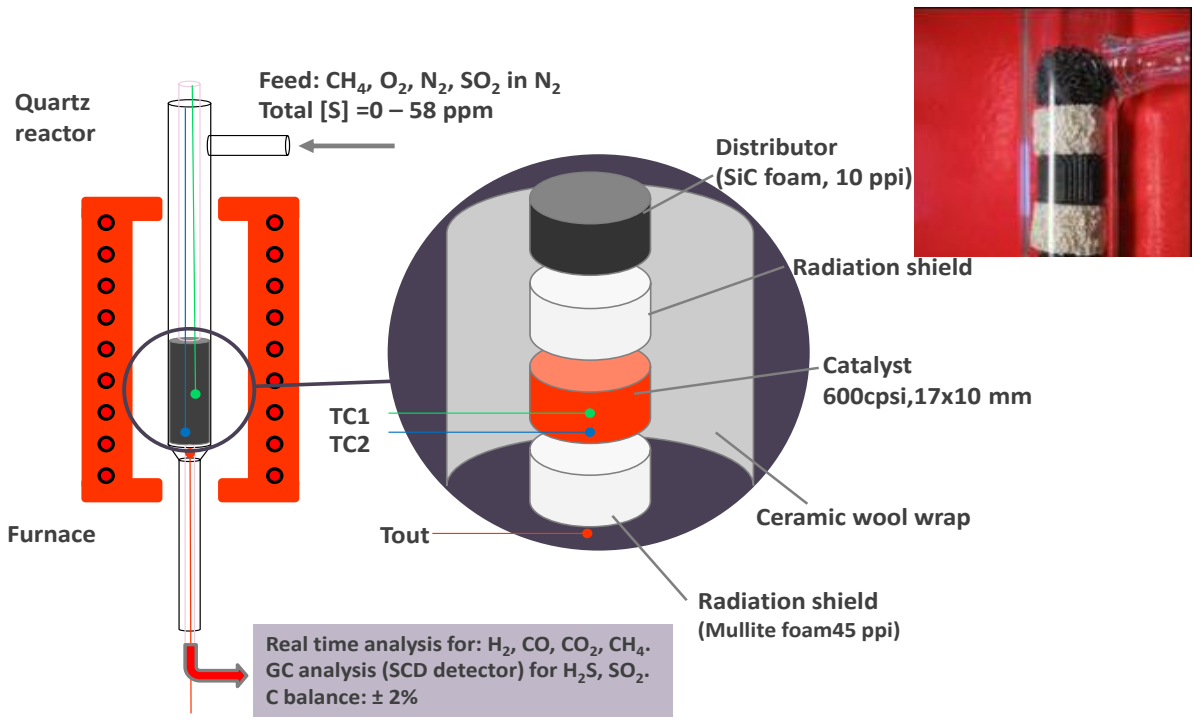

Figure 2: CPO experimental apparatus.

Hot product gases passed through a condenser and a $CaCl_2$ trap to remove water, and a continuous analyzer (syngas GEIT) was employed to measure the concentrations of CO, CO_2 and CH_4 (ND-IR), O_2 (ECD), and H_2 (TCD, with cross sensitivity corrections). O_2 was always completely converted under steady state operation as well as during transient addition/removal of S to the feed. H_2O production was calculated from the O-balance. Carbon and hydrogen balances were closed within ±1% and ±2%, respectively. Methane conversion, yields and selectivities to CO and H_2 were calculated according to the following definitions based on measured dry mol fractions:

$$x_{CH4} = 100\left(1 - \frac{{CH_4}^{out}}{{CH_4}^{out} + {CO_2}^{out} + {CO}^{out}}\right)$$

$$Y_{CO} = 100\left(\frac{{CO}^{out}}{{CH_4}^{out} + {CO_2}^{out} + {CO}^{out}}\right)$$

$$S_{CO} = 100\frac{Y_{CO}}{x_{CH4}}$$

$$Y_{H2} = \frac{100}{2}\left(\frac{{H_2}^{out}}{{CH_4}^{out} + {CO_2}^{out} + {CO}^{out}}\right)$$

$$S_{H2} = 100 \times 2\frac{Y_{H2}}{x_{CH4}}$$

The fate of sulphur was determined by gas chromatography employing a high sensitivity dual plasma sulphur chemiluminescence detector (SCD, Agilent) and a GasPro column. It was confirmed that under the typical CPO operating conditions, i.e. high H_2 partial pressure and high temperatures (> 700 °C), all of the sulphur is transformed into H_2S (with traces of COS), in agreement with thermodynamic predictions [3].
Equilibrium calculations with constant enthalpy and pressure were performed using CHEMKIN 4.1.1 software excluding solid carbon formation, which was never observed experimentally.

2.2.2 Catalytic Partial Oxidation of ethane

The CPO of ethane was studied under self-sustained pseudo-adiabatic conditions in the same experimental setup previously described. The impact of sulphur addition (up to 58 ppm) was studied at two different C_2H_6/O_2 ratio, respectively 1 and 2, the former stoichiometric for syngas

production and the latter for the ethylene formation. The CPO performance with sulphur addition was investigated under both transient and steady state operation.

Product gases were splitted to a continuous syngas analyzer (GEIT), employed to measure concentrations of CO, CO_2 and CH_4 (ND-IR), O_2 (ECD), H_2 (TCD, with cross sensitivity corrections) and an on line GC equipped with a GasPro 0.32 mm × 30 m column (Agilent) and a FID, optimized to measure C_2H_6, C_2H_4, C_2H_2, CH_4,C_3H_8, C_3H_6 and other eventual hydrocarbons up to C_4. Also during CPO of ethane, O_2 was always completely converted under steady state operation as well as during transient addition/removal of S to the feed. Carbon and hydrogen balances were always closed within ±1.5% by measuring the total flow rate of dry products.

2.2.3 Dry reforming of methane

Dry reforming of methane was studied under atmospheric pressure in a fixed-bed vertical steel reactor containing an alumina tube (inner diameter 5 mm) which was operated in a down flow mode. In the reactor, the pelletized catalyst ($d_{particles}$=500-710 μm) was held on a quartz wool bed and a thermocouple was placed outside of the reactor to control the oven temperature.

The pretreatment of the catalyst in situ was carried out by increasing the temperature from room temperature to 850 °C at a rate of 5 °C/min in a H_2 / N_2 flow (100 ml/min) without holding at 850°C. After reduction, the feed gases (CH_4/CO_2/N_2 = 1/1/2) were introduced into the catalyst bed at a flow rate of 100 ml/min, which for a 50.0 mg catalyst corresponds to a space velocity of $1.2*10^5$ ml/(h g).

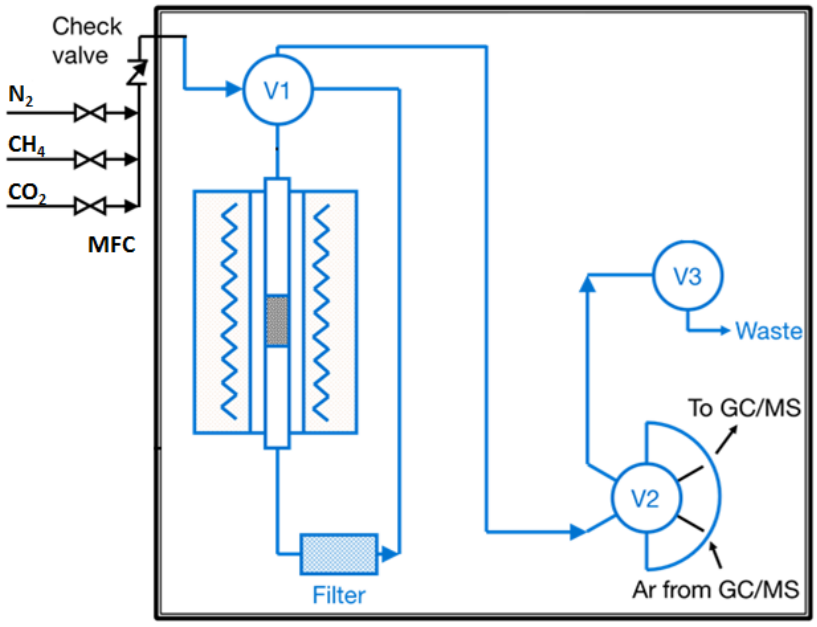

Figure 3: Dry reforming experimental apparatus.

Dry reforming was used as a model reaction to test the effect of P doping by directly comparing the results obtained over doped and undoped on Rh catalysts tested under identical conditions for more than 16 hours on stream, under severe temperature conditions and taking account of probable coke formation.

The reactants and products were analyzed with an on-line gas chromatograph GC-2010 Plus by Shimadzu (including FID and TCD detectors) equipped with a HP-Plot-Q capillary column (for CO_2 and H_2O) and HP-plot Molesieve (for H_2, N_2, CH_4 and CO). In order to satisfactorily separate the products, the temperature setting inside the GC columns was programmed varying with time. In the first 4.5 min, the temperature was constant at 50°C, it was then increased steadily by the rate of 10°C per min until 150°C. Finally, the temperature was decreased to 50°C. The analytical method applied is an internal standardization in which the peak area is related to the molar concentration through the response factor (RF):

$$RF = \frac{mole\ fraction}{peak\ area}$$

Mass balances ranged between -0.5% and 3% for carbon, and from -0.5% to 1.5% for hydrogen.

Methane and carbon dioxide conversion were calculated according to the following definitions based on measured mol fractions:

$$CH_4 conversion\ (\%) = \frac{moles\ {CH_4}^{in} - moles\ {CH_4}^{out}}{moles\ {CH_4}^{in}} x\ 100$$

$$CO_2 conversion\ (\%) = \frac{moles\ {CO_2}^{in} - moles\ {CO_2}^{out}}{moles\ {CO_2}^{in}} x\ 100$$

$$\frac{H_2}{CO} ratio = \frac{moles\ of\ {H_2}^{out}}{moles\ of\ CO^{out}}$$

The reaction equilibrium compositions were calculated using the HSC software.

2.3 Catalyst characterization techniques

A variety of well-known techniques have been utilized to characterize the catalysts synthesized and a brief description of those used in this thesis is presented in the following section.

BET specific surface area measurements were performed with a Quantachrome Autosorb 1-C by N_2 adsorption at (-196°C). The powder sample of approximately 0.2 grams was first loaded into a round bottom sample tube, dried and degassed at 150 ºC under vacuum for about 2 hours and then cooled to liquid nitrogen temperature (-196 ºC) by immersing the sample tube into liquid nitrogen. Desorption followed adsorption in pore distribution measurements. The equipment automatically measured, recorded and calculated nitrogen adsorption at various pressures. In the case of honeycomb catalysts the surface area was assigned only to the active washcoat layer (SA of cordierite substrate ≤ 1 m^2/g).

Elemental content was quantitatively determined on selected fresh and used catalysts by inductively coupled plasma spectrometry (ICP) on an Agilent 7500 ICP-MS instrument, after microwave-assisted digestion of samples in nitric/hydrochloric acid solution.

The active metal surface area and metal dispersion (i.e. fraction of active metal atoms on the catalyst surface) of the catalysts were determined by CO chemisorption measurements using a Quantachrome Autosorb 1-C equipment. Rh catalysts and their corresponding alumina supports (200 mg) were pre-treated at 400°C under a flow of pure H_2 for 1 h in order to obtain surfaces reasonably free from impurities [4], then evacuated for 2h at the same temperature and cooled under vacuum to 40°C, where CO adsorption was performed using the method of the double isotherm [4] with an intermediary treatment under vacuum (P= 0.001 mmHg).
Pretreatment and operating conditions are determining for the subsequent chemisorption and it is essential to define a procedure likely to give reproducible and reliable results [4].The first isotherm gives the total amount of chemisorbed CO, the second isotherm gives the reversible part of chemisorbed CO, the difference between the two isotherms giving the irreversible part of chemisorbed CO. The two isothermal curves were drawn with 5–10 experimental points in the 20–800 mmHg pressure domain. The total and reversible adsorption curves did not always exhibit a saturation plateau; the monolayer CO chemisorption was obtained from the extrapolation at zero pressure of the linear part of the irreversible strong adsorption [4]. Since CO may adsorb on Rh in several forms (linear, bridged, di-carbonyl species) [4-7] mainly depending on metal dispersion,

type of support and catalyst pre-treatment, the adsorption stoichiometry (CO/M) is not known a-priori, and it was assigned by the corresponding DRIFTS study.

Temperature-programmed reduction (TPR) is among the most commonly used techniques for catalyst characterization, it provides information on the reducibility of metal oxides. The reduction of a metal oxide MOn by hydrogen to its metallic form is described by equation (2.1).

$$MO_n + nH_2 \rightarrow M + nH_2O \quad (2.1)$$

In this work TPR experiments were carried out with a Micrometrics AutoChem 2020 equipped with a TC detector on catalysts and supports pre-treated in air at 550°C. The sample powder (200-400 mg) was heated at 10 °C min^{-1} between room temperature and 900 °C in flowing 2% H_2/Ar mix (50 cm^3/min). The exit gas from the reactor was passed through a cold trap (isopropanol cooled by liquid nitrogen) to remove any water formed during the experiment.

Thermogravimetric analysis of uncalcined powder samples were run in Perkin Elmer Pyris TGA by ramping up to 900°C at 10 °C min^{-1} in flowing air or 2% H_2/N_2 mixture. Gaseous products, sampled via a heated transfer line, were analyzed with a FTIR spectrometer (Perkin Elmer Spectrum GX) in a gas cell recording spectra every 1 minute using PE TimeBase software.

XRD (crystallographic analysis) was performed on powder samples with a Bruker D2 Phaser diffractometer (operated at diffraction angles ranging between 10 and 80° 2θ with a scan velocity equal to 0.02°2θ s^{-1}).

Scanning electron microscopy (SEM) was carried out on honeycomb catalysts with a FEI Inspect microscope equipped with an energy dispersive X-ray (EDX) probe.

Infrared spectroscopy (IR) is one of the most important tools in catalysis research and has been a workhorse technique for materials analysis in the laboratory for many decades [8]. The two most frequently used IR techniques for catalyst characterization are transmission infrared and diffuse reflectance spectroscopy [8].

IR spectroscopy of adsorbed carbon monoxide [9] is a well-known technique for the characterization of metal surfaces in the cases of both bulk and supported metal catalysts. The spectroscopy of the surface carbonyl species formed upon CO adsorption allows us to have information on the state and the nature of the adsorbing metal species [10]. This technique has been widely applied to supported Rh catalysts [11].

Diffuse reflectance is, by definition, that process in which the angle of reflection is different from the angle of incidence. In the diffuse reflectance mode, samples can be measured as loose powders instead of self-supported wafers. DRIFTS is a common technique that collects and analyzes scattered IR energy. When a beam of infrared radiation impinges onto a fine particulate material it essentially undergoes reflection in one of several ways. It can undergo reflection, refraction, scattering absorption to a varying degree, before re-emerging as diffuse reflectance (Figure 2.3).

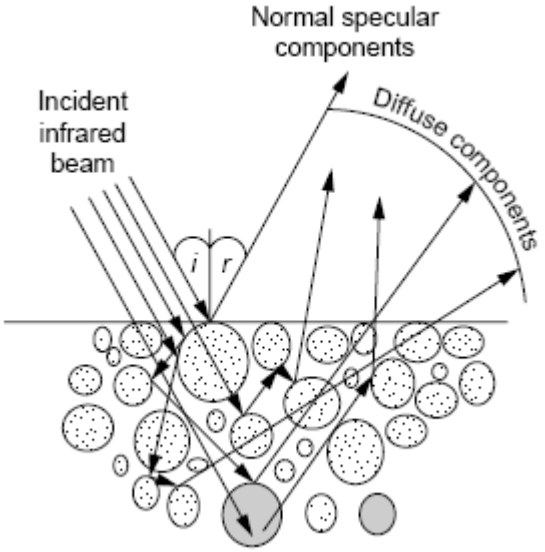

Figure 4: Interaction of IR beam on a powdered sample.

On these bases, in this work, the nature of metal species was investigated by diffuse reflectance infrared Fourier transform spectroscopy (DRIFTS) using CO as a probe molecule. DRIFTS experiments were performed in a PerkinElmer Spectrum GX spectrometer equipped with a liquid-N2 cooled MCT detector with a spectral resolution of 4 cm^{-1} and averaged over 50 scans. For each experiment approximately 30 mg of finely ground powder sample was placed into the ceramic cup of a commercial PIKE Diffuse-IR cell equipped with a heat chamber (Fig.5) which allows the sample to be heated from room temperature up to 900°C within the chamber. Any temperature can be set between this range and can be controlled automatically. The environment within the chamber can be inert gas, vacuum, reaction mixture etc. in order to create various measurement conditions. Inserting and changing samples is easily accomplished by opening and closing the screw cap which holds the ZnSe window. The cell is also equipped with an internal cooling system, which prevents excessive heating of the sample compartment. Samples can be loaded into either a ceramic or stainless steel sample cup. Reactants are introduced in the cell through a 1-mm (i.d.) pipeline and released close to the sample.

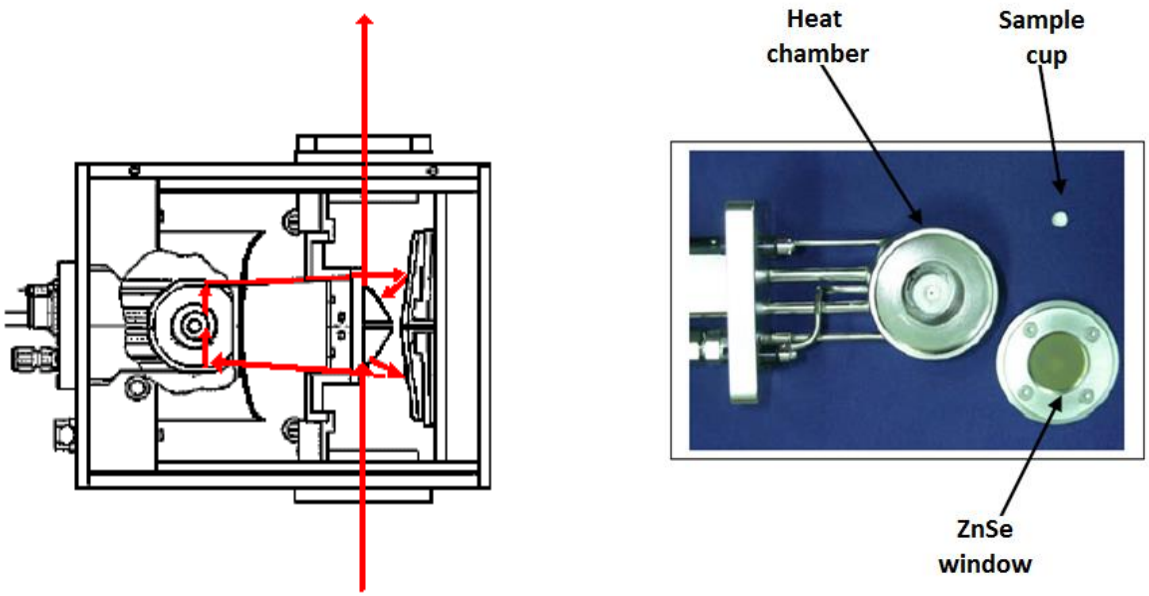

Figure 5: Schematic representation of the Diffuse Reflectance attachment and the heat chamber.

The sample was treated following similar steps, where possible, to those used before quantitative CO chemisorption: (i) prior to the experiments it was reduced in pure H_2 for 1 hour at 400°C, purged with Ar (100 cm^3/min) for about 60 min and then cooled down to 40°C under the same flow before a background spectrum was recorded; (ii) CO was adsorbed at this temperature by flowing a 5% CO/N_2 mixture (100 cm^3/min) for 60 minutes. IR spectra were recorded both under CO flow and during prolonged flushing with Ar (100 cm^3/min). All spectra were ratioed against the corresponding background spectra collected on the adsorbate-free sample at 40°C.
Sulphurization of catalysts was performed in the same cell: the sample was heated up to 800°C under a 2% H_2/N_2 flow, followed by exposure to $H_2S/H_2/N_2$ mixture (20ppm/1.8%/rest, 200 cm^3/min) for 1h, and then purged and cooled down under Ar flow, before CO adsorption. The effect of regeneration of sulphurized catalysts by reduction at 400 °C under a H_2 flow for 1h (and purging at the same temperature) was also investigated.

The catalysts prepared at TUM, were in part therein characterized. The BET surface areas were determined by N_2 adsorption at (-196°C) using a Sorptomatic 1990 Series instrument after the activation of the sample in vacuum at 300°C for 2 h. Elemental analyses were performed by the Microanalytical Laboratory of TUM using an Atomic Absorption Spectrometer AAS 280FS (Varian).
The fraction of accessible Rh atoms was determined by H_2 chemisorption using a Sorptomatic 1990 Series instrument. Approximately 0.1 g of catalyst was pretreated in H_2 at 300°C for 1 h, followed by outgassing in vacuum at 35°C for 2 h. The sorption isotherms were measured at 35°C. The

amount of chemisorbed hydrogen was obtained after removing physisorbed hydrogen from the sample by evacuation at 35°C for 2 h. The metal dispersion was determined by extrapolating the differential isotherm to zero H_2 pressure by assuming H/Rh ratio of 1. The particle sizes of Rh were calculated by the relationship between dispersion and crystallite size assuming spherical particles.

The dispersion results obtained at TUM laboratories with H_2 chemisorption were compared with those achieved on the same samples by CO chemisorption performed in a Quantachrome Autosorb 1-C instrument, as described above.

TEM images were measured on a JEM-2010 Jeol transmission electron microscope operating at 120 kV. Prior to the measurements, catalyst was ground, suspended in ethanol, and dispersed by ultrasonic treatment. The dispersion was dropped on a copper grid-supported carbon film.

References

1) Hayes J. R., Bowker R. H., Gaudette A. F., Smith M. C., Moak C. E., Nam C. Y., Pratum T. K., Bussell M. E. J. of Catal. 276 (2010) 249-258
2) Cimino S., Landi G., Lisi L.,Russo G., Catal. Today 117 (2006) 454-461
3) Bitsch-Larsen A., Degenstein N.J., Schmidt L.D.; Appl. Catal. B. 78 (2008) 364-370
4) Perrichon V., Retailleau L., Bazin P., Daturi M., Lavalley J.C., Appl. Catal., A 260 (2004) 1-8
5) Maroto-ValienteA., Rodriguez-RamosI., Guerrero-RuizA., Catal. Today 93–95 (2004) 567-574
6) RaskóJ., BontovicsJ., Catal. Lett. 58 (1999) 27-32
7) TrautmannS., BaernsM., J. Catal. 150 (1994) 335-344
8) Lercher J.A., Grundling C., Eder-Mirth G., Catal. Today 27 (1996) 353
9) Lear, T.; Marshall, R.; Lopez-Sanchez, J. A.; Jackson, D. D.; Klapotke, T. M.; Baumer, M.; Rupprechter, G.; Freund, H.-J.; Lennon, D. J. Chem. Phys. 123 (2005) 174706
10) FinocchioE., BuscaG., ForzattiP., GroppiG., BerettaA., Langmuir 23 (2007) 10419-10428
11) Hadjiivanov K. I., Vayssilov G. N., Adv. Catal. 47 (2002) 307-511

3. Effect of Phosphorous doping on Rh catalysts during the Catalytic Partial Oxidation and Dry Reforming of methane

3.1 Introduction

3.1.1 Sulphur tolerance of a P-doped $Rh/\gamma Al_2O_3$ catalyst during the partial oxidation of methane to syngas

The catalytic partial oxidation (CPO) of methane over noble metal catalysts represents an attractive way to obtain syngas (CO and H_2) in autothermal reactors at very short contact times (10^{-2} to 10^{-4} s) and high selectivity to syngas [1-2]. Rh-based systems are the best performing catalysts in terms of both activity and selectivity [1-2]. Recently the possible poisoning effects of sulphur on the costly Rh catalysts was recognized as a serious issue. Poisoning is due to the adsorption of S onto Rh active sites causing a (reversible) suppression of their steam reforming activity, with an associated risk of catalyst overheating during CPO autothermal operation [3-5]. In recent studies on the effect of several inorganics on methane steam reforming activity of $Rh/\gamma Al_2O_3$ catalysts poisoned ex situ, Schmidt and co-workers [6] reported that sulphur decreased the methane conversion the most, followed by phosphorus. Even if phosphorous is recognized as a common poison for metal catalysts [6,7], a substantial body of literature has shown that metal phosphide catalysts have promising hydrodesulphurization (HDS) properties [8-15]. For example Rh_2P/SiO_2 catalysts readily obtained by reduction of oxide precursors [27-28]have displayed superior activity, and sulphur tolerance than the corresponding supported Rh catalyst (either sulphided or not) during deep HDS [16-17]. The authors concluded that the presence of P in the Rh_2P particles improved their resistance to S-poisoning inhibiting the irreversible adsorption of S at the particle surface as well as the incorporation of S into the bulk (i.e. to form Rh sulphide) [16]. The main purpose of this chapter is the investigation of the possible beneficial effect of P-doping of Rh supported on La-γ-Al_2O_3 on the catalytic performance and particularly on its S-tolerance during the self-sustained methane CPO at short contact time.

3.1.2 Dry reforming of methane over a P-doped Rhodium catalyst

During a six-month period spent as a visiting scientist at the Chemistry Department of Technical University in Munich (TUM- Technische Universität München), a P-doped Rh catalyst therein prepared has been tested in the dry reforming reaction.

$CH_4 + CO_2 \leftrightarrow 2\ CO + H_2$, $\quad \Delta H_r^{298K} = +247$ kJ/mol (3.1)

The DRM reaction has been getting increasing interest from academic and industrial point of views in the past few years since it provides a syngas with a low H_2/CO ratio (≤1) suitable for downstream

processes towards chemicals and synthetic fuels. Moreover it involves utilization of CH_4 and CO_2 which are two major greenhouse effect gases contributing to global warming [18-21]; thus, the utilization of these reactants in many chemical processes could drastically improve the quality of the environment [22]. Although the environmental benefits and economic a↔dvantages presented by dry reforming, there are only a few commercial processes based on this reaction (i.e., the CALCOR [23] and SPARG [24] processes). The success of the concept is highly dependent on the catalyst activity and selectivity. From an industrial point of view, it is more practical to develop and optimize Ni-based catalysts as their relative low cost. A major limitation that arises from the use of nickel is the formation of carbon deposits, which can cause significant deactivation of the catalyst. Coke is mainly produced via methane (CH_4) decomposition (3.2) and Boudouard (CO disproportionation) reactions (3.3) which are thermodynamically feasible.

$CH_4 \leftrightarrow C + 2H_2$, ΔH_r^{298K} = +75 kJ/mol (3.2)

$2CO \leftrightarrow C + CO_2$, ΔH_r^{298K} = -172 kJ/mol (3.3)

Several authors [20,25-26] presented calculations to predict thermodynamic potential of carbon deposition as a function of operating conditions suggesting operation for the DRM reaction at higher temperature, ~727°C, and with CO_2/CH_4 ratios far above unity to avoid regions where there is a potential for carbon formation. However, to avoid such severe conditions, different studies have been performed to develop a catalyst which incorporates a kinetic inhibition of carbon formation with CO_2/CH_4 ratios near unity [27-28]. Rostrup-Nielsen and Hansen [27] reported that the amount of carbon deposited on metal catalysts decreases in the order Ni >> Rh > Ir = Ru > Pt ≈ Pd at 773 K and Ni > Pd = Rh > Ir > Pt >> Ru at 923 K. Hence, the noble metal catalysts exhibit higher selectivity and much less carbon deposition than the nickel catalyst. According to Zhang et al [28], the specific activity of Rh catalysts was found to be strongly sensitive to the particle size, decreasing as the metal size increased. As regards Rhodium based catalysts, recently Schmidt and his coworkers [6], as already reported, observed a poisoning impact of phosphorous on this noble metal beside sulphur, although in a less extent, during steam reforming of methane performed on 2.5 wt% $Rh/\alpha Al_2O_3$ spheres. In particular they found that a fraction of spheres appeared black due to coke deposition after a test of 5 hours, attributing this phenomenon to the presence of phosphorous. Since dry reforming is a reaction which potentially leads to carbon deposition requiring an active and stable catalysts, it has been exploited as a model reaction for phosphorous addition to Rh catalysts. In view of the negative results obtained by Chakrabarti et al. with this kind of systems, P doped Rh samples were prepared at TUM following a similar procedure utilized to prepare Rh-P/LA destined to CPO, and they were tested during dry reforming of methane ($CH_4/CO_2/N_2$=1/1/2) at 850°C and atmospheric pressure, focusing on the role of phosphorous on

the noble metal activity and deactivation. In other words, these experiments have been carried out to further confirm the good results achieved with the novel active phase tested during the CPO of methane related to the higher dispersion of the materials containing phosphorous and good interaction achieved between noble metal and dopant, on the contrary of the previous cited findings that marked phosphorous as a poison.

3.2 Experimental Procedure

As regards the experiments of CPO of methane in the presence of sulphur, the P-doped Rh/La_2O_3-Al_2O_3 (Rh-P/LA) and the two reference catalysts (excluding either phosphorous or rhodium, Rh/LA and P/LA) were prepared by the incipient wetness impregnation method as described in Chapter 2.1.1. The catalytic tests were carried out on monolith samples as reported in Chapter 2.2.1. Catalysts were characterised by techniques described in Chapter 2.3.

Rh-P/LA_T and Rh/LA_T were prepared by the incipient wetness impregnation method as described in Chapter 2.1.1 and tested in DR of methane as reported in Chapter 2.2.1.

3.3 Results and Discussion

3.3.1 Characterization of Rh catalysts for CPO of methane

Table 1 illustrates catalysts denomination and final pre-treatment, loading of active phase in honeycombs, elemental composition and BET specific surface area.

	Pretreatment	Loading g/cm^3 [a]	Rh	P	La	BET m^2/g [b]
			w/w % [b]			
LA	As received		-		2.6	143
P/LA	TPR 900°C		-	0.3	2.6	139.8
Rh-P/LA	TPR 900°C		0.98	0.19	2.7	130.6
Rh/LA	TPR 900°C		0.9	-	2.6	122.2
Honeycombs						
Rh-P/LA	TPR 900°C	0.11	0.99	0.2		122.6
	Aged in CPO	0.11				112.5

a) Weight of active washcoat per unit volume of honeycomb catalyst
b) With respect to the weight of active catalyst (cordierite substrate excluded)

Table 1: Denomination of catalysts and supports, final pre-treatment, honeycomb loading, elemental composition and BET surface.

The effect of calcination and reductive pretreatment on the weight change of bulk mono basic ammonium phosphate and impregnated on the La-γ-Al_2O_3 (LA) support , is illustrated in Figure 1.

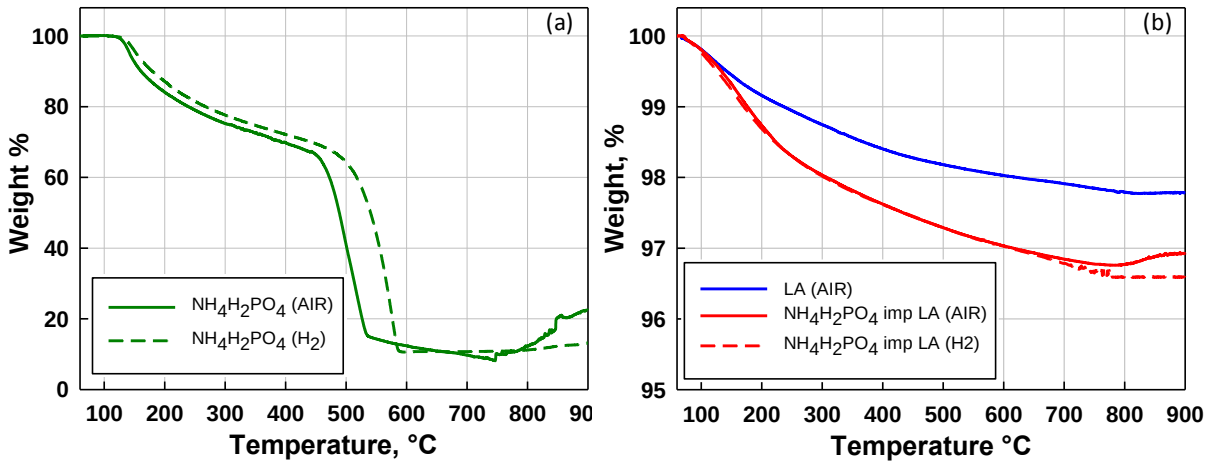

Figure 1: Weight loss curves for bulk ammonium mono basic ammonium phosphate (a) and impregnated on the La-γ-Al_2O_3 (LA) support (b). Heating rate 10 °C/min under flowing air or 2%H_2/N_2 mixture. The reference curve for LA is also reported. Nominal P content in the impregnated LA sample was ca. 5 times larger than in the Rh-P/LA catalyst.

These preliminary thermogravimetric analysis of the ammonium phosphate precursor (Fig. 1a) confirmed that its decomposition in air proceeded in 2 main steps: roughly 30% of the initial weight was lost in the temperature range from 130 to ca. 400°C corresponding to the evolution of ammonia and water; the remaining phosphorous oxide was quickly and completely devolatilized above 430°C [29]. A similar behaviour was observed when heating in H_2/N_2 flow, with an increase in this critical temperature by 50-60°C. In contrast, TGA profiles of the LA alumina support impregnated with the same phosphorous precursor (Fig. 1b), indicated that no significant loss of phosphorous occurred when heating up to 900°C (in air or H_2/N_2) due to the strong interaction with alumina and possible formation of superficial amorphous aluminium or lanthanum phosphate [10], which, however were not detected by XRD analysis (see fig.4).

Accordingly, the amount of elemental phosphorous found by ICP-MS in the catalysts after the final TPR treatment at 900°C (Table 1) was in line with its nominal content (0.2%); Rh and La were also detected at levels close to their nominal ones.

Values of the BET specific surface area are reported in Table 1: phosphorous addition to the commercial La- γ-Al_2O_3 (LA) and following reducing treatment at 900°C did not alter the initial surface area of the support (140 m^2/g). The presence of rhodium determined a limited decrease in this value down to roughly 131 m^2/g for the reduced Rh-P/LA sample, and 122 m^2/g for the reference Rh/LA sample, thus suggesting a positive stabilizing effect obtained via doping with

phosphorous. The active layer in honeycomb Rh-P/LA catalysts displayed a value of 123 m^2/g, only slightly lower than the reference powder catalyst, possibly due to a small contribution coming from the pseudo-bohemite binder used in the washcoating step [30]. The exposure to CPO operation for a total of 38 h, both determined a further limited decrease in the surface area of Rh-P/LA honeycomb catalyst down to 112-115 m^2/g.

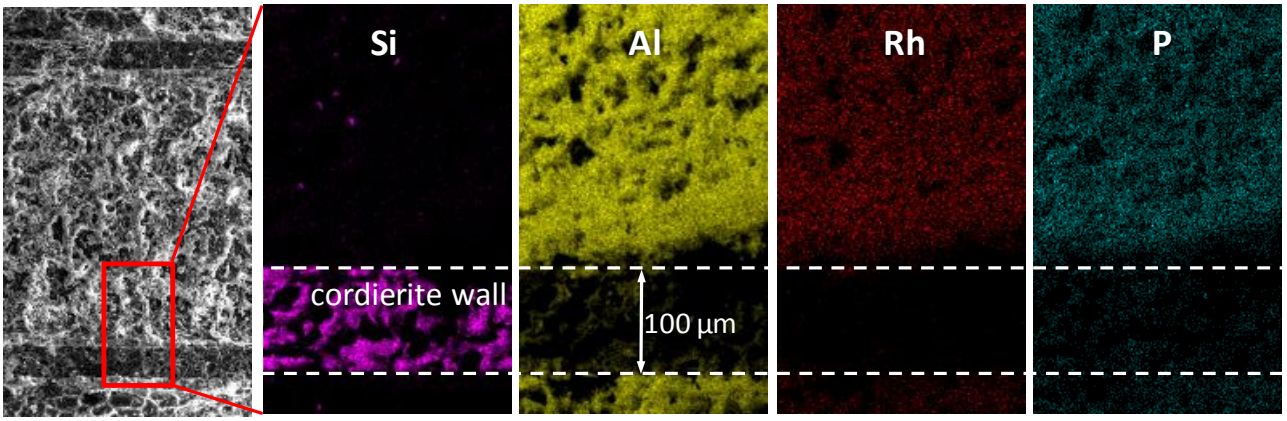

Figure 2: SEM image of a longitudinal section of the Rh-P/LA honeycomb catalyst after TPR at 900°C (1st panel) and maps (false colour) for elemental distribution of Si, Al, Rh and P in the highlighted area.

SEM observation of longitudinal sections of the honeycomb catalyst (after reduction at 900°C) revealed that all channels were coated with a rough porous layer consisting of interconnected aggregates of submicronic γ-Al_2O_3 particles which were firmly anchored to the underlying cordierite walls. The average thickness of the washcoat layer was in line with its nominal value (ca 20 µm, estimated by assuming an uniform deposition on the wet geometrical area of honeycomb channels). EDAX mapping of elemental distributions (Fig.2) confirmed the simultaneous occurrence and uniform concentration of Rh and P throughout the Al washcoat layer, and not within the macroporous cordierite walls.

Temperature programmed reduction profiles of Rh-P/LA, Rh/LA, and P/LA samples pre-calcined in air at 550°C are compared in Figure 3; the corresponding amount of hydrogen taken up and referred to the actual Rh content is reported in Table 2.

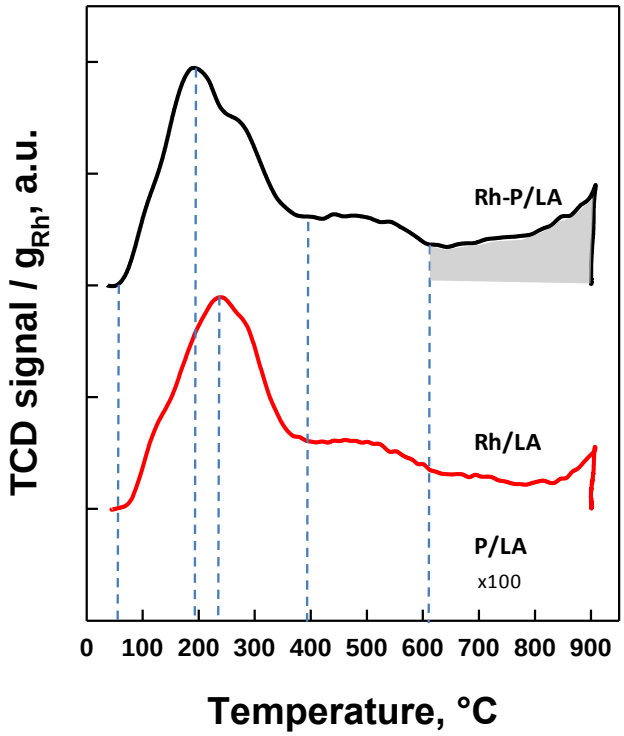

Figure 3: H_2-TPR profiles for the Rh-P/LA and Rh/LA catalysts and P-LA support calcined at 550°C in air. For comparison purpose the signal was referred to the actual weight of Rh in catalysts (ca. 1% wt), and multiplied x100 for the support.

Sample	**T max**	**H_2^{uptake} / Rh [a]**		**P / Rh [a,b]**	**H_2^{uptake}/ P [a,d]**
		up to 600°C	total [c]		
R-P/LA	195 °C	1.50	2.44	0.64	1.47
R/LA	237 °C	1.49	1.73	–	–

a) Molar ratio
b) By ICP-MS after TPR at 900°C
c) After 1h at 900°C
d) From H_2 uptake at T>600°C

Table 2 H_2-TPR analysis up to 900°C of the R-P/LA and R/LA samples

The reference P-LA support showed an almost flat baseline up to 870°C; above this temperature it started to develop a hardly detectable peak, which, in line with previous reports, could be assigned to the reduction of surface aluminium phosphate [10]. H_2 consumption on Rh-LA and Rh-P/LA catalysts started at ca. 65°C and showed peak maxima respectively at 195°C and 237°C with shoulders at 125°C and 275°C. Such complex pattern is typical of the reduction of Rh_2O_3 clusters not strongly interacting with the alumina support to metallic Rh [31]. The left shift of the peak

temperature observed for the P-doped catalyst is likely related to a higher superficial dispersion of the Rh oxide particles, possibly due to the co-impregnation procedure employing Rh^{+3} and $H_2PO_4^-$ precursors. A broad and small reduction peak (in the range 350-600°C) centred at ca. 485°C appeared in the TPR traces of both Rh catalysts which can be assigned to the reduction of RhO_x species interacting more strongly with the alumina [32]. The hydrogen consumption calculated from TPR profiles of Rh/LA and Rh-P/LA catalysts up to ca. 600°C and referred to the measured content of Rh in each sample (Table 2) corresponded to the complete reduction of Rh^{3+} to Rh^0 for both samples. A further significant reduction event occurred only for the Rh-P/LA sample starting at temperatures around 600C, which was completed under the isothermal step at 900C (highlighted area in Figure 3). That peak, which was absent in the TPR of reference Rh/LA sample, can be assigned to the reduction of phosphate species. Recalling that the reduction of superficial $AlPO_4$ was reported to occur above 830°C [10] and in our reference P-LA sample it only started above 870°C, the easier reducibility of phosphates in the Rh-P/LA catalyst was probably due a spill-over effect on Rh sites, which appear to be close enough to interact with phosphorous emerging from the support and to form Rh phosphide species [10]. Assuming that the surplus H_2 consumption (with respect to the full reduction of Rh) was employed to reduce P^{5+} to P^0, then roughly 60% of the initial phosphorous was reduced to the zero oxidation state at the end of TPR. This value can be regarded as an upper limit since the reference Rh-LA also showed some H_2 consumption at high temperatures, which could be related to the surface reduction of aluminium oxide, enhanced by the presence of Rh via a spill-over effect. Therefore, due to the high stability of the superficial $AlPO_4$ species, not all of the phosphorous was available to form a stoichiometric Rh_2P phase even after H_2 reduction at 900°C: the possible formation of sub-stoichiometric Rh phosphides, or, more simply, the simultaneous presence of both Rh and Rh_2P entities on the surface of Rh-P/LA catalyst cannot be ruled out.

XRD analysis after the TPR treatment at 900°C (Figure 4) failed to identify the formation of Rh_2P species in the Rh-P/LA catalyst, which showed the typical reflections of γ-alumina with incipient formation of transitional δ and θ phases [33]. That is most probably associated to the low loading of active phase, and its high dispersion and possibly its amorphous nature.

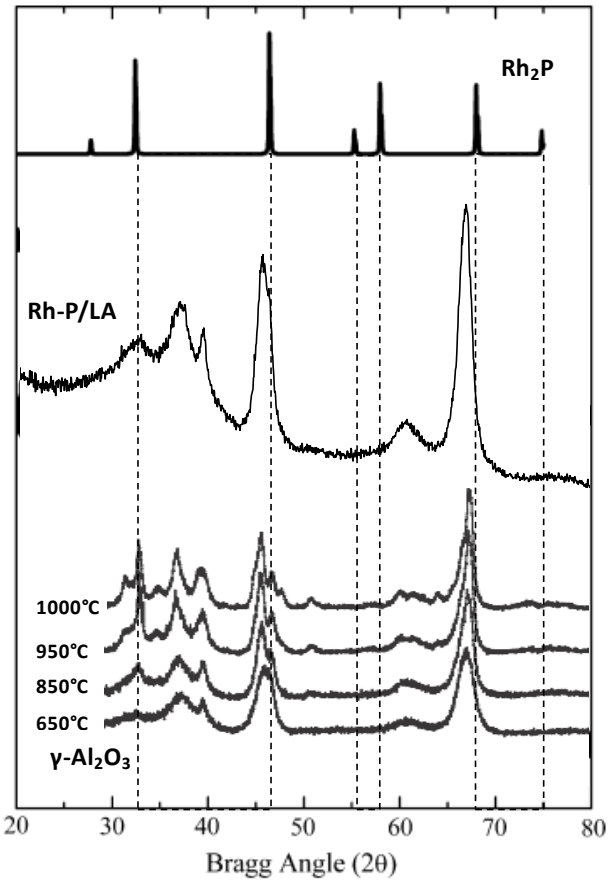

Figure 4: XRD pattern of Rh-P/LA catalyst after TPR at 900°C as well as reference patterns for Rh_2P [14] and γ-alumina calcined in air at 650°C, 850°C, 950°C and 1000°C showing progressive formation of transition δ and θ phases [33].

3.3.2 DRIFT and volumetric study of adsorbed CO

DRIFTS spectra of adsorbed CO on reduced catalysts provides information on the state and morphology of the rhodium component as the adsorption mode of CO is sensitive to different rhodium structures. In order to gain insight into the nature of the Rh active sites during the CPO of methane in the absence and presence of sulphur under self-sustained reaction conditions at high temperatures, DRIFTS experiments were carried out at room temperature before and after sulphurization of the sample at 800°C under H_2S/H_2-N_2 reaction mixture.

After CO adsorption at 40°C (1h P_{CO} = 38 mmHg) on freshly reduced catalysts, DRIFT spectra were collected at fixed time intervals under a flow of Ar in order to investigate the nature of surface species and to evaluate the strength of the CO/surface interaction. A common trend was obtained for Rh-P/LA and Rh/LA (Figure 5), which can be described as follows.

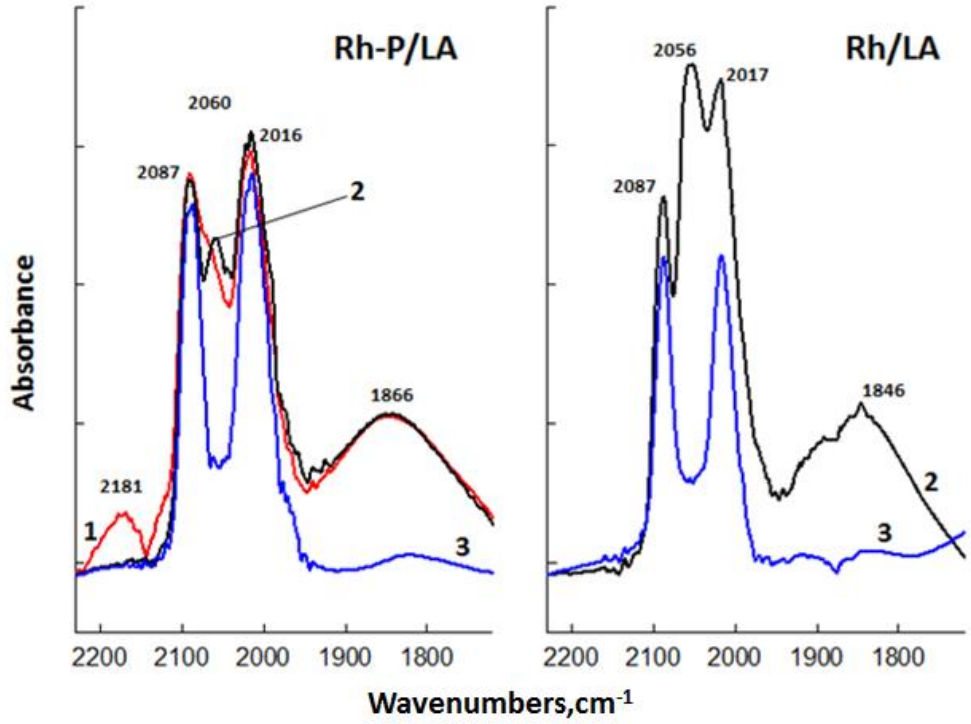

Figure 5: DRIFT spectra of CO adsorbed over freshly reduced Rh-P/LA and Rh/LA catalysts: (1) under flowing CO/N_2; (2) after 60 min and 120 min (3) of purging with Ar flow.

Upon switching to Ar flow, a characteristic band of gaseous CO centred at ca. 2180 cm^{-1} (Figure 5, spectrum 1) rapidly disappeared and the resulting spectra (exemplified by those (2) recorded after 60min Ar purging) were characterized by IR bands in the ranges 2055-2065 cm^{-1} and 1840-1870 cm^{-1}, respectively, attributed to linear and bridged CO adsorbed on large metal particles [34-37]. Such large Rh clusters are not subjected to the disruption of Rh-Rh bond which only takes place when the adsorbed CO is in close proximity of support hydroxyl groups, that is when rhodium species are small and highly dispersed [38-40]. In that case $Rh^{I}(CO)_2$ gem-dicarbonyl species are formed, according to the following reaction [37]:

$$Rh^0 + 2CO + OH^- \rightarrow O^{2-} + Rh(I)(CO)_2 + 1/2H_2 \quad (3.4)$$

They are characterized by symmetric and asymmetric stretching bands around 2090 and 2020 cm^{-1} [34-40], which indeed were detected in the spectra of Figure 5 for both catalysts. P doping of Rh particles entailed a significant reduction in the relative intensity of the signal due to linear Rh^0CO species, which was compensated by the simultaneous increase in the bands of gemdicarbonyl species, whereas the intensity of the broad band due to bridged bond CO was roughly unaltered. The wavenumber values of the gem-dicarbonyl stretching bands (2087 and 2016 cm^{-1}) were not affected by P-doping, whereas the *ν*CO for linear and bridge bonded CO shifted to higher frequencies, likely due to the transfer of electron density from Rh to P, as also observed for alumina supported nickel-phosphorous catalysts [13,41]. IR bands of bridge- and linear-bonded carbonyls

coordinated over metallic Rh particles progressively disappeared (in that order) from the spectra recorded on both catalysts during prolonged purging in Ar (Figure 5, curves 3), possibly because of the weak nature of their σ-bond [37,42] making those species relatively less stable [43]. On the other hand gem-dicarbonyl species are quite stable as a result of a strong covalent σ-bond and π-back bond [37,43], and indeed their characteristic IR bands persisted even after prolonged purging. A direct comparison of the spectra recorded after purging for 120 min (3) confirms the higher intensities of those signals on the P-doped catalyst.

Regarding sulphurized catalysts, H_2S chemisorption on Rh is reported to be mainly dissociative [44-46] with H_2 evolution; adsorbed S atoms are preferentially bonded to defect sites such as steps [46]. For this reason smaller Rh particles, with their lower surface coordination number and higher density of defect sites are more seriously affected by S poisoning [5,7,47], which in turn is reported to be highly selective at low coverages.

DRIFT spectra of CO adsorbed over the catalysts previously sulphurized at 800°C (and purged in Ar at the same temperature) are reported in Figure 6, and show a general decrease in the intensities of the relevant bands due to an overall lowering of chemisorption capacity.

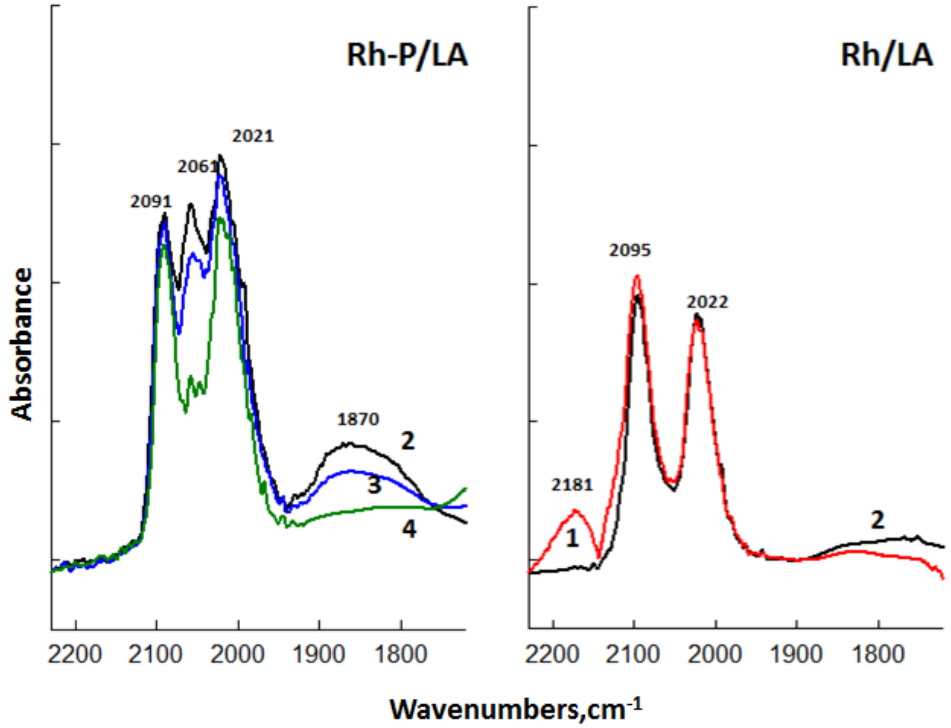

Figure 6: DRIFT spectra of CO adsorbed over Rh/LA and Rh-P/LA catalysts following sulphurization (800°C H_2S/H_2: (1) under flowing CO/N_2; after purging with Ar flow for 60 min (2), 120 min (3) and 180 min (4).

Sulphur had a much stronger impact on the reference Rh/LA catalyst: IR bands corresponding to linear and bridge-bonded CO species disappeared completely already from the spectrum (1)

recorded under a constant partial pressure of CO. The nonoccurrence of bridge-bonded CO is easily rationalized by the conventional site blocking model; even at low sulphur coverages, the remaining surface Rh atoms become isolated from each other [48]. However, the lack of linear CO species suggests a high degree of sulphur coverage with extensive formation of surface Rh sulphides. The only mode of CO adsorption over Rh/LA after sulphurization was related to formation of gemdicarbonyl species, whose characteristic doublet bands were detected at 2022 cm^{-1} and 2095 cm^{-1} and were retained even after prolonged purging with Ar (exemplified by spectrum (2) after 60 min). The wavenumber values were clearly shifted to higher frequencies with respect to the freshly reduced catalyst, which could be explained by withdrawing of the electron density from the metal particles induced by adsorbed sulphur [7,13,41,49]. In conclusion, the electronegative sulphur atoms might leave adjacent Rh atoms with a net positive charge thus facilitating the adsorption of 2 CO molecules [48]. In this case, the occurrence of gem-dicarbonyl species in sulphurized sample would not be necessarily (or cannot be directly) associated to the morphology and size of supported Rh particles [48 and ref therein].

As also shown in Figure 6, the addition of phosphorous in Rh-P/LA catalyst limited the impact of the sulphurization on the following CO adsorption performed without pre-treating the sample in H_2. In contrast to what observed for the unpromoted catalyst, the IR spectra revealed the simultaneous presence of all the three modes of CO adsorption, and confirmed a higher stability of geminal species upon prolonged purging. In particular, in the spectrum (2) collected 60 min after removing gaseous CO the intensity of the band at 2061 cm^{-1} assigned to linear CO species became comparable to those doublet bands of geminal carbonyls respectively at 2091 cm^{-1} and 2021 cm^{-1}; at the same time, bridged CO species showed a broad band with a lowered relative intensity and a maximum shifted to 1870 cm^{-1}. Therefore sulphurization determined an upward shift of all the characteristics wavenumbers of CO adsorption modes: however, this was less pronounced for the Rh catalyst promoted with P, possibly suggesting a lower weakening of the metal-CO bond related to the perturbation in the electronic state induced by adsorbed S [13,50].

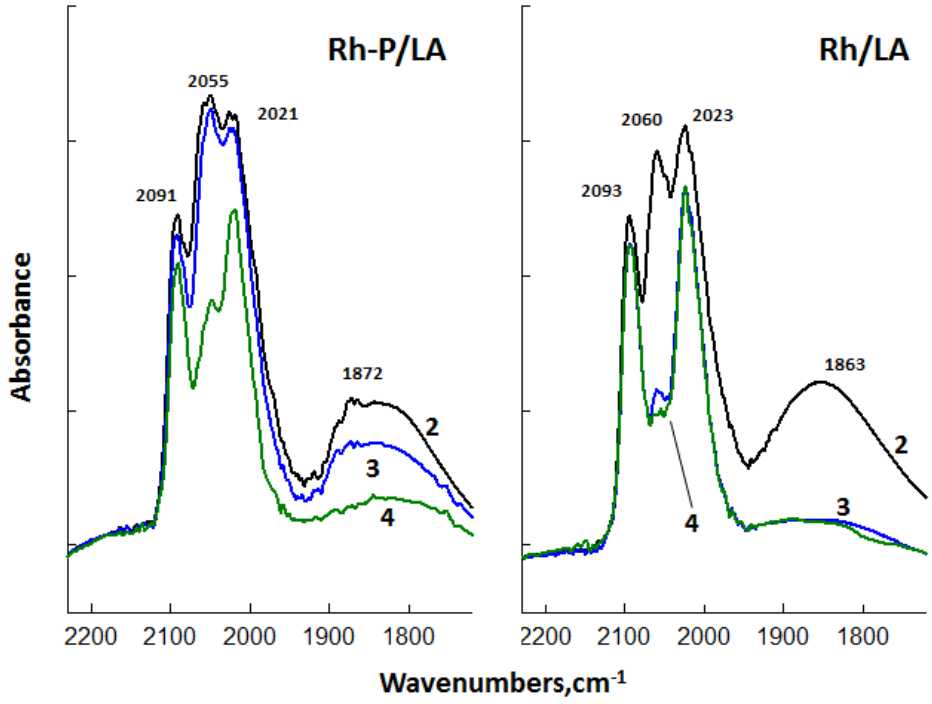

Figure 7: DRIFT spectra of CO adsorbed over Rh/LA and Rh-P/LA catalysts following regeneration (H_2 at 400°C) : (1) under flowing CO/N_2; after purging with Ar flow for 60 min (2), 120 min (3) and 180 min (4).

Following regeneration in H_2 at 400°C, as it is shown in fig.7(b), the IR bands of linear and bridge bonded CO re-appeared over the sulphurized Rh/LA catalyst: as for the freshly reduced sample, those species showed a relatively weak bond and progressively disappeared during purging with Ar. On the contrary, the intensities of bands for gem-dicarbonyl CO species were not affected significantly by this regeneration and persisted during purging. Due to the high stability of adsorbed S species their desorption as H_2S is unlikely under such regeneration conditions [46]. However it is conceivable that the reformation of linear- and bridge-bonded CO was related to surface reconstruction and/or partial hydrogenation at 400°C causing the exposure of some additional Rh sites capable of weakly adsorbing CO [48]. It should be noted that the disappearance of the linear CO adsorption mode on sulphurized Rh/alumina catalyst was not found in previous literature reports since the catalysts were pretreated in H_2 prior to readsorbing CO [48].

As for the unpromoted Rh/LA catalyst, regeneration in H_2 at 400°C of Rh-P/LA sulfurized sample caused some partial surface reconstruction/hydrogenation which in turn increased only the intensity of the bands for bridge and linear-bonded CO. In particular the band for linear CO shifted to 2055 cm^{-1} and became the predominant feature in spectrum (2) taken after 60 min Ar purging and decreased more slowly than for the freshly reduced sample, being still well evident after 180 min (spectrum 4).

The quantitative results of CO chemisorption measurements performed at 40°C on reduced samples and following sulphurization at 800°C (+ H_2 regeneration at 400°C) are summarized in Table 3.

	CO strong ads.	CO weak ads.	SA[a]s	SA[b]w	SA s+w	dispersion	D
Sample pretreatment	µmol/g_{cat}		m^2/g_{cat}			%	Nm
Rh-P/LA	80.4	8.7	1.82	0.39	2.21	51.3	2.14
Rh/LA	49.5	7.6	1.12	0.34	1.46	37.5	2.93
P/LA	0	0	–	–		–	–
H_2S/H_2 800°C + H_2 400°C							
Rh-P/LA	34.8	17.8	0.79	0.81	1.60	37.0	
Rh/LA	14.3	13.7	0.32	0.61	0.93	23.8	
P/LA	0	0	–	–		–	–
LA	0	0	–	–		–	–
H_2S/H_2 800°C + H_2 800°C							
Rh-P/LA	43.3	12.9	0.98	0.59	1.57	36.3	
Rh/LA	35.7		0.81				
LA	5	0	–			–	–

[a] CO/Rh =2

[b] CO/Rh =1

Table 3: Results of CO chemisorption measurement at 40°C on freshly reduced and sulphurized samples: strong and weak chemisorbed CO (at zero pressure), corresponding values of exposed metal surface areas (SAs,SAw), percentage metal dispersion and average diameter of crystallites (d).

P-LA and LA supports had identical adsorption isotherms, which only accounted for a reversible CO physisorption, thus excluding any direct contribution of phosphorous; furthermore CO adsorption on the supports was not altered by the sulphurization treatment.

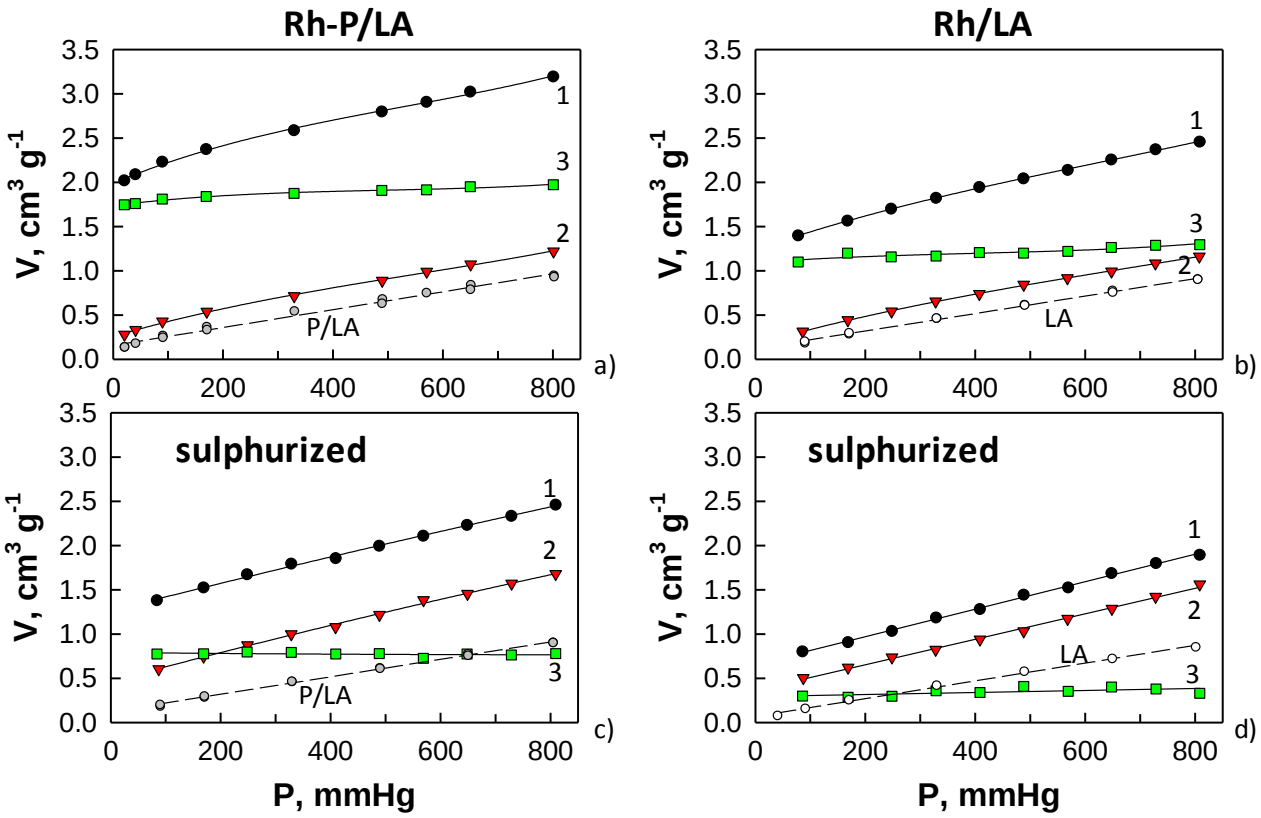

Figure 8: CO adsorption at 40°C on freshly reduced Rh-P/LA (a) and Rh/LA catalysts (b) and after sulphurization for 1h at 800°C in H_2S/H_2 mix (c, d). Each panel presents the total (1), weak (2) and irreversible (3) adsorption curves for the catalyst as well as the total=weak adsorption curve on the corresponding support (P/LA or LA). Sample pre-treatment at 400°C: 1h in flowing H_2 + 1h evacuation

Figure 8 shows for each of the two catalysts the total (1) and the weak (2) CO adsorption curves as well as the corresponding irreversible adsorption curve (3) obtained as the difference from the previous two. The (reversible) adsorption isotherm on the corresponding support is also reported in each panel of Figure 8. A direct comparison of the relevant curves for the freshly reduced catalysts confirms the addition of surface phosphorous did not suppress CO adsorption on Rh and in fact it caused a significant increase in the amount of irreversibly chemisorbed CO, which was ca. 60% higher for the Rh-P/LA sample than for the undoped Rh/LA (Table 3 first column). It is also clear from Figure 8 a-b that the weak isotherm recorded over the catalysts containing Rh was higher than the curve corresponding to the physisorption of CO on the support. Thus some additional CO was absorbed on the noble metal and bonded to its surface more weakly, since it didn't resist to sample evacuation: the corresponding CO amounts were estimated by extrapolating to zero pressure the difference between the two reversible adsorption curves and were similar for the two catalysts (CO weak, Table 3).

In agreement with previous reports [34,37-38], DRIFT experiments of CO adsorption at room temperature on P-doped and undoped Rh catalysts reported in this work, showed the simultaneous presence of prevailing gemdicarbonyl species, together with some linear bonded and bridged CO species on larger Rh clusters. However, those last two species disappeared progressively when purging the sample with Ar. Based on those results, CO/Rh stoichiometric coefficients were assumed equal to 2 and 1 respectively for the strong and weak adsorption components on Rh, allowing to distinguish the contribution of isolated Rh sites (SAs) and larger metal clusters (SAw) to the total exposed surface area (Table 3). The contribution from bridge bonded CO species to the weak adsorption was neglected according to previous literature data on Rh/alumina reporting high values of the linear to bridging adsorbed CO ratio (above 20 [37]).

The addition of phosphorous effectively increased metal dispersion up to 51.3 % corresponding to an average diameter of the metal particles down to 2.1 nm, as opposed to 37.5 % dispersion and 2.9 nm calculated for the reference undoped Rh catalyst.

Figure 8 c-d presents the CO adsorption isotherms obtained after sulphurization for 1h at 800°C with the H_2S/H_2 mix, and following a new pre-treatment at 400°C for 1h in H_2; corresponding values of strongly and weak adsorbed CO and exposed metal surface area are also reported in Table 3. It should be noted that the samples tested under these conditions can be considered as regenerated catalysts. Indeed, the H_2 pretreatment at 400°C was necessary due to the exposure to air after sulphurization carried out ex-situ.

The strong sulphur adsorption occurring on Rh sites caused a reduction in the total CO adsorption capacity at each pressure (curve 1), which was also accompanied by an increase in the amount of weakly bonded CO (2). As a consequence the difference (3) between the two isotherms was significantly lower, but still independent of the pressure level and precise enough to calculate the irreversible fraction adsorbed CO (Table 3). Due to the presence of phosphorous, the Rh-P/LA catalyst preserved an irreversible chemisorption capacity which was more than two times larger than on the reference Rh/LA system. This agrees well with previous results [16] showing that following a H_2S/H_2 treatment at 300°C the site blockage by S on a Rh_2P/SiO_2 catalyst was roughly halved with respect to its reference Rh/SiO_2 sample. Following sulphurization, both catalysts adsorbed weakly on their metal particles almost twice as much CO as their freshly reduced counterparts (Table 3).

The strong decrease in the amount of irreversibly adsorbed CO suggests that highly dispersed Rh sites, are preferred targets for S adsorption [7,47,51], whilst larger metal clusters appear less affected. The simultaneous increase in the amount of weakly bonded CO confirms the qualitative

trend observed during DRIFT experiments and was related to the partial surface reconstruction/hydrogenation occurring on the sulfurized sample during the H_2 treatment at 400°C.
Assuming unaltered stoichiometric coefficients, the residual metal surface areas available for CO adsorption on Rh-P/LA and Rh/LA catalysts were lowered respectively to 72 % and 63 % of their initial values. However, if the impact of sulphur is assumed limited on the metal sites capable to strongly adsorb CO, the values (SAs) for Rh-P/LA and Rh/LA dropped to 42 % and 24 % of their initial levels. It clearly comes out that P-addition helped to preserve a much higher active surface area (0.79 m^2/g vs. 0.32 m^2/g) of those isolated and coordinatively unsaturated Rh surface atoms which are generally reported to decrease the energy required to form relevant transition states for the initial C–H bond activation step in reforming reactions [52]. Increasing further the temperature of the H_2 pre-treatment (1h) up to 800 °C, the sulphurized Rh-P/LA catalyst recovered some but not all of its strong CO chemisorption capacity (Table 3), suggesting that complete regeneration is a rather slow process and/or some catalyst reconstruction had occurred. However a precise evaluation of the various modes of CO adsorption was somehow precluded by a strong contribution coming from the support, possibly due to its partial superficial reduction.
To sum up, the interaction of phosphorous with Rh showed several positive effects: i) it formed a metallic surface capable to strongly adsorb CO; ii) it improved the metal dispersion on the alumina support; iii) it significantly inhibited the strong sulphur adsorption and lowered the resulting surface S coverage with special regards to those sites capable of strong CO adsorption.
Accordingly to TPR results, not all of the phosphorous interacted with Rh to form a new metallic phase in the Rh-P/LA catalyst; thus it can be argued that an even better S-tolerance might be achieved if one manages to force the formation of the Rh-P active phase.

3.3.3 Catalytic partial oxidation performance testing

After stabilization of the CPO performance of the Rh-P/LA honeycomb monolith under self-sustained conditions at CH_4/O_2 =2 in air (Tcat = 730°C, complete O_2 conversion), the impact of sulphur was studied by following the transient response of the catalytic reactor to a step addition of SO_2 to the feed. The typical temporal profiles of methane conversion, temperature inside the catalyst (Tcat) and selectivity to CO and H_2 are reported in Figure 9 a-d for the addition and subsequent removal of 20ppm of SO_2.

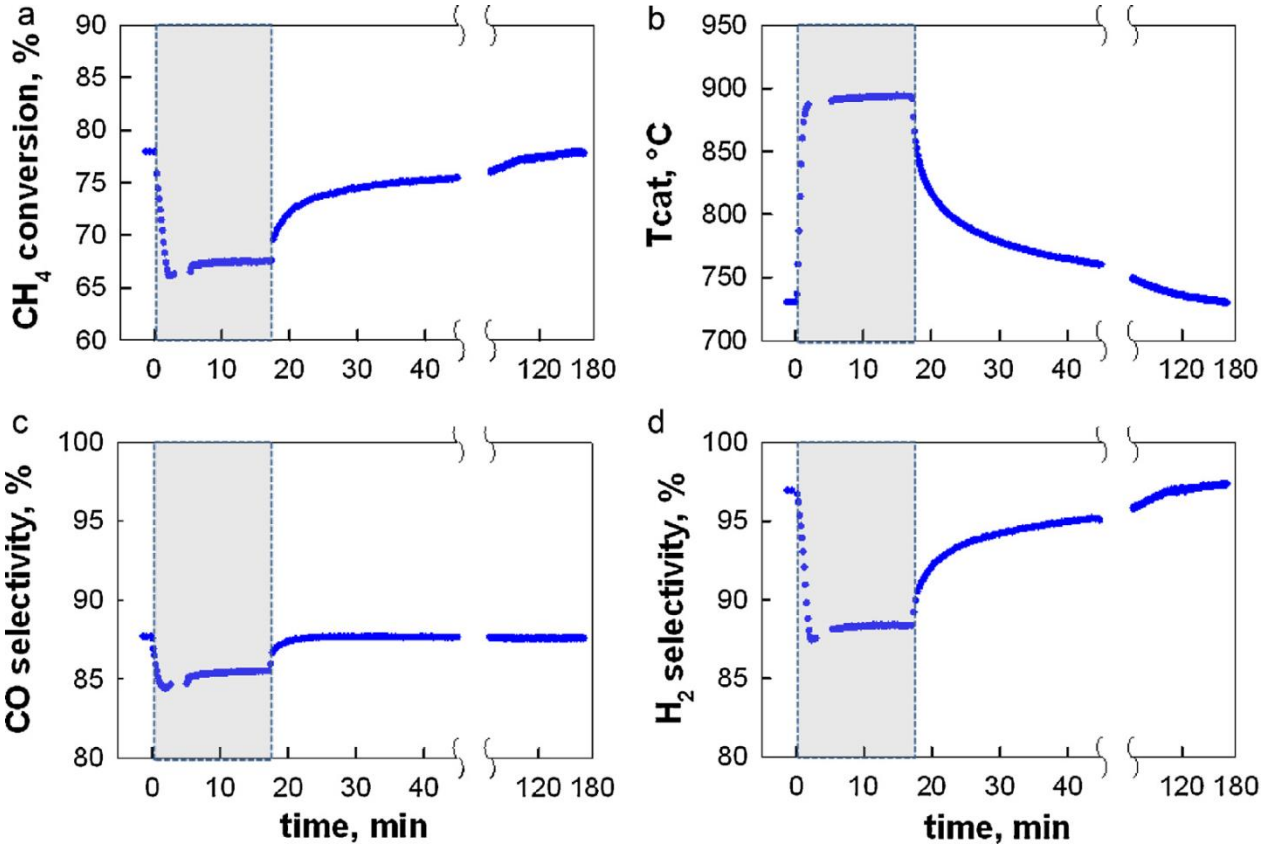

Figure 9:Transient response to SO_2 addition (20 ppm) and removal during the CPO of methane on Rh-P/LA honeycomb: (a) methane conversion, (b) temperature in the middle of catalyst, selectivities to (c) CO and (d) H_2. Feed CH_4/O_2 = 2, air as oxidant.

In line with recent results with Rh catalysts supported on various stabilized aluminas [4,5,51,53-54] the step addition of S to the feed to the CPO reactor resulted in a rapid decrease in CH_4 conversion and selectivity to H_2, which was accompanied by a corresponding sharp increase in the catalyst temperature, whereas the selectivity to CO was only marginally reduced. Such peculiar behaviour has been associated [4-5] to the inhibiting effect of sulphur on the kinetics of the endothermic methane steam reforming reaction (eq. 3.2), which significantly contributes to syngas formation over Rh catalyst [36-37] consuming part of the heat generated by the catalytic oxidation reactions. At the same time oxygen conversion from Rh-P/LA CPO reactor (not shown) remained complete, in good agreement with results of Bitsch-Larsen et al. who reported that the rates of O_2 consumption on Rh (i.e. O_2 spatial profiles along the CPO reactor) were independent of the sulphur level, likely because the kinetics of the oxidation reactions remained much faster than the transport phenomena even in the presence of sulphur.

$$CH_4 + H_2O \leftrightarrow CO + 3H_2, \qquad \Delta H_r^{298K} = +206 \text{ kJ/mol} \tag{3.5}$$

For each level of S in the feed (up to 58 ppm) the Rh-P/LA catalyst reached a novel steady state within ca. 10-15 min, without any visible sign of further loss/modification of its catalytic

performance during time on stream in the presence of SO_2, at least on a time scale of a few additional hours (not shown). This suggests a dynamic equilibrium between S adsorbing on the surface of the active sites and S desorbing into the gas phase, which is governed by the catalyst temperature and sulphur concentration [5]. Upon removing the SO_2 from the reaction feed, the activity/selectivity of the Rh-P/LA catalyst was found to increase immediately although it required a relatively longer time in order to completely recover the initial levels, as opposed to the fast regeneration occurring on the undoped Rh/LA catalyst [5]. Therefore the interaction between Rh and P, which was shown to reduce the amount of S taken up by the metal, slowed down the desorption of a part of the surface S via reaction with gas phase H_2. A similar slow recovery effect was previously observed due to the presence of Ce in a Rh/CeO_2-γ-Al2O_3 foam catalyst [4]. The complete reversibility of the S-poisoning effect under the studied reaction condition was also confirmed by the unchanged values of the temperatures measured at three different locations along the reactor before the addition and after the removal of sulphur, indicating the development of identical temperature (and reactivity) profiles inside the catalytic honeycomb.

Having ruled out any further decay of activity induced by progressive S-poisoning, steady state performance of Rh-P/LA and reference Rh/LA monolith [5] can be compared in Figure 10 a-c as a function of the S load in the feed.

Under S free conditions both Rh based honeycombs displayed similar performance in terms of CH_4 conversion and yield to CO and H_2. This result is particularly significant in view of the lower loading of active washcoat on the Rh-P/LA honeycomb (0.11 g/cm^3) with respect to its Rh/LA counterpart (0.17g/cm^3), which was completely compensated by the larger active surface area measured on Rh-P/LA catalyst (Table 3). In fact it was demonstrated that during methane CPO over structured Rh-based catalysts, oxidation reactions are so fast to proceed under fully external mass transfer control, consuming all of the molecular oxygen in the very first part of the reactor [55-57]. On the other hand, the catalytic methane steam reforming (3.6), which significantly contributes to syn-gas formation [55-56], is a much slower reaction that occurs under kinetic control on Rh, spreading all over the catalytic reactor [58].

The Water Gas Shift reaction (3.7) is generally equilibrated at the exit of Rh-based CPO reactors [56,58].

$CH_4 + H_2O \leftrightarrow CO + 3H_2$, $\quad \Delta H_r^{298K}$ =+206 kJ/mol (3.5)

$CO + H_2O \leftrightarrow CO_2 + H_2$, $\quad \Delta H_r^{298K}$ = -41 kJ/mol (3.6)

These results suggest that the addition of phosphorous to Rh with the possible formation of a new metallic phase enhanced the intrinsic activity for methane steam reforming (per gram of catalyst), likely through the increased metal dispersion, while not significantly affecting the oxidation reaction path. This contrasts with recent results showing an evident poisoning effect caused by the addition of P to a 2.5 wt% Rh/α-Al_2O_3 during the steam methane reforming at 700°C, which eventually resulted in the formation of carbon filaments with large rhodium particles at the tip [6]. Those authors reported a much lower initial dispersion of Rh on α-Al_2O_3 (ca. 10%) which was further decreased down to 3.6% (with Rh particles of ca 30nm) after the addition of 1 atom of P for every 5 atoms of Rh. The striking discrepancy in the effect of P may thus originate from differences in the initial metal dispersion, as well as from the lack of a H_2 prereduction at high temperature [6] which is required for a favourable structural reconstruction.

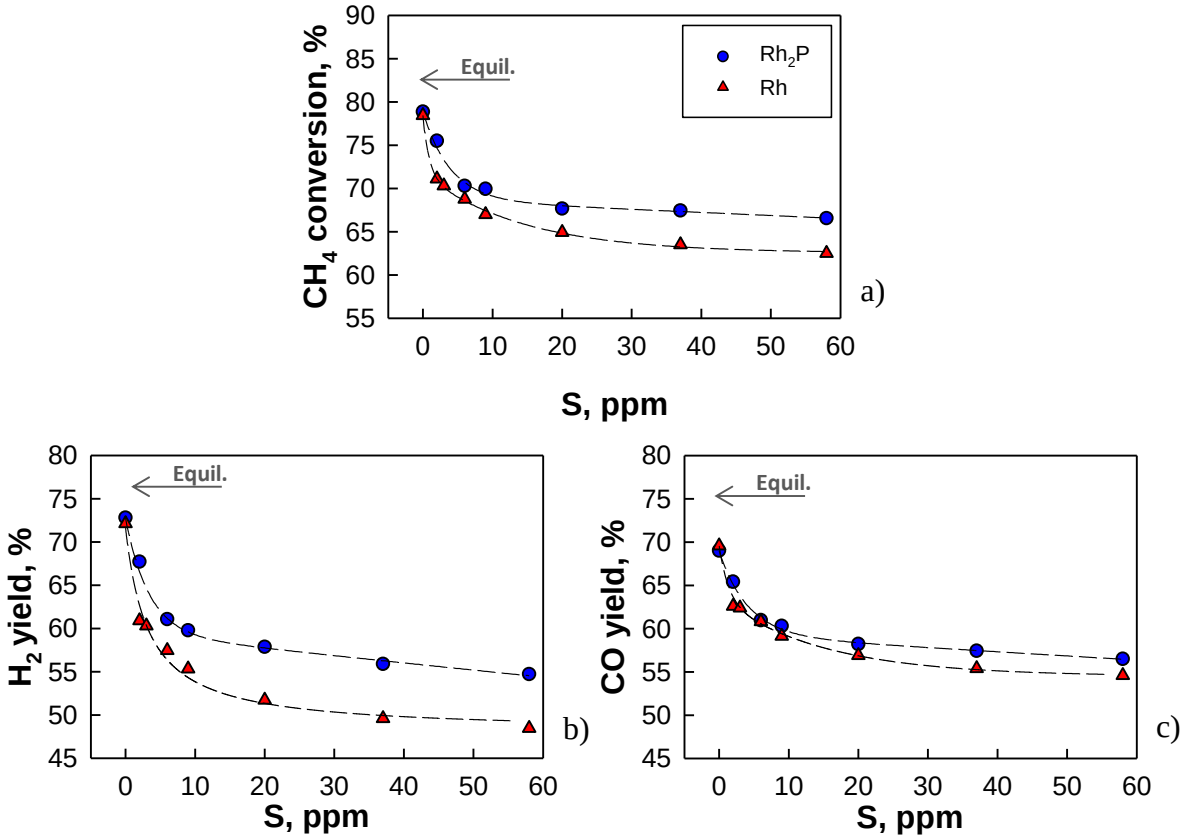

Figure 10: Effect of SO_2 addition on CH_4 conversion (a), yield to H_2 (b) and to CO (c) from the CPO over RhP/LA honeycomb catalyst. Feed CH_4/O_2=2, air as oxidant. Arrows indicate thermodynamic equilibrium values (P, h =constant).

Upon addition of sulphur the extent of deactivation of the P-doped Rh catalyst was always significantly lower than its metallic counterpart showing higher methane conversion and yields to syngas (and particularly to H_2, Figure 10 a-c) and a corresponding smaller jump in the catalyst temperature (Figure 11).

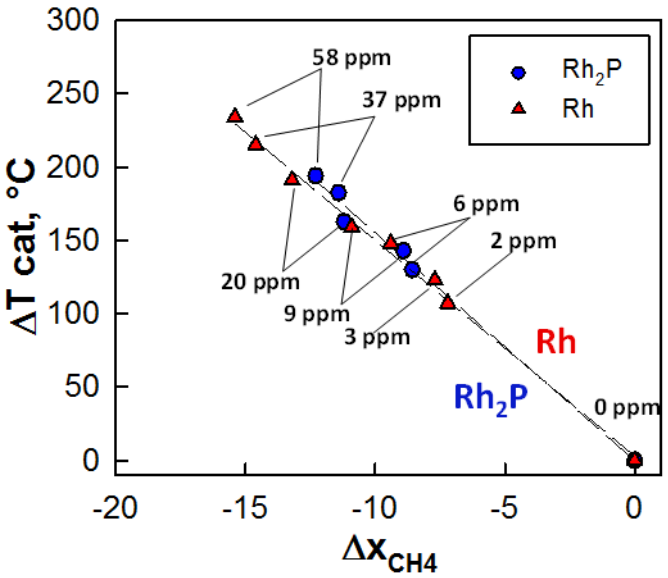

Figure 11: Increase in catalyst temperature as a function of the variation of fuel conversion measured upon the addition of sulphur to the feed during the steady state CPO of methane over Rh-P/LA and Rh/LA honeycomb catalysts. Labels indicate sulphur content in the feed (CH_4/O_2=2 in air).

As an example, at the maximum S level added to the feed (58ppm), Rh-P/LA catalyst converted ca. 66.6 % of methane, with 55 % yield to H_2 and 56.5 % yield to CO, as opposed to 62.5 %, 48.5 % and 54.6 % measured respectively on the reference Rh/LA honeycomb. In fact the temperature rise measured in the honeycomb upon addition of S was proportional to the corresponding drop in methane conversion on each catalyst (Fig.11). Starting from this observation, a simple heat balance on the gas phase was proposed [5] in order to calculate a lumped value for the heat of the reaction involving methane which was inhibited by S,

$$\Delta H_r^{T_0} = \frac{-W c_p}{F_{CH4}} \left(\frac{\Delta T}{\Delta x_{CH4}}\right) \qquad (3.7)$$

where Cp is the specific heat of the product gas mixture, W is the total molar flow rate, and F_{CH4} is the hydrocarbon feed molar flow rate. By assuming a thermal equilibrium between gas and solid (i.e. exit gas temperature is equal to the measured catalyst temperature) and substituting the value of $\Delta T/\Delta x_{CH4}$ obtained from the slopes of the line in Fig.11 [5,51], the heat of reaction was estimated to be in the range +225 – 240 kJ/mol at 700°C for both catalysts which corresponds well to the heat of reaction of methane steam reforming (3.5) at that temperature. The inhibition of steam reforming is further corroborated by the change in the flows of products from Rh-P/LA catalyst induced by S-addition, exemplified in Table 4 for the case of 9 ppm SO_2 in the feed.

		SO_2		Differences*
CH_4/O_2=2		0 ppm	9ppm	Δ (9-0)
X_{CH4}	(%)	78.9	70.0	- 8.9
Y_{H2}	(%)	72.8	59.8	- 26.0
Y_{CO}	(%)	69.0	60.3	- 8.7
Y_{H2O}	(%)	6.1	10.2	+8.2
Y_{CO2}	(%)	9.9	9.7	-0.2

* Molar differences of each species produced from a feed of 100 CH_4

Table 4. Changes in the steady state performance of methane CPO over Rh-P/LA honeycomb induced by the addition of 9ppm SO_2. Feed CH_4/O_2=2, air as oxidant.

In agreement with the results on Rh/LA [5] and Rh/CeO_2-γ-Al_2O_3 [4], the measured change in CO production corresponded to the drop in converted methane (i.e. unchanged S_{CO}), while the drop in the H_2 flow was almost three times larger, accordingly to the stoichiometry of reaction (3.6).

3.3.4 Equilibrium considerations

In order to better quantify the effect of sulphur the experimental values of the proportionality constant for steam reforming (3.8) and water gas shift (3.9) reactions were calculated, according to the definitions:

$$K_{exp,SR} = \frac{P_{H2}^3 P_{CO}}{P_{H2O} P_{CH4}} \quad (3.8)$$

$$K_{exp,WGS} = \frac{P_{H2} P_{CO2}}{P_{H2O} P_{CO}} \quad (3.9)$$

Those values were compared (Figure 12 a-b) to the corresponding equilibrium constants K_{SR} and K_{WGS} calculated at the temperature at the exit of the catalytic honeycomb.

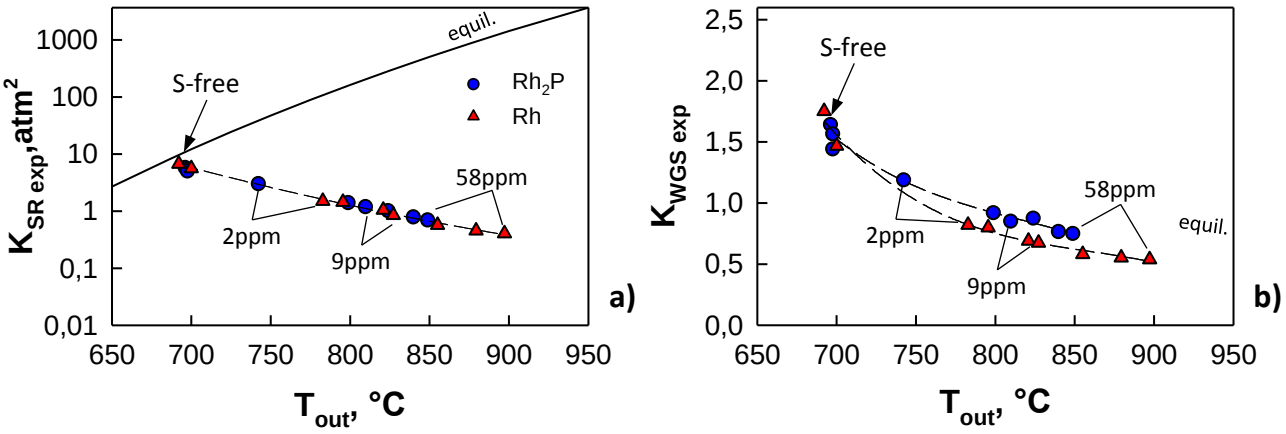

Figure 12: Values of the proportionality constant for steam reforming (a) and water gas shift (b) reactions calculated at the exit temperature from Rh-P/LA and Rh/LA honeycomb catalysts during methane CPO under S-free operation and in the presence of SO_2 added to the feed (2-58 ppm). Continuous lines represent the corresponding equilibrium constants for each reaction at P=1.1atm.

For both catalysts the WGS reaction was equilibrated under S-free feed conditions; however the $K_{exp,SR}$ /K_{SR} ratio was in the range 0.4 - 0.5, confirming that methane steam reforming was kinetically limited, which was expected also considering the heat losses from the CPO reactor whose thermal efficiency was estimated at ca. 80% - 85% [59].

As already discussed, sulphur addition progressively inhibited methane steam reforming without completely stopping it, as shown by the continuous decrease in the $K_{exp,SR}$ values which followed the opposite trend of the equilibrium constant and collapsed in a single line for the two catalysts because the temperature increase was indeed caused by the inhibition of the steam reforming. However P doping significantly enhanced the S tolerance of the Rh-P catalyst as shown by its higher $K_{exp,SR}$ at each S level. The WGS reaction was also partially inhibited by sulphur on both Rh-based catalysts [6,60], although the detrimental effect was markedly lower than for steam reforming, and smaller for Rh-P/LA as demonstrated by the closer approach to the equilibrium curve in Figure 12b.

A rough and preliminary estimate of the impact of sulphur on the rate of methane steam reforming over the two catalysts was attempted through the inclusion of an “activity coefficient” in the kinetic expression as suggested by [57], assuming that sulphur only caused a reduction in the number of active sites (unchanged activation energy). The activity coefficient corresponds to the ratio of the pre-exponential factors in the SR kinetic constants with and without sulphur and was estimated by the measured drop in methane conversion, taking into account the variation in the average temperature of the catalyst (second part of the reactor). The correction factor for the approach to equilibrium was neglected at least for the case with S-addition in agreement with results of Figure 12a.

The CPO reactor was schematically simplified as the series of two reactors: in the first one oxidation reactions proceed under external mass transfer regime and consume all of the molecular oxygen and some methane to form both partial and total oxidation products; in the second part unconverted methane and water react together via steam reforming producing some more syngas [4,56]. In fact it was shown that steam reforming spreads all over the CPO reactor due to the zero concentration of oxygen on the surface of Rh based catalysts which works under external mass transfer limitation [58].

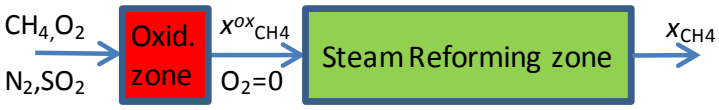

Figure 13: Schematization of CPO reactor.

For the purpose of this calculation, the inhibiting effect of sulphur on methane conversion was assumed to be limited to the second steam reforming reactor. In fact Bitch–Larsen et al. [4] demonstrated by detailed spatial profiles within a Rh-Ce/γ-Al_2O_3 foam catalyst during methane CPO that the length of the first oxidation zone was not affected by the presence of sulphur in the feed, and the conversion of methane at the exit of this zone, constantly remained around 45%. For the SR reaction rate it was assumed a first order dependence on methane concentration, neglecting any other dependency apart from the approach to equilibrium:

$$r_{SR} = k_{SR} C_{CH4} (1 - \eta_{SR}) \qquad \text{[mol/(g s)]} \qquad (3.10)$$

$$k_{SR}(T) = A_{SR} \exp\left(-\frac{E_{a,SR}}{RT}\right) \qquad \text{[Nm}^3\text{/(g s)]} \qquad (3.11)$$

$$E_{a,SR} = 92 \qquad \text{[kJ/mol]} \quad [57]$$

$$\eta_{SR} = \frac{K_{P,SR}}{K_{eq,SR}} \qquad (3.12)$$

$$K_{P,SR} = \frac{P_{CO} P_{H2}^3}{P_{CH4} P_{H2O}} \qquad \text{[atm}^2\text{]} \qquad (3.13)$$

$$C_{CH4} = C_{CH4}^0 (1 - x_{CH4}) \qquad \text{[mol/Nm}^3\text{]} \qquad (3.14)$$

Under the experimental conditions explored the steam reforming reaction was always far away from equilibrium ($1 - \eta_{SR} \cong 1$) when sulphur was added to the feed to the CPO reactor with each of the two catalysts (Figure 14). For S free conditions at the end of the CPO reactor $1 - \eta_{SR}$ was roughly

0.8 with both catalysts; thus, in order to calculate the apparent kinetic constant k_{SR}, $1-\eta_{SR}$ was averaged between inlet (=1) and outlet conditions of the steam reforming zone and set at a constant value of 0.9.

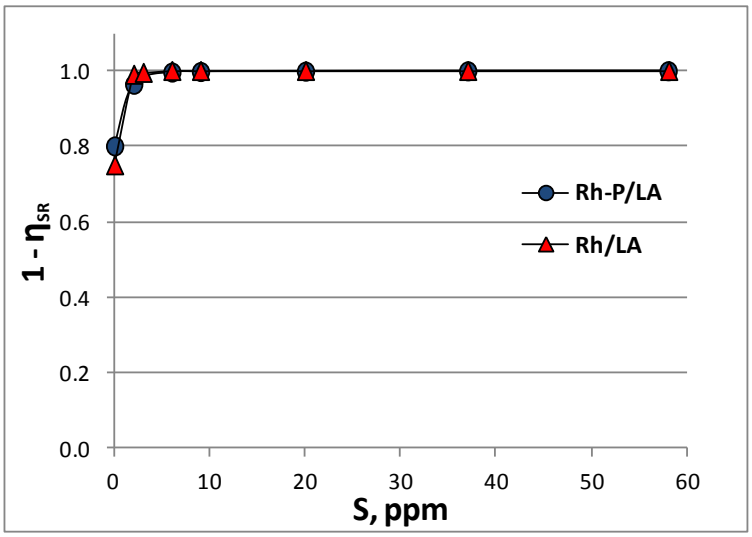

Figure 14: Thermodynamic driving force for methane steam reforming reaction calculated for Rh-P/LA and Rh/LA catalyst from steady state compositions and temperature of the effluent gas from the CPO reactor as a function of the S concentration in the feed.

Assuming an ideal isothermal PFR reactor in which methane is only consumed by steam reforming the apparent average kinetic constant for the SR reaction can be expressed in terms of methane conversion (x_{CH4}), both under S-free conditions:

$$\ln(1-x_{CH4}) - \ln(1-x_{CH4}^{ox}) = -\bar{k}_{SR}\frac{W}{Q}(1-\eta_{SR}) \tag{3.15}$$

And with sulphur added to the feed ($1-\eta_{SR} \cong 1$):

$$\ln(1-x_{CH4}^{S}) - \ln\left(1-x_{CH4}^{ox,S}\right) = -\bar{k}_{SR}^{S}\frac{W}{Q} \tag{3.16}$$

where W is the mass of catalyst in the SR reactor, Q is the gas flow rate, superscript ox and S denote respectively conditions at the exit of the first oxidation reactor (inlet of steam reforming zone) and the presence of sulphur in the feed. As already pointed out, $x_{CH4}^{ox} = x_{CH4}^{ox,S} = 0.45$ were set according to literature data obtained during the CPO in air at CH_4/O_2=2 with a Rh based foam catalyst [4].

Also the amount of catalyst in the steam reforming reactor zone and the gas flow rate are unaffected from the presence of sulphur.

Thus the ratio of the apparent kinetic constants $\bar{k}^{S}_{SR}/\bar{k}_{SR}$ with or without sulphur added to the feed was calculated for each of the two catalyst from the above equations (3.15) and (3.16) at each sulphur concentration (2–58 ppm) by considering the methane conversion values experimentally measured at the exit of the CPO reactors. Assuming the activation energy of SR reaction is unchanged by sulphur poisoning, an "activity coefficient" due to the inhibiting effect of sulphur can be defined as the ratio of the pre-exponential factors in the Arrhenius expression for the apparent kinetic constant of SR:

$$activity\ coefficient_{SR} = \frac{A^{S}_{SR}}{A_{SR}} = \frac{\bar{k}^{S}_{SR}}{\bar{k}_{SR}}\ exp\left(-\frac{E_{a,SR}}{R}\left(\frac{1}{\bar{T}} - \frac{1}{\bar{T}^{S}}\right)\right) \tag{3.17}$$

where $\bar{T}$ represents an average temperature in the SR reactor, which was simply estimated as the mean of the experimental values measured in the second portion of the catalytic monoliths (centre and exit, respectively at 5mm and 10 mm from the inlet):

$$\bar{T} = \frac{T^{5mm}_{cat} + T^{10mm}_{cat}}{2} \quad [K] \tag{3.18}$$

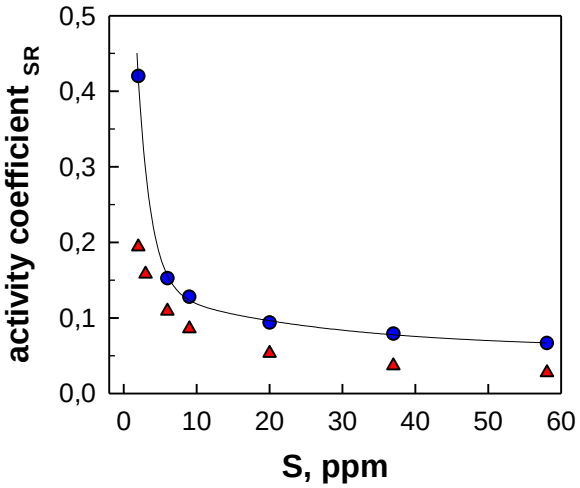

Figure 15: Activity coefficient accounting for S poisoning of the steam reforming reaction over RhP/LA and Rh/LA honeycomb catalysts as a function of S level in the feed during methane CPO (CH_4/O_2=2 in air).

The activity coefficient values followed similar trends for the two catalysts (Figure 15), decreasing markedly for the initial addition of few ppm of S to the feed, and then approaching a saturation value at the highest S level. In particular for the Rh-P/LA catalyst the activity coefficient was estimated in the range from 0.4 to 0.1, being as much as 2 times higher than for the reference Rh/LA catalyst. Those results reflect the higher tolerance of P-promoted Rh towards strong sulphur

chemisorption, which in turn resulted in a higher residual active metal surface (Table 3). In fact activity coefficients suggest that the drop in the rate of methane steam reforming is mainly connected to the loss of those active sites capable of strongly chemisorb CO rather than on the total exposed metal sites [52].

3.3.5 Dry reforming tests

3.3.5.1 Catalysts characterization

	Elemental analysis*		S BET* [m^2/g]
	%Rh (wt)	%P (wt)	
1% Rh-P/LA_T	0.9 [b]	0.1 [b]	117
1% Rh/LA_T	0.9 [b]	-	120
1% Rh-P/LA	1 [c]	0.19 [c]	130.6
1% Rh/LA	0.9 [c]	-	122.2

a)After reduction at900°C
b)By AAS at TUM
c)By ICP-MS

Table 5: Denomination of catalysts, elemental composition and BET surface.

Actual content of metals and BET measurements, shown in Tab.5, were performed to confirm the analogy between the samples synthesised with slightly differences in the preparation methods (see section 2.1.1). The amount of Rh after the final TPR treatment at 900 °C , was the same for both the catalysts prepared at TUM and similar to the values of noble metal loading of their corresponding sample utilized in CPO. The presence of phosphorous, though with a lower value than the expected loading, indicated that no significant loss occurred after the thermal treatment at 900°C. The BET surface areas of both Rh-P/LA_T and Rh/LA_T were in line with the results obtained with the catalysts previous prepared, showing a limited decrease in the surface area in comparison to the bare support (LA_{BET} =140 m^2/g) due to the presence of rhodium in all the cases.

	H_2 uptake[a]	Dispersion[b]	Diameter	CO uptake[c] (weak+strong)	Strong (CO gem.)	Weak (CO linear)	Dispersion	Diameter
	[µmol/g]	[%]	[nm]	[µmol/g]			[%]	[nm]
Rh-P/LA_T	87	44.8	2.4	57.9	47.2	10.7	39.2	2.8
Rh/LA_T	38	19.7	5.5	30.5	26.1	4.1	19.6	5.6
Rh-P/LA[c]	-	-	-	89.1	80.4	8.7	51.3	2.1
Rh/LA[c]	-	-	-	57.1	49.5	7.6	37.5	2.9

a) chemisorption measured at 35°C
a) stoichiometry H/Rh=1
c) see section (3.3.2)

Table 6: Results of H_2 and CO chemisorption measurements, percentage metal dispersion and average diameter of crystallites.

In table 6, results obtained with H_2 and CO chemisorption are reported. The dispersion values have been calculated with a stoichiometry H/Rh=1, while in the case of CO adsorption the stoichiometry has been assumed equal to 2 and 1 respectively for the strong and weak adsorption components on Rh accordingly to DRIFT experiments reported in section 3.3.2.

As regards the samples prepared at TUM, H_2 and CO chemisorption data show a good agreement, with a very slight difference for Rh-P/LA_T, while perfectly coincident for the undoped catalyst. Through the very similar comparative data, obtained with techniques employing different adsorbate molecules, it is possible to confirm the reliability of dispersion calculations of Rh metal particles by means of CO distinguishing between strong and weak adsorption. It must be emphasized, that the efficiency of CO measurements is also supported by the utilization of higher amount of catalyst (up to 1 gram) than the H_2 tests, that together to a higher stoichiometry CO/Rh (=1-2) than H_2/Rh (0.5), allows to measure a significant uptake. Moreover, it is claimed that if H_2 chemisorption is carried out at room temperature, hydrogen spillover processes on the support can easily occur in presence of a metallic phase [61]. Thus, the relative higher value of dispersion calculated for Rh-P/LA_T by H_2 in comparison to that calculated by CO could be related to a higher H/Rh ratio than the real value, due to the spillover effect. Despite all, focusing on the dispersion results, it is clear that the P addition leads to a higher dispersion of Rh particles: in the lower case (i.e. CO measurements) RhP/LA_T has a double dispersion than the reference sample and an average diameter of the metal particles equal to 2.8 instead of 5.6 nm calculated for Rh/LA_T. In table 2, the value of dispersion and dimension of particles relative to Rh-P/LA and Rh/LA already described in section 3.3.2 are also recalled for the sake of comparison. Their dispersion values are slightly higher than those corresponding to the catalysts prepared later, thus resulting in lower dimension of crystallites; although phosphorous results in an improved dispersion in both the cases, the difference is probably

ascribed to the changes in the preparation routes, especially taking account the different precursor for phosphorous used to prepare Rh-P/LA (see section 2.1.1).

In order to have a further probe on the difference of dispersion between the doped catalyst and its counterpart, TEM images were taken. Unfortunately, the pictures collected (not shown) for the two samples didn't allow to estimate particles mean size and particles size distribution. Indeed, for high surface areas supports, the TEM observation becomes more difficult because of the low contrast between the small metallic particles and the support and it is not easy to obtain quantitative data on metal dispersion [61].

3.3.5.2 Dry reforming catalytic tests

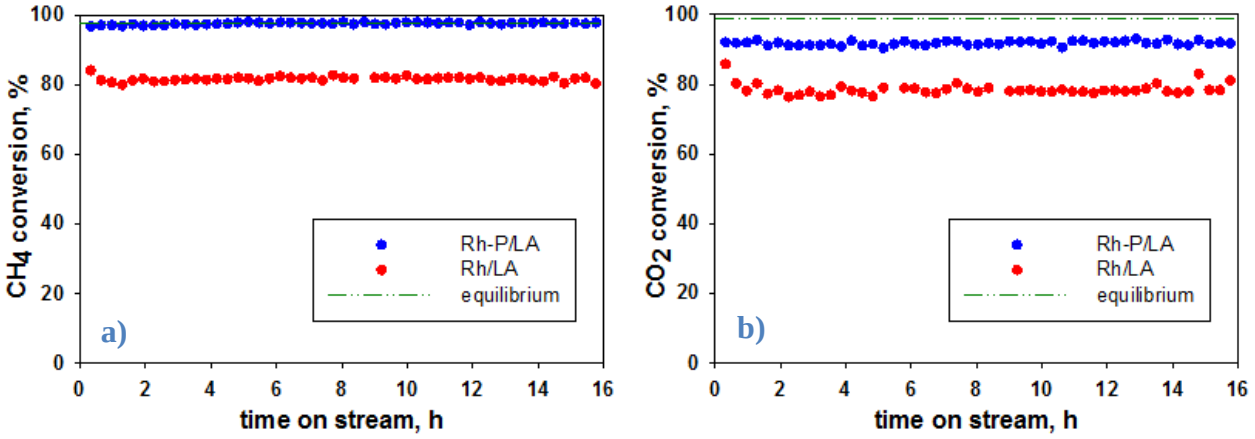

*Figure 16: Time-dependent conversions of CH_4 (a) and of CO_2 (b) over Rh-P/LA_Tand Rh/LA_T , P=1 atm, T furnace=850°C, P 1 atm, space velocity 1.2*10^5 ml/(h g).*

The time-dependent activities of supported Rh catalysts are plotted in Fig. 16. The conversions of CH_4 and CO_2 remained unchanged during the period of study, 16 h. Especially the P doped sample, which conversion values are arranged in a straight line, didn't show any sign of deactivation. Both methane and CO_2 conversions approached the equilibrium prediction for Rh-P/LA_T, resulting in an H_2/CO ratio equal to 1, as it is shown in fig. 17, while the activity of undoped catalyst slightly departed from the equilibrium lines.

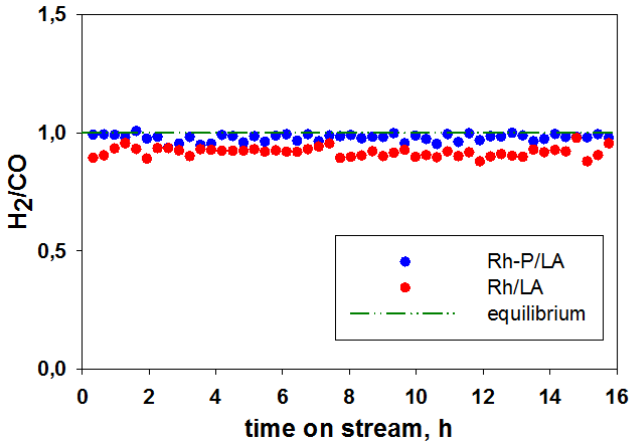

*Figure 17: Time-dependent H_2/CO ratio over Rh-P/LA_Tand Rh/LA_T , P=1 atm, T furnace=850°C, P 1 atm, space velocity 1.2*10^5 ml/(h g).*

Altough the good stability and high activity of both the samples, Rh-P/LA_T displayed a better overall performance, i.e. higher conversion than the reference Rh/LA_T. This occurrence is likely ascribed to the higher metal dispersion of P doped Rh catalyst. Indeed, Wang and Ruckenstein [62] investigated the effect of particle size on the specific activity of Rh for the CO_2-reforming of CH_4 over the Rh/γAl_2O_3 catalyst. They changed the particle size by varying the Rh loading: the turnover frequency (TOF) was found strongly dependent on the particle diameter of Rh in the range of 1–7 nm. This result suggested to the authors that the reforming reaction is structure sensitive on γAl_2O_3 supported Rh catalyst. These findings agree with the results obtained in this work, as higher activity is achieved with the more dispersed Rh-P/LA which average particle diameter is half in comparison to the reference Rh/LA.

Equilibrium calculations (shown in fig.18) indicated the occurrence of very small amount of solid carbon (0.58% mol) at operative conditions used in this work. However, during reforming operations, coke formation is possible even when it is not predicted by thermodynamics. For example, Rostrup-Nielsen investigating the carbon deposition reactions over Ni catalysts [27] stated that the Boudouard and methane decomposition reactions are catalyzed by Ni, causing carbon to grow as a fibre/whisker. In the context of steam methane reforming, in which the primary carbon deposition route is methane decomposition, Rostrup-Nielsen described carbon formation related also to a kinetic allowance in spite of overall thermodynamics leading to methane decomposition into carbon (instead of reacting with steam).

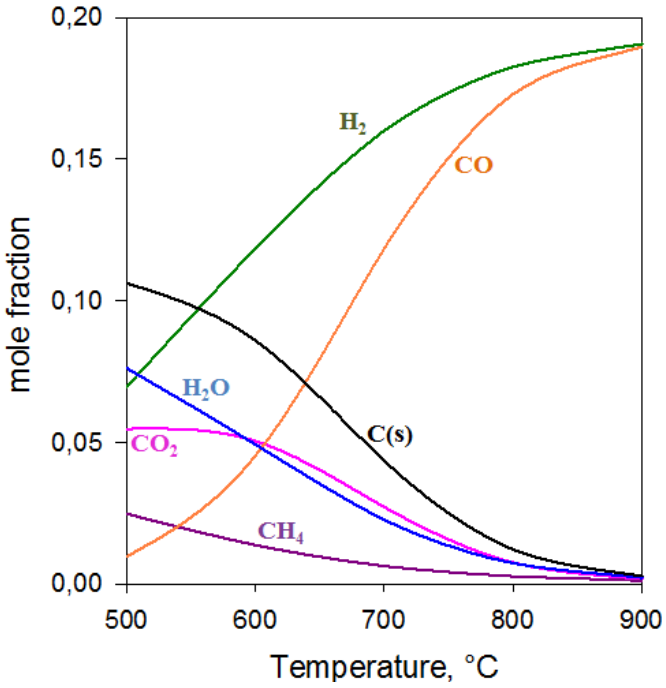

Figure 18: Equilibriun mole fraction versus temperature calculated at atmospheric pressure and $CH_4/CO_2/N_2=1/1/2$.

Under dry reforming conditions, this situation may even get worse in comparison to steam reforming, since the absence of steam as reactant that can gasify deposits of solid carbon.

In this work, both catalysts investigated, showed an excellent stability without any decay in conversion of CH_4 and CO_2, whose occurrence is generally explained through coke formation during dry reforming operations. This outcome is especially relevant for Rh-P/LA indicating the maintenance of a strong interaction between Rh and P also under severe reaction conditions, avoiding losses of phosphorous at high temperature. In addition to the stability results, visual inspection of the alumina tube in which the catalysts were allocated, didn't show any carbon deposition after testing runs. The non-occurrence of coke formation is of particular relevance for Rh-P/LA_T, since the previous studies of Chakrabarti et al [6] found a negative effect of phosphorous addition (1 atom of P for every 5 atoms of Rh) to the catalysts during steam reforming of methane, in terms of conversion and carbon deposition. As above mentioned, they argued that phosphorous decreased the dispersion of Rh-αAl_2O_3 spheres from a value of 10% to 3% (with Rh particles of ca30nm). Moreover, they demonstrated through SEM images of P doped systems, the formation of carbon filaments on the catalyst after performance testing. They observed the presence of whisker carbon species, tipically formed on Ni catalysts due to methane decomposition and Bodouard reaction, attributing this situation to the poison effect of Phosphorus on the surface–carbon gasification reactions, leading to accumulation of carbon on surface of rhodium. The impressive discrepancy in the effect of P is likely related to the different dispersions of doped

catalysts as well as to the absence of a H_2 pretreatment at high temperature [6] which is required to obtain an effictive interaction between the two metals.

3.4 Conclusions

A novel monolith catalyst with Rh supported on γ-alumina and doped with phosphorous was prepared by temperature-programmed reduction of oxidic precursors in flowing H_2 and tested for the first time in the CPO of methane at short contact time and high temperature in the presence of sulphur. The interaction of phosphorous with Rh showed several positive effects:

i) it formed a metallic surface capable to strongly adsorb CO;
ii) it improved the metal dispersion on the alumina support;
iii) it significantly inhibited the strong sulphur adsorption and lowered the resulting surface S coverage with special regards to those sites capable of strong CO adsorption.

Reaction of phosphorous with the alumina also enhanced the stability of the support probably through the formation of surface $AlPO_4$ but partially prevented a complete reaction of P with Rh. Direct comparison of CPO performance data with the reference undoped Rh catalysts showed a significant enhancement of the specific steam reforming reaction rate, which can be correlated to the higher metal dispersion, and markedly contrasts with previous reports on the poisoning effect of P on Rh/α-Al_2O_3. Above all, the P doped Rh catalyst was significantly more S-tolerant then the reference undoped system, guaranteeing a higher methane conversion and H_2 selectivity at any S level in the feed up to 58ppm, while reducing the risk of excessive catalyst overheating due to the S-inhibition of the endothermic steam reforming reaction path. The higher residual steam reforming activity of the Rh-P catalyst during the CPO of methane in the presence of sulphur appears to be correlated to the larger exposed active metal surface capable to strongly bond CO (as gem-dicarbonyl species) at room temperature.

The beneficial effect of P-doping has also been demostrated during the dry reforming tests carried out at TUM, further confirming the promising results found for CPO of methane in the presence of sulphur. Indeed, also in this reaction, the enhanced dispersion relative to phosphorous addition leads to higher activity than the reference undoped catalyst and excellent stability, without any deactivation due to coke formation, on the contrary of previous results reported in literature on detrimental effect on dispersion and steam reforming activity of ethane for P doped systems.

References

1) Enger B.C. , Lødeng R., Holmen A.; Appl. Catal. A, 346 (2008) 1–27
2) G.J. Panuccio, B.J. Dreyer, L.D. Schmidt, AIChE Journal 53 (2007) 187–195
3) Hulteberg C.; Int. J. Hydrogen Energy 37 (2012) 3978-3992
4) Bitsch-Larsen A., Degenstein N.J., Schmidt L.D.; Appl. Catal. B. 78 (2008) 364–370
5) Cimino S. , Torbati R., Lisi L., Russo G.; Appl. Catal. A. 360 (2009) 43–49
6) Chakrabarti R., Colby J.L., Schmidt L.D., Appl. Catal. B 107 (2011) 88–94
7) Bartholomew C.H.; Appl. Catal. A. 212 (2001) 17–60
8) R. Prins, M.E. Bussell, Catalysis Letters 142 (2012) 1413–1436
9) S.T. Oyama, T. Gott, H. Zhao, Y. Lee, Catalysis Today 143 (2009) 94–107
10) ClarkP., OyamaS.T., J. Catal. 218 (2003) 78–87
11) A.W. Burns, K.A. Layman, D.H. Bale, M.E. Bussell, Applied Catalysis A 343 (2008) 6876
12) T. Montesinos-Castellanos, A. Zepeda, B. Pawelec, J.L.G. Fierro, J.A. de los Reyes, Chemistry of Materials 19 (2007) 5627–5636
13) S.J. Sawhill, K.A. Layman, D.R. Van Wyk, M.H. Engelhard, C. Wang, M.E. Bussell, Journal of Catalysis 231 (2005) 300–313
14) Z. Wu, F. Sun, W. Wu, Z. Feng, C. Liang, Z. Wei, C. Li, J. Catal. 222 (2004) 41–52
15) F. Sun, W. Wu, Z. Wu, J. Guo, Z. Wei, Y. Yang, Z. Jiang, F. Tian, C. Li, J. Catal. 228 (2004) 298–310
16) Hayes J. R., Bowker R. H., Gaudette A. F., Smith M. C., Moak C. E., Nam C. Y., Pratum T. K., Bussell M. E. J. of Catal. 276 (2010) 249–258
17) Y. Kanda, C. Temma, K. Nakata, T. Kobayashi, M. Sugioka, Y. Uemichi, Appl. Catal. A 386 (2010) 171–178
18) Energy Information Administration, Annual Energy Review 2006 (2007)
19) Mark, M.F., Maier, W. F. J. Catal. 164 (1996) 122-130
20) Gadalla, A.M.; Bower, B. *Chem. Eng. Sci.* 1988, 43, 3049-30624
21) Arbag H., Yasyerli S., Yasyerli N., Dogu G., Int. J. Hydrogen Energ. 35 (2010) 2296-2304
22) J. M. Ginsburg, Juliana Pina, Tarek El Solh, Hugo I. de Lasa Ind. Eng. Chem. Res. 2005, 44, 4846-4854
23) Teuner, St. C.; Neumann, P.; Von Linde, F. The Calcor Standard and Calcor Economy Processes. Oil Gas Eur. Mag. 2001,3, 44
24) Udengaard, N. R.; Bak Hansen, J. H.; Hanson, D. C.; Stal, J. A. Sulfur promoted Reforming Process lowers Syngas Hydrogen/Carbon Monoxide Ratio. Oil Gas J. 1992, 90 (10), 62

25) Sacco, A. Jr.; Geurts, F.W.A.H.; Jablonski, G.A.; Lee, S.; Gatell, R.A. J. Catal. 1989, 119, 322
26) Bradford, M.C.J.; Vannice, M.A. Catal. Rev. Sci. Eng. 1999, 41, 1–42
27) Rostrup-Nielsen, J.R.; Bak Hansen, J-H. J. Catal. 1993, 144, 38-49
28) Zhang, Z. L.; Tsipouriari, V.A.; Efstathiou, A.M.; Verykios, X.E. *J. Catal.* **1996**,158, 51-63.
29) Erdey L., Gál S., Liptay G., Talanta 11 (1964) 913–940
30) Cimino S., Landi G., Lisi L.,Russo G., Catal. Today 117 (2006) 454–461
31) Torbati R. , Cimino S., Lisi L., Russo G.;,Catal Lett 127 (2009) 260–269
32) Wang D., Dewaele O., Groote A.M., Froment G.F., J. Catal. 159 1996, 418
33) Boumaza A., Favaro L., Lédion J., Sattonnay G., Brubach . B., Berthet P., Huntz A. M., Royc P., Teto tR., J. Solid State Chem. 182 (2009) 1171–1176
34) Maroto-ValienteA., Rodriguez-RamosI., Guerrero-RuizA., Catal. Today 93–95 (2004) 567–574
35) Trautmann S., Baerns M., J. Catal. 150 (1994) 335–344
36) Raskó ., Bontovics J., Catal. Lett. 58 (1999) 27-32
37) Finocchio E., Busca G., Forzatti P., Groppi G., Beretta A., Langmuir 23 (2007) 10419–10428
38) Solymosi F., Pasztor M., J. Phys. Chem. 89 (1985) 4789–4793
39) Paul D. K., Marten C. D., Yates Jr.J. T., Langmuir, 15 (1999) 4508–4512
40) Basu P., Panayotov D. , Yates J. T., J. Am. Chem. Soc. 110 (1988) 2074–2081
41) Layman K. A., Bussell M. E., J. Phys. Chem. B 108 (2004) 10930–1094
42) Hadjiivanov K. I., Vayssilov G. N., Adv. Catal. 47 (2002) 307–511
43) BulushevD. A., FromentG. F., J. Mol. Catal. A: Chem. 139 (1999) 63–72
44) Jackson S. D., Brandreth B. J., Winstanley D., J. Chem. Soc., Faraday Trans. 1 83 (1987) 1835-1842
45) NewtonM. A., DentA. J., Diaz-MorenoS., FiddyS. G., JyotiB., EvansJ., Chem. Commun. 0 (2003)1906–1907
46) McAllister B., Hu P., J. Chem. Phys. 122 (2005) (Article number 84709)
47) Oudar J., Catal. Rev.: Sci. Eng. 22 (1980) 171–195
48) Konishi Y., Ichikawa M., Sachtler W., J . Phys. Chem. 91 (1987) 6286–6291
49) Nasri N. S., Jones J. M., Dupont V. A., Williams A., Energy Fuels, 12 (1998) 1130–1134
50) Chuang S.S., Pien S.-I., Sze C., J. Catal. 126 (1990) 187–191
51) Cimino S., Lisi L., Russo G., Torbati R.; Catal. Today 154 (2010) 283–292
52) Wei J., Iglesia E., J. Catal. 225 (2004) 116–127
53) Cimino S., Lisi L., Russo G., Int. J. Hydrogen Energy 37 (2012) 10680-10689
54) Hong J., Zhang L., Thompson M., Wei W., Liu K.; Ind. Eng. Chem. Res. 2011, 50, 4373–4380

55) Horn R., Williams K.A., Degenstein N.J., Bitsch-Larsen A., Dalle Nogare D.,Tupy S.A., Schmidt L.D. J. of Catal. 249 (2007) 380–393
56) Horn R., Williams K.A., Degenstein N.J., Schmidt L.D., J. Catal.242 (2006) 92–102
57) Beretta A., Groppi G., Lualdi M., Tavazzi I., Forzatti P., Ind. Eng.Chem. Res. 48 (2009) 3825–3836
58) Michael B.C., Nare D.N., Schmidt L.D. Chem Eng Sci 65 (2010) 3893-3902
59) Cimino S., Lisi L., Mancino G., Musiani M., Vázquez-Gómez L., Verlato E., International Journal of Hydrogen Energy 37 (2012) 17040–17051
60) Cimino S., Lisi L., Russo G., Int. J. Hydrogen Energy 37 (2012) 10680–10689
61) Perrichon V., Retailleau L., Bazin P., Daturi M., Lavalley J.C., Appl. Catal., A 260 (2004) 1-8
62) Wang H.Y., Ruckenstein E., Appl. Catal. A, 204 (2000) 143-152

4. Effect of sulphur during the catalytic partial oxidation of ethane to syngas over Rh and Pt honeycomb catalysts

4.1 Introduction

In addition to methane, other fuel feedstocks, such as light hydrocarbons heavier than CH_4, could be considered to feed a CPO reactor to obtain syngas. Since the natural gas is typically composed of methane and ethane, the objective of obtaining syngas from ethane is a direct use of natural gas as feed at the on-site gas field without separating respective components.

In the case of CH_4 CPO over Rh and Pt it is largely accepted that the gas-phase paths are negligible at atmospheric pressure and the catalytic route dominates [1-4]. However, the gas phase chemistry can play an increasingly important role for higher alkanes following the progressive lower stability of the C-H bond [5,6], as in the case of CPO of ethane or propane [7,8], when large quantities of ethylene can be formed with Pt based catalysts (but not with Rh) mainly through homogeneous reactions if proper conditions are met [5,7-12].

The adverse impact of sulphur compounds on catalytic performance is well known [13,14], however, only few publications are available in the field of sulphur poisoning during CPO of higher hydrocarbons. Since the S inhibition of the highly endothermic reforming reactions causes the reactor temperature to rise considerably [15-18] and in turn increases the risk of catalyst deactivation due to overheating by hot-spot formation close to the entrance section [4], the issue of catalyst stability may become even more serious during the CPO of ethane or propane due to their higher reaction enthalpy as compared to CH_4 [19]. However, regarding the effect of the hydrocarbon fuel type (form methane up to diesel) on syngas production by CPO on Rh-based catalyst, it was reported that increasing both the molecular weight and the aromaticity makes the fuel more sulphur tolerant for H_2 generation. In particular with propane feed, a small addition of SO_2 (5 ppm) caused a somehow surprising, small but still appreciable increase of H_2 production [20], which was reduced by any further increase of S level.

Moreover, it was also found that Pt-based catalysts have lower activity but greater tolerance than Rh to sulphur poisoning [15,17].

The object of this chapter is the study of the effect of sulphur addition to the feed during the CPO of ethane for syngas production (C_2H_6/O_2=1) over γ-alumina supported Rh and Pt catalysts anchored to honeycomb monoliths.

4.2 Experimental Procedure

Standard supported Rh and Pt catalysts (respectively 1 and 2% by weight of the alumina, in order to obtain similar atomic concentrations) were prepared via repeated incipient wetness impregnations as described in Chapter 2.1.1. The catalytic tests were carried out on monolith samples as described in Chapter 2.2.1, under self-sustained pseudo-adiabatic conditions conditions at fixed pre-heating (235 °C or 350 °C) and an overall pressure of P=1.2 bar, respectively using air or enriched air (O_2:N_2 = 1:2) as oxidant. The impact of sulphur addition (2 and 58 ppmv SO_2) was investigated at fixed C_2H_6/O_2 feed ratio=1 (stoichiometric for syngas production), under both transient and steady state conditions.

4.3 Results and Discussion

4.3.1 Rh catalyst

Sulphur poisoning on Rh catalysts during the CPO of ethane was rapid and completely reversible, in analogy with what found over Rh/La and Rh-P/LA catalysts with methane feed.

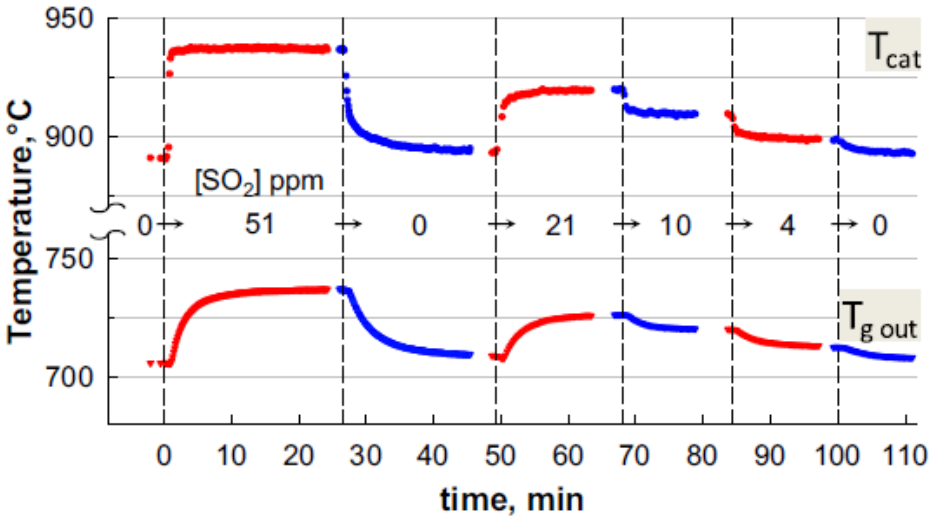

Figure 1: Transient response to SO_2 addition and removal on the temperatures measured in the centre of the catalytic monolith and in the gas leaving the reactor during ethane CPO over Rh/LA catalyst. Feed C_2H_6 25 Sl/h,C/O=1, enriched air (N2:O2=2:1), GHSV 5.8x10^4 h^{-1},pre-heating 350 °C.

Fig. 1 shows that the step addition of 51 ppmv of S to the feed to the CPO reactor resulted in a sharp but moderate increase in the temperature of the catalyst by roughly 40°C, followed by a corresponding increase in the outlet temperature of the product gas. A new steady state of the CPO

reactor was reached within roughly 10 min, characterized by stable catalytic performance with a somewhat lower activity towards syngas formation (Fig. 2).

In fact the oxygen conversion was always 100% and was not affected by sulphur poisoning, in good agreement with results of Bitsch-Larsen et al. [15] who reported that the rates of O_2 consumption (i.e. O_2 spatial profiles along the reactor) and the initial CH_4 conversion are independent of the sulphur level. This is most likely due to the kinetics of the oxidation reactions which remain much faster than the transport phenomena even in the presence of sulphur.

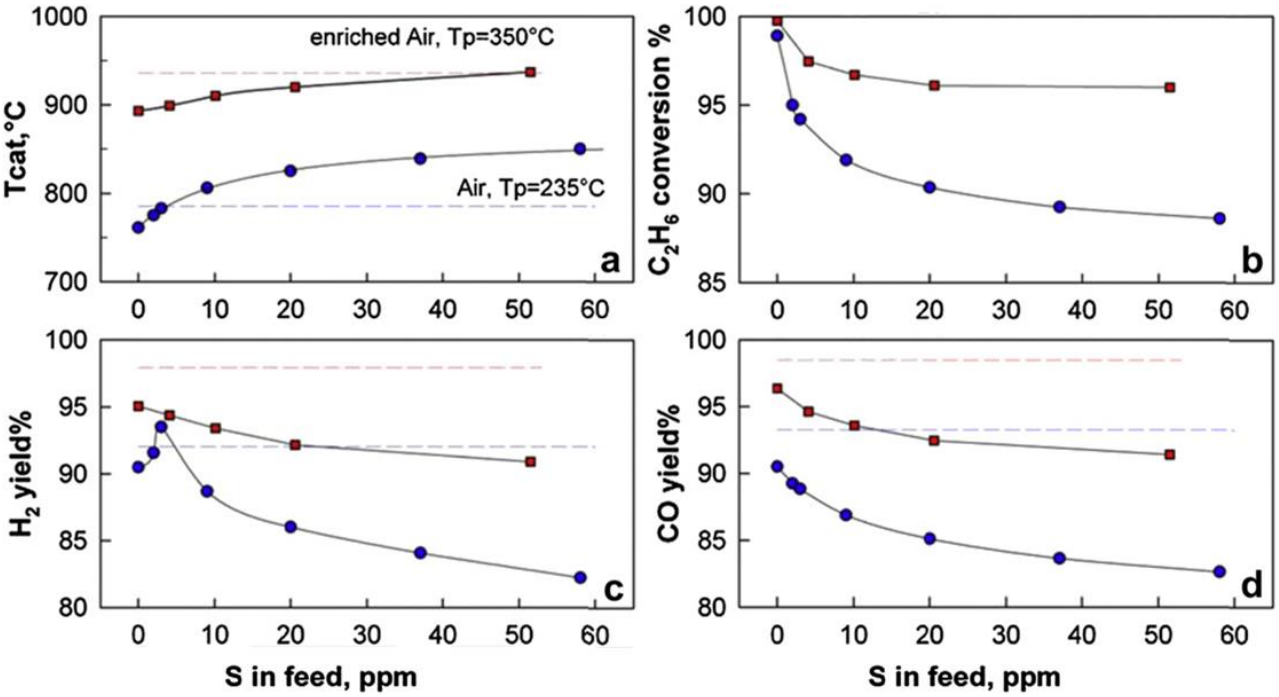

Figure 2: Effect of SO_2 addition on the temperature of the catalyst, C_2H_6 conversion, yields to H_2 and CO during the CPO of ethane over Rh/LA monolith operated at C/O=1 with air or enriched air as the oxidant, respectively at feed pre-heating of 235 °C and 350 °C, GHSV=5.8x10^4 and 6.7x10^4 h^{-1}.

The complete reversibility of the S-poisoning effect under the studied reaction condition was confirmed by the identical values of the temperature measured in the reactor before the addition and after the removal of sulphur (Fig. 1). The temperature of the catalyst was found to decrease immediately and the initial level was regained on a time scale that is comparable to that of the poisoning process. A further step addition of 21ppm SO_2 followed by progressive step reductions in the S-level back to sulphur free conditions (Fig. 1) confirmed the qualitative repeatability of the observed catalytic behaviour and demonstrated that the poisoning effect is directly dependant on S-concentration. In the absence of sulphur Rh catalyst showed an almost complete conversion of ethane feed (Fig. 2b) and yields to CO and H_2 (Fig. 2c,d) close to the corresponding values

predicted by adiabatic equilibrium (dashed lines), which are higher when the CPO reactor is operated at a higher temperature (Fig. 2a), i.e. with enriched air and a high pre-heating level.

Heat losses from the hot CPO reactor are responsible for small losses in fuel conversion and selectivity to syngas with the consequent deviation from equilibrium in the distribution of products [19]. At steady state the addition of S to the feed to Rh-based monolith caused a monotonic increase in the temperature of the catalyst and a corresponding reduction in the conversion of ethane (Fig. 2a,b) which was more pronounced when the CPO reactor was operated at higher dilution (i.e. in air) and at lower pre-heating. Moreover, the inhibiting effect appears to saturate for lower levels of S if the initial (S-free) operating temperature of the catalyst is higher. In agreement with previous results of CH_4 CPO on Rh based catalysts, also discussed in this dissertation, it is suggested that the inhibiting effect of S depends on the equilibrium coverage of the most active, highly dispersed Rh sites due to the (reversible) formation of surface Rh-sulphide species, which is favoured by high values of P_{H2S}=P_{H2} ratio and low temperatures [16,17,21].

Regarding the effect of S on steady state yields CO and H_2 reported in Fig. 2 c,d, they both decreased along with fuel conversion upon S addition when the C_2H_6 CPO reactor was run at high temperature (≥900°C). However, when operating the Rh catalyst on air at lower temperatures (≈750 °C), small concentrations of S in the feed caused an unexpected increase in the H_2 yield, which passed through a maximum exceeding its equilibrium value for [S] ≈ 3 ppmv. On the other hand, the yield to CO decreased progressively for increasing S level in the feed, following the same trend of ethane conversion. A similar, though less evident, promoting effect of low concentrations of S on the hydrogen production was previously identified during the CPO of propane over Rh catalyst but was not discussed further [20]. In order to get some more insights into the origin of such unexpected increase in H_2 selectivity induced by S on Rh catalyst, Fig. 3 depicts the flows of major species from the CPO reactor running on air, as a function of S in feed; the same data are also reported in Table 1 for some selected S levels.

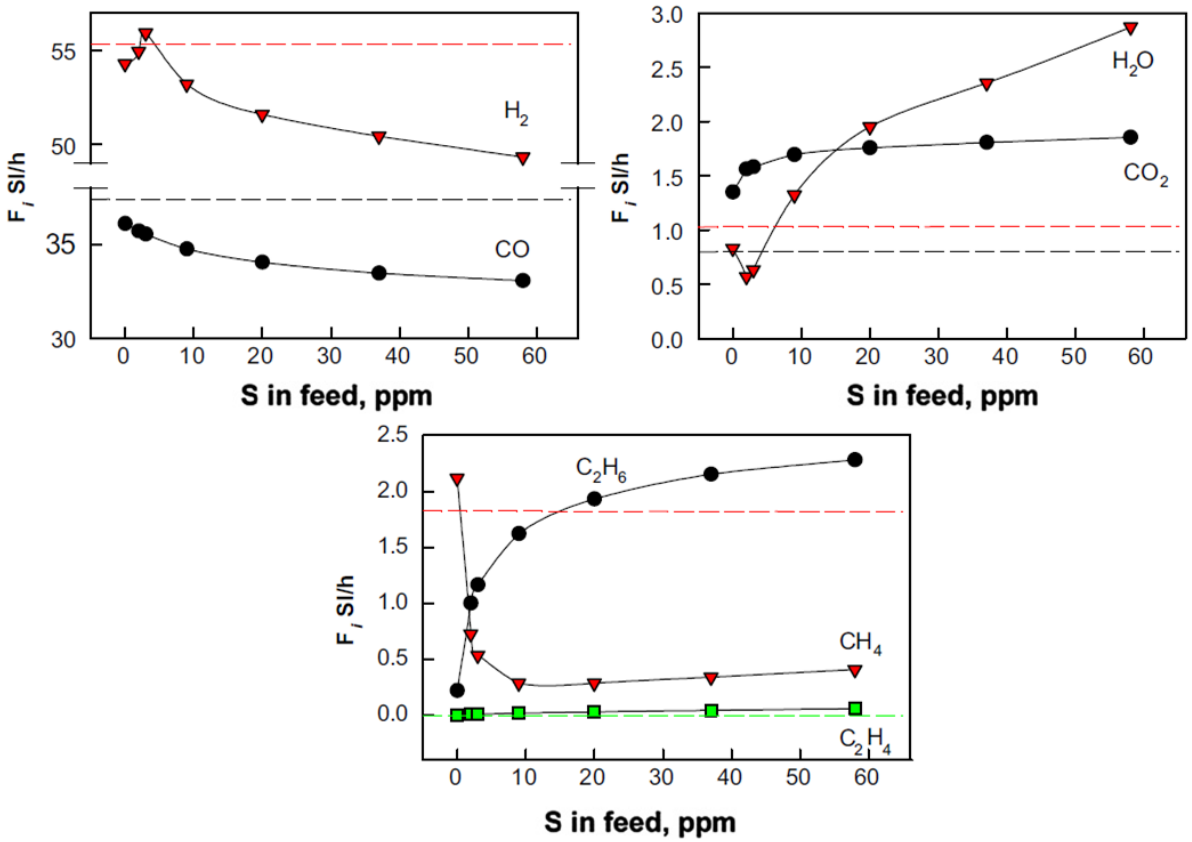

Figure 3: Effect of SO_2 addition on the steady state flows of products from the Rh/LA monolith during the CPO of ethane in air. Feed C_2H_6 20 Sl/h, C/O=1,GHSV = 6.7x10^4 h^{-1}, pre-heating 235°C.

	Product flows (Sl/h)					Differences			
S (ppm)	0	2	3	37	58	Δ(2-0)	Δ(37-2)	Δ(37-3)	Δ(58-3)
C_2H_6	0.22	1	1.16	2.15	2.28	0.78	1.15	0.99	1.12
CH_4	2.12	0.73	0.53	0.34	0.41	-1.39	-0.39	-0.19	-0.12
C_2H_4	1.8e-3	6.8e-3	8.8e-3	0.044	0.058	5e-3	0.037	0.035	0.049
CO	36.1	35.7	35.5	33.5	33.1	-0.39	-2.24	-2.07	-2.47
CO_2	1.35	1.56	1.6	1.81	1.85	0.21	0.24	0.21	0.26
H_2	54.3	54.9	55.9	50.4	49.33	0.65	-4.51	-5.49	-6.6
H_2O	0.83	0.57	0.63	2.36	2.87	-0.26	1.79	1.72	2.24
H_2/CO	1.5	1.54	1.57	1.51	1.49	-	-	-	-

Table 1: Effect of SO_2 addition at various concentrations on the steady state flows of products from the Rh/LA.

As already pointed out, in the absence of sulphur, H_2 and CO were produced with stoichiometric ratio (=1.5) at levels close to their corresponding equilibrium values (Fig.3a), with a slight deficit

which is mainly due the small fraction of unconverted C_2H_6 leaving the reactor (Fig.3c). The other main species CH_4, CO_2 and H_2O were close or slightly above their predicted values (dashed lines). Traces of ethylene (≈10ppmv) were measured in the product stream though its expected equilibrium concentration is lower by 2 order of magnitude. The maximum in H_2 production observed at low concentrations of S was accompanied by a simultaneous increase of unconverted C_2H_6 and a significant drop in CH_4 production (Fig. 3c, Table 1), which then levelled off for higher values of S. The differences in the flows of C_2H_6, CH_4 and H_2 produced with or without 2 or 3 ppm of S (Table 1) suggest that the first measurable effect of S at low concentrations is the inhibition of ethane hydrogenolysis (4.1).

$C_2H_6 + H_2 \rightarrow 2CH_4$, ΔH_r^{298K} = -65 kJ/mol (4.1)

$CO + 3H_2 \leftrightarrow CH_4 + H_2O$, ΔH_r^{298K} = -206 kJ/mol (4.2)

This reaction is reported to proceed at significantly fast rates on Rh [22-25], being responsible for the high CH_4 production observed on supported Rh/YSZ during the steam reforming of ethane [22], particularly in the presence of added H_2. In the same work [22] the authors ruled out any contribution to CH_4 formation via methanation ((4.2), the reverse of methane steam reforming) whereas this catalytic reaction was recently invoked to justify a complex evolution of CH_4 along Rh/α-Al_2O_3 based honeycombs during CPO of propane to syngas [6] under conditions similar to those used in the present study. C-C bond breaking during hydrogenolysis of alkanes (in particular ethane) is known to be a structure sensitive process [23-27], mainly catalyzed by step sites on the surface of Group VIII metals (in particular Ru, Os, Rh, Ir, and Ni [23-25]). Active step sites can be selectively removed or poisoned and their activity can be strongly suppressed by, for example, alloying with inactive metals (Ag or Cu on Ni [23,26,27]) or by presulphidation (on Ru [23], on Ir/Al_2O_3 and, to a lower extent, on the less active Pt/Al_2O_3 [24]): this approach has been applied in the design of industrial reforming catalysts to increase the selectivity for dehydrogenation versus hydrogenolysis [23].

Coming back to the flows of products from the Rh-based monolith, Fig. 3b shows that CO_2 had a slight increase with the initial S addition and then reached a plateaux, whereas H_2O was slightly reduced for the first addition of S and then increased progressively following the opposite trend of H_2. The simultaneous increase in H_2 and CO_2 product flows discovers a second effect of S addition at low concentrations involving the water gas shift reaction (and it reverse) (WGS (4.3)), which is normally equilibrated on Rh catalysts under short contact time CPO conditions [1,2,22,28,29].

$CO + H_2O \leftrightarrow CO_2 + H_2$, ΔH_r^{298K} = -41 kJ/mol (4.3)

$C_2H_6 + 2H_2O \leftrightarrow 2CO + 5H_2$, ΔH_r^{298K} = +347 kJ/mol (4.4)

$C_2H_6 + 2CO_2 \leftrightarrow 4CO + 3H_2$, ΔH_r^{298K} = +429 kJ/mol (4.5)

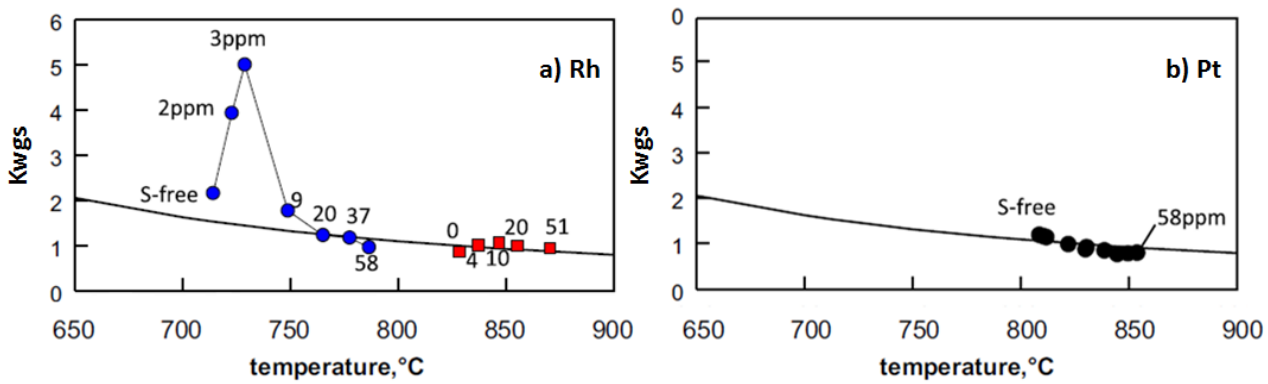

Fig. 4: Comparison between WGS equilibrium constant and values calculated from the measured concentrations of products during ethane CPO over Rh and Pt based monoliths, at varying SO_2 concentration in the feed (see legend), as a function of the gas temperature at the exit of the catalyst. CPO operation at C/O=1, with air and preheating at 235°C (circles), or enriched air at 350 °C (squares).

Fig. 4 illustrates that the WGS constant calculated from the experimental concentrations of H_2, CO_2, CO and H_2O produced with the Rh catalyst operated under S-free conditions in air approaches the corresponding theoretical value calculated at the exit temperature of the CPO reactor (Fig. 4a), being slightly higher than it. However, with 2-3 ppm of S in the feed, the WGS reaction was not equilibrated anymore: the sharp increase in the experimental value of the WGS constant indicates a kinetic limitation of the endothermic reverse WGS pathway, which was not able to consume the excess of H_2 made available due to the inhibition of ethane hydrogenolysis. The reduction in the number of available active sites due to the strong chemisorption of S on Rh [16] can slow down the WGS kinetics, as found during methane steam reforming at 700 °C over S-doped Rh/α-Al_2O_3 spheres [29]. However, increasing further the concentration of sulphur in the feed, the experimental value of the WGS constant approached again its theoretical equilibrium value, probably due to the simultaneous increase in the temperature level (above 750 °C) which sped up the kinetics on residual free Rh sites. In fact, when the Rh catalyst was operated at a higher temperature level the WGS reaction was always equilibrated, regardless of the presence of S (square symbols in Fig. 4a), thus explaining why the maximum in the yield to H_2 was found only during operation in air. Fig. 4b shows that WGS reaction was equilibrated also on Pt catalyst during CPO of ethane in air, either in the absence or in the presence of up to 58 ppm of SO_2 in the feed. This circumstance is justified by the higher temperature level at the exit of Pt catalyst comparable to the case of Rh operated with enriched air and higher pre-heating shown in Fig. 4a: Pt is reported to be less active than Rh for WGS reaction [28] but also more S-tolerant [15,21].

A third effect of sulphur appears clearly for concentrations exceeding 3 ppm (Fig. 3 b, c; Table 1): the increase in the unconverted ethane flow proceeded in a 1:2 ratio with the increase in the water

flow. The selectivity of the process to H_2 was progressively reduced, since roughly 5 moles of H_2 disappeared for every additional mole of ethane which was not converted, whereas C-atom selectivity to CO was unchanged since 2 moles of CO disappeared for every additional mole of unconverted ethane. This effect is fully compatible with the inhibition of the endothermic steam reforming of ethane (SR (4.4)). As shown in Fig. 5, the temperature increase measured in the second (reforming) part of the Rh-based monolith upon variation of S from 3 up to 58 ppm of S is proportional to the reduction in ethane conversion, which agrees well with the data collected for the CPO of methane over Rh/LA catalyst [see Chapter 3]. Following the analogy with the CPO of methane, the hypothesis on the adverse impact of sulphur on SR can be further supported by a simple heat balance in the gas phase (Eq. (4.6)), assuming adiabatic operation and thermal equilibrium between solid and gas in the second part of the reactor [19,28], which makes possible to calculate an apparent heat of reaction for ethane from the slope of the lines in Fig. 5:

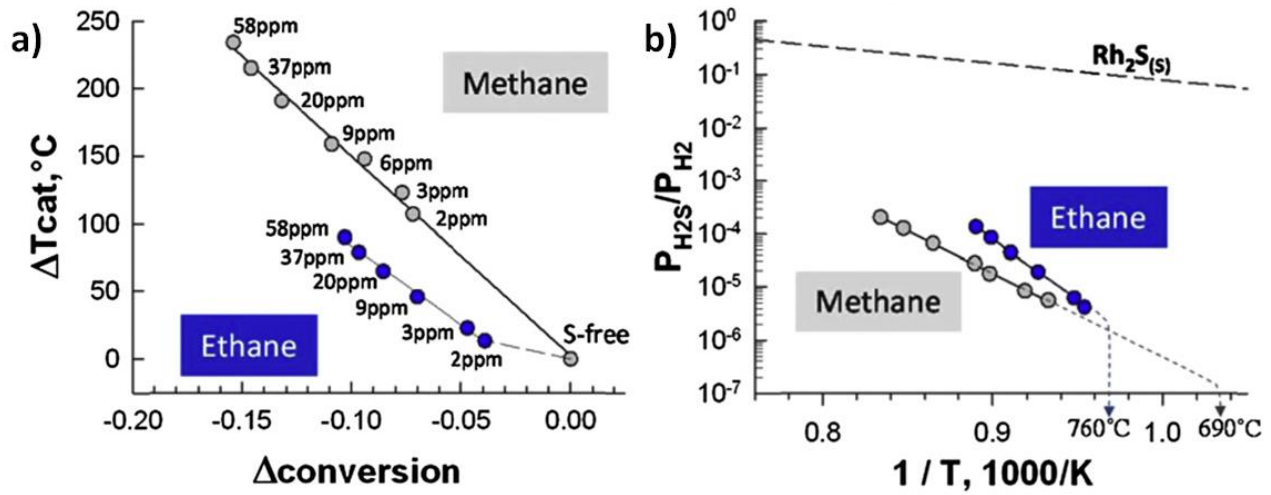

Fig. 5: CPO of methane or ethane over the same Rh/LA monolith: a) increase in catalyst temperature as a function of the variation of fuel conversion measured upon the addition of sulphur to the feed; b) comparison of the apparent thermodynamic activity of sulphur chemisorbed on Rh for $P_{H2S}=P_{H2}$ at the exit of the catalytic monolith with that of bulk Rh_2S; arrows indicate the catalyst temperature for S-free operation with methane [16] or ethane. Feed: methane or ethane at C/O=1, air as oxidant (O_2 20 Sl/h), pre-heating 235 °C.

$$\Delta H_r^{T_0} = \frac{-W c_p}{F_{fuel}} \left(\frac{\Delta T}{\Delta x_{fuel}} \right) \qquad (4.6)$$

where Cp is the specific heat of the product gas mixture, W is the total molar flow rate, and F_{fuel} is the hydrocarbon feed molar flow rate. For the case of ethane, with a Rh catalyst operating at roughly 750 °C with S-free feed and air as oxidant, it turns out that $\Delta H_r^{750\ °C}$ =+360 kJ per mole of C_2H_6, which corresponds well to the heat of the ethane steam reforming reaction at that temperature level. The superimposed and larger poisoning effect of the exothermic ethane hydrogenolysis

(Table 1) found for the addition of 2-3 ppm of S, is the cause of the initial low temperature increase and change in the slope of the curve relevant to ethane feed in Fig. 5a. The simultaneous inhibition of SR and r-WGS occurring at low concentrations of S sum to each other, and result in an apparent poisoning effect compatible with the stoichiometry of ethane dry reforming (Eq. (4.5)): moving from 0 to 2 ppm of sulphur, the drop in the CO flow was roughly 2 times the increase in CO_2 and 4 times that of C_2H_6 (Table 1), after subtracting the contribution from inhibited hydrogenolysis (from Eq. (4.1) $C_2H_6 + H_2 \rightarrow 2CH_4$). However no evidence of a direct dry reforming route was found during CPO of CH_4 with added CO_2 on Rh catalysts, and the present data suggest a marginal role of this reaction due to the slow kinetics with respect to steam reforming and direct/reverse WGS [5].
The adverse impact of sulphur on the rate of SR on Rh catalyst is significantly lower in the case of ethane with respect to methane: at the maximum concentration of S tested (58 ppm), the measured drop of fuel conversion ascribed to the inhibition of SR exceeds 15 points % for methane, with a corresponding $\Delta T = +230°C$, whereas it accounts for only 6 points % for ethane ($\Delta T = +90°C$). A comparative study of steam reforming reactivity with a Rh/YSZ catalyst demonstrated that ethane reacts significantly faster than methane under sulphur free conditions [22]. Steam reforming of methane on supported Rh catalysts was reported to proceed at higher rates on steps and corners surface sites [30], i.e. on small, highly dispersed metal crystallites which strongly interact with the support, particularly alumina. The inverse spillover of adsorbed H_2O from the support to the metal was recognized as a key step in the overall steam reforming reaction since it is an effective source of H_2O for the Rh sites on which dissociation occurs [31,32]. The resulting adsorbed oxygen and hydroxyl then oxidize the adsorbed CH_x species [32]. In a previous work [17] it was shown that under CPO conditions sulphur preferentially chemisorbs on those highly dispersed Rh crystallites, hindering the reaction with the surface hydroxyl groups of the alumina. However, the access of reactants to larger metal sites is less affected by chemisorbed sulphur [17] and H_2O adsorbed on the metal not only results from inverse spillover from the support [32]: therefore some residual activity for steam reforming is preserved [17,29]. It is reasonable that the reforming activity on those free Rh active sites is higher for ethane rather than for methane, which in turn explains the lower adverse impact of S on the conversion of the fuel to syngas and on the corresponding temperature increase. As a consequence, for the same value of $P_{H2S}=P_{H2}$ at the exit of catalytic reactor, the same Rh catalyst self-sustained higher temperatures during CPO of methane rather than of ethane (Fig. 5b), whereas the opposite holds for S-free feeds. The slight increase in CH_4 flow at high S levels (Fig. 3c), which was observed for CPO experiments on Rh at both temperature levels but not on Pt (see Fig. 7), could be related to the inhibition of the SR consuming some methane formed in the gas phase, in analogy with what observed in the CPO of CH_4 over the same Rh catalyst [16], or to the

re-activation of the hydrogenolysis reaction. Many investigations of ethane CPO at higher C/O feed ratios report that production of C_2H_4 occurs in the gas phase [7-12], though it is very low in the presence of Rh catalysts [26], whereas molar yields in excess of 60% can be attained on Pt based systems [7,9-12]. Recently it was shown by detailed spatial and temperature profiles that a definite correlation can be made between C_2H_4 production and reactor temperature, since >750 °C are required for the onset of homogeneous (oxygenative) dehydrogenation reaction [2]. Nevertheless, for any net C_2H_4 production to be measured, ethylene consumption routes have to be slower than its formation rate [5-6]: it was suggested that the high reforming activity of Rh, opposed to that of Pt, competes with cracking chemistry that occurs in the gas phase, by consuming both the reactant C_2H_6 and the product C_2H_4 [5-6]. This interpretation is herein supported by the progressive increase in the C_2H_4 flow from Rh monolith (Fig. 4 and Table 1), that is associated to the inhibiting effect of S on reforming reactions.

It was already recalled that reforming of C_2H_4 and C_2H_6 proceeds at similar rates on Rh/YSZ [22], with slight differences that can be attributed to the activation of hydrogenolysis in the case of ethane feed. Therefore, it can be argued that S inhibits simultaneously those reforming reactions, thus favouring the homogeneous ethylene formation chemistry, since also the temperature level increases, due to the lack of endothermic heterogeneous chemistry [6].

4.3.2 Pt catalyst

Fig. 6 compares the catalytic activities of supported Pt and Rh catalysts during the CPO of ethane with air in the absence or with various concentrations of SO_2 in the feed.

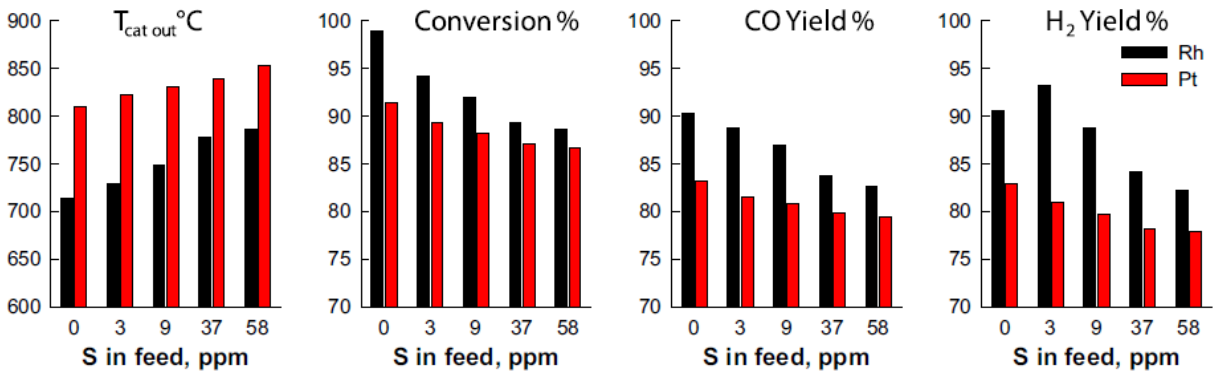

Figure 6: Comparison of steady state temperatures (at the exit of the catalysts), C_2H_6 conversions, CO and H_2 yields on Rh- and Pt-based monoliths in the absence and presence of SO_2. Feed C_2H_6: 20 Sl/h, C/O=1, air as oxidant, pre-heating 235 °C

Regardless of the sulphur level, the Pt catalyst showed lower ethane conversion and yield to syngas than Rh, while operating at higher temperature in the last section of the catalytic monolith. Previous works clearly demonstrated that Rh more rapidly consumes O_2 (under full external mass transfer control) in the first part of the reactor where a hot spot forms due to the large exothermicity confined in a small region [1,4-6]; on the other hand the slower reaction between C_2H_6 and O_2 on Pt can extend over the entire length of the catalyst resulting in an increase in temperature along the monolith with a maximum close to its exit [5]. Furthermore, Rh displays a significantly higher reforming activity compared to Pt: the activity gap between the two noble metals increases further moving from CH_4 to C2H6, since the reported order of activity was C_2H_6>CH_4 on Rh and the opposite on Pt [22].

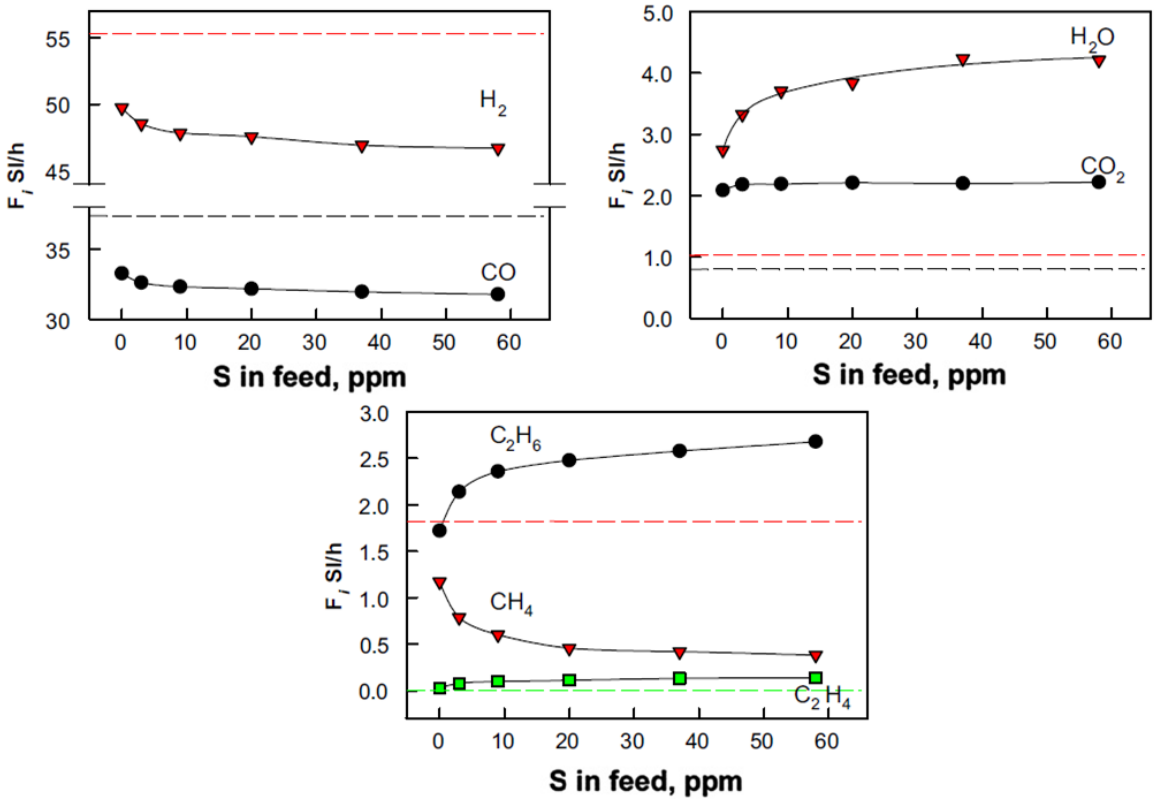

Fiure 7: Effect of SO_2 addition on the steady state flows of products from the Pt/LA monolith during the CPO of ethane in air. Feed C_2H_6: 20 Sl/h, C/O=1,GHSV 6.7x10^4 h^{-1}, pre-heating 235 °C.

	Product flows (Sl/h)			Differences	
S (ppm)	0	3	58	Δ(3-0)	Δ(58-3)
C_2H_6	1.72	2.14	2.68	0.42	0.54
CH_4	1.17	0.79	0.38	-0.38	-0.40
C_2H_4	0.024	0.079	0.137	0.055	0.058
CO	33.27	32.61	31.76	-0.66	-0.85
CO_2	2.08	2.19	2.22	0.09	0.03
H_2	49.74	48.54	46.71	-1.20	-1.83
H_2O	2.74	3.32	4.21	-0.58	0.89
H_2/CO	1.5	1.49	1.47	-	-

Table 2: Effect of SO_2 addition at various concentrations on the steady state flows of products from the Pt/LA monolith during the CPO of ethane in air. Feed C_2H_6: 20 Sl/h, C/O=1, pre-heating 235°C.

A closer look at flow rates of products from the Pt catalyst under S-free conditions (Fig. 7a-c and Table 2) shows that methane production was about the half with respect to the Rh catalyst (Table 1), in good agreement with the higher hydrogenolysis activity of Rh in comparison to Pt [22-25]. Apart from that, the lower flows of H_2 and CO formed on Pt in comparison to Rh, and the associated higher amount of H_2O, stoichiometrically correspond to a lack of contribution from steam reforming of ethane. However the Pt catalyst displayed a higher tolerance to sulphur addition than its Rh-based counterpart (Figs. 6 and 7, Table 2): the temperature at the exit of the Pt monolith showed a progressive but rather limited increase (only 40 °C for 58 ppm of SO_2); ethane conversion, as well as the yields to H_2 and CO were negatively affected by sulphur, but the corresponding drops were generally smaller in comparison to those measured on Rh catalyst for the same level of S. In a qualitative analogy with the case of Rh catalyst, sulphur addition adversely impacted on the catalytic conversion of ethane to methane also over Pt (Fig. 7c), but the decrease in CH_4 flow for increasing S levels was not as steep as for Rh and it accounted for less than a half of the surplus ethane found in the product stream with respect to S-free conditions (Table 2). Moreover the catalytic steam reforming of ethane and ethylene were partly inhibited also on Pt as suggested by the parallel increase of reactants C_2H_6, C_2H_4 and H_2O (Fig. 7b,c; Table 2). Moving from 0 to 58 ppm of SO_2 in the feed to the ethane CPO reactor, the net production of ethylene increased much more over the Rh catalyst (from $2.4*10^{-2}$ to $13.7*10^{-2}$ Sl/h) than over Pt catalyst (from $0.18*10^{-2}$ to $5.8*10^{-2}$ Sl/h) (Tables 1 and 2), thus confirming what was previously argued that (ethylene)

reforming activity is an important distinguishing characteristic in determining higher yields of C_2H_4 over Pt than Rh [5-6]. Here two further observations can be made: a) the limited reforming activity of Pt still competes with the homogeneous chemistry of formation of C_2H_4; b) the balance between the contributions of the homogeneous formation of C_2H_4 and its heterogeneous consumption can be altered by the poisoning effect of sulphur on the catalytic steam reforming and hydrogenolysis reactions. Therefore, the selective S-poisoning of the catalytic sites responsible for the undesired reactions consuming both C_2H_6 and C_2H_4 can be proposed as a strategy to increase the selectivity and the yield to ethylene during the oxygenative dehydrogenation of ethane at short contact time (i.e. with feed ratio C/O=2/1) over Pt based catalysts. Further investigation to check this approach have been discussed in Chapter 5.

4.4 Conclusions

Sulphur poisoning during the CPO of ethane to syngas under self-sustained conditions at high temperature was studied over Rh- and Pt-based honeycomb catalysts. Steady state and transient experiments with addition/removal of up to 58 ppm of SO_2 to the feed demonstrated that S-poisoning is rapid, completely reversible, directly dependant on S-concentration, and leads to a new steady state characterised by a higher surface temperature of the catalyst and a correlated drop in fuel conversion and yield to syngas. Rh catalyst, which is more active than Pt with S-free feed, mainly due to its higher activity for steam reforming and hydrogenolysis of ethane, is also more prone to the adverse impact of sulphur, which strongly and preferentially adsorbs on highly dispersed Rh crystallites. A close examination of the variation in the flows of the main products from the Rh-based monolith and a simplified heat balance of the CPO reactor indicate that sulphur selectively inhibits ethane hydrogenolysis and, to a lower extent, steam reforming of ethane and ethylene, in good agreement with the reported structure sensitivity of those reactions on supported metals. A third inhibiting effect of sulphur on the kinetics of the reverse water gas shift reaction was observed only for operation with Rh at temperatures below 750 °C, and prevented the WGS equilibrium to be reached, in contrast to what normally observed during CPO over Rh. The combined poisoning effect of hydrogenolysis and r-WGS at low sulphur concentrations during ethane CPO in air with Rh-based catalyst explains the apparently surprising increase in the H_2 yield above its equilibrium value recorded with a simultaneous drop in fuel conversion. The higher reforming reactivity of ethane in comparison to methane limits the adverse impact of sulphur on the overall production of syngas and on the associated risk of catalyst overheating during CPO.

Finally, it was shown that sulphur poisoning significantly increases the net production of ethylene particularly over Rh catalyst, but also over Pt, discovering the role of heterogeneous reactions consuming both the reactant (ethane) and the product (ethylene) of the gas phase dehydrogenation chemistry, which occurs simultaneously supported by the high temperatures in the CPO reactor. Thus selective S-poisoning of catalytic sites can be used as a strategy to alter the balance and synergy between homogeneous and heterogeneous chemistry in the CPO of highly reactive feeds.

References

1) Horn R., Williams K.A., Degenstein N.J., Bitsch-Larsen A., Dalle Nogare D.,Tupy S.A., Schmidt L.D. J. of Catal. 249 (2007) 380–393
2) Michael BC, Nare DN, Schmidt LD. Chem Eng Sci 2010; 65: 3893-3902
3) Horn R., Williams K.A., Degenstein N.J., Schmidt L.D., J. Catal.242 (2006) 92–102
4) Beretta A, Groppi G, Lualdi M, Tavazzi I, Forzatti P., Ind Eng Chem Res 48 (2009) 3825-3836
5) Michael BC, Donazzi A., Schmidt LD. J Catal, 265 (2009) 117–129
6) Donazzi A, Livio D, Maestri M, Beretta A, Groppi G, Tronconi E, Forzatti P.; Angew Chem Int Ed 2011; 50: 3943-3946
7) Bodke A, Olschki D, Schmidt LD, Ranzi E.; Science 1999; 285: 712-715.
8) Lange JP, Schoonebeek RJ, Mercera PDL, Van Breukelen FW.; Appl. Catal. A 2005; 283: 243-253
9) Beretta A, Ranzi E, Forzatti P.; Chem Eng Sci 2001; 56: 779-787.
10) Donsì F, Cimino S, Di Benedetto A, Pirone R, Russo G.; Catal. Today 2005; 105: 551-559
11) Cimino S., Donsì F., Russo G., Sanfilippo D.; Catal. Today 2010; 157: 310-314.
12) Cimino S, Donsì F, Russo G, Sanfilippo D.; Catal Lett 2008; 122: 228-237.
13) Bartholomew C.H.; Appl. Catal. A. 212 (2001) 17-60
14) Oudar J. Catal Rev Sci Eng 22 (1980) 171-195
15) Bitsch-Larsen A., Degenstein N.J., Schmidt L.D.; Appl. Catal. B. 78 (2008) 364-370
16) Cimino S. , Torbati R., Lisi L., Russo G.; Appl. Catal. A. 360 (2009) 43–49
17) Cimino S., Lisi L., Russo G., Torbati R.; Catal. Today 154 (2010) 283–292
18) Hong J., Zhang L., Thompson M., Wei W., Liu K.; Ind. Eng. Chem. Res. 2011, 50, 4373–4380
19) Livio D, Donazzi A, Beretta A, Groppi G, Forzatti P. Top. Catal. 54 (2011) 866-872
20) Fisher G. B., Rahmoeller K. M., DiMaggio C. L., Wadu-Mesthrige K., Weissman J. G., Tan E. C., Chen L., Kirwan J.E.; NAM Meeting, 2007
21) Hulteberg C. Int J Hydrog Energ 37 (2012) 3978-3992
22) Graf P, Mojet B, Van Ommen J., Lefferts L.; Appl. Catal. A 2007; 332: 310-317.
23) Rodriguez JA, Goodman DW. Surf Sci Rep 14 (1991)1-107.
24) Rice R, Keptner D. Appl Catal A 262 (2004) 233-239.
25) Zeigarnik AV, Valdes-Perez RE, Myatkovskaya ON. J Phys Chem B 104 (2000) 10578-10587.
26) Vang R, Honkala K, Dahal S, Vestergaard E, Schnadt J, Laegsgaard E. Nat. Mater. 4 (2005) 160-162
27) Rovik A, Klitgaard S, Dahl S, Christensen C, Chorkendorff I. Appl Catal A 358 (2009) 269-278.
28) Wheeler C, Jhalani A, Klein EJ, Tummala S, Schmidt LD. J Catal 223 (2004) 191-199

29) Chakrabarti R, Colby JL, Schmidt LD. Appl Catal B 107 (2011) 188-94.
30) G. Jones, J. G. Jakobsen, S. S. Shim, J. Kleis, M. P. Andersson, J. Rossmeisl, F. Abild-Pedersen, T. Bligaard, S. Helveg, B. Hinnemann, J. R. Rostrup-Nielsen, I. Chorkendor, J. Sehested, J. K. Norskov, J. Catal. 259 (2008) 147-160.
31) Walter K., Buyevskaya O.V., Wolf D., Baerns M., Catal Lett 29 (1994) 261-270.
32) J. W. Wang, A. C. Johnston-Peck and J. B. Tracy, Chem. Mater.,2009, 21, 4462–4467.

5. Ethane Catalytic Partial Oxidation to Ethylene with Sulphur and Hydrogen Addition over Rh and Pt Honeycombs

5.1 Introduction

Light olefins are the most important building blocks for the polymers industry and the world demand for ethylene and propylene is expected to increase significantly in the next decade [1-2].
Ethylene and Propylene are obtained primarily through Steam Cracking which is carried out in process equipment similar to a steam methane reformer and represents also the most energy consuming process in the chemical industry [3] despite the technological improvements occurred in more than 50 years. The catalytic oxidative conversion of light alkanes to olefins has attracted some interest as an alternative technology with potentially low capital investment, improved energy efficiency and reduced NO_x and CO_2 emissions [4-6]. It is accepted that the formation of ethylene in a catalytic partial oxidation (CPO) reactor is the result of a complicated chemistry with interacting hetero-homogeneous reaction paths. In order to have any net production of ethylene, the catalytic reforming reactions which consume both the reactant and the product, have to be slower than the homogeneous formation of the desired olefin.
Sulphur is recognized as the responsible for the inhibition of endothermic reforming reactions during the CPO of methane and ethane to syngas, as established in the last two chapters: its detrimental effect is higher on Rh than Pt, in fact, Pt has a lower activity in steam reforming reaction but is more S-tolerant. The purpose of this chapter is to explore the selective S-poisoning of catalytic steam reforming of C_2H_6 and C_2H_4 as a strategy to increase the process selectivity and yield to ethylene during the CPO of ethane to ethylene, allowing at the same time to shed light on the complex interaction of hetero-homogeneous chemistry available in a C_2H_6 CPO reactor. Accordingly, it has been investigated the effect of S addition during the CPO of ethane for ethylene production (feed ratio $C_2H_6/O_2=2$) over γ-alumina supported Rh and Pt catalysts washcoated onto honeycomb monoliths. It has been also studied the effect of sulphur addition during the CPO of ethane with H_2 co-fed as sacrificial fuel, to further probe the differences between Pt and Rh.

5.2 Experimental Procedure

Standard supported Rh and Pt catalysts (respectively 1 and 2% by weight of the alumina, in order to obtain similar atomic concentrations) were prepared via repeated incipient wetness impregnations as describe in Chapter 2.1.1. The catalytic tests were carried out on monolith samples as described

in Chapter 2.2.1, under self-sustained pseudo-adiabatic conditions and an overall pressure of P=1.2 bar, with a C_2H_6/O_2 feed ratio=2 (stoichiometric for ethylene production via oxidative dehydrogenation), with or without the addition of H_2 as a sacrificial fuel (H_2/O_2= 2). The impact of sulphur addition to the feed (up to 51 ppmv SO_2) was investigated under both transient and steady state operation of the CPO reactor at fixed preheating and nitrogen dilution (respectively, 350◦C and 25 %vol; 295°C and12.5 %vol with H_2 co-feed).

5.3 Results and Discussion

5.3.1 CPO operation at C_2H_6/O_2 = 2

Feed $C_2H_6/O_2/H_2/N_2$	T_{ad}	X C_2H_6	Y_C C_s	Y_C CO	Y_C CO_2	Y_C CH_4	Y_C C_2H_4	Y_C C_2H_2	Y_H H_2	Y_H H_2O
	°C	(%)								
2/1/0/1 @ 350°C	730	100	54.2	35.2	3.3	7.3	0.0	0.0	84.7	5.5
excluding C_s	950	99.9	----	50.0	0.0	46.8	2.1	1.0	35.7	0.0
2/1/2/1 @ 295°C	713	100.0	51.9	32.5	3.3	12.3	0.0	0.0	76.3	7.3
excluding C_s	857	100.0	----	50.0	0.0	49.9	0.1	0.0	33.4	0.0

Table 1. Predicted adiabatic equilibrium values with initial conditions as for the ethane CPO experiments: temperature, ethane conversion, C- and H- yields to the main species were calculated with or without solid carbon formation and H_2 addition as sacrificial fuel.

Adiabatic equilibrium for a feed ratio C_2H_6/O_2 = 2 predicts (Table 1) complete oxygen and ethane conversions with a yield to solid carbon C_s in excess of 50% and no formation of C_2H_4, which, together with C_2H_2, can be regarded as intermediates in the decomposition of C_2H_6 towards equilibrium. In fact if one excludes C_s formation from equilibrium calculations (Table 1), ethane conversion remains complete but it yields a large formation of CH_4 (ca. 47%) with a concomitant drop in H_2 production, and a bit of C_2H_4 (ca. 2%) and C_2H_2 (1%). A similar picture is obtained when the feed contains also H_2 (H_2/O_2=2), with the only difference that C_2H_4 is hardly seen also when excluding C_s formation from the equilibrium (Table 1). The presence of 50 ppm of SO_2/H_2S does not alter the equilibrium compositions of the mixtures.

During the initial phase of operation (30-60 min after ignition) with the Pt honeycomb catalyst, the non-closure of carbon balance between feed and products (ca. -3%) indicated the formation of solid carbon deposits. After that initial transient phase, carbon accumulation (if any) was not evident. Visual inspection of the reactor assembly, as well as temperature profiles and CO_x evolution during oxidation tests performed in an air stream just after operation in the CPO of ethane, confirmed the presence of solid carbon deposits both on the surface of the Pt catalyst as well as on the back radiation shield (Figure 1). This was not observed during ethane CPO with the Rh-based honeycomb.

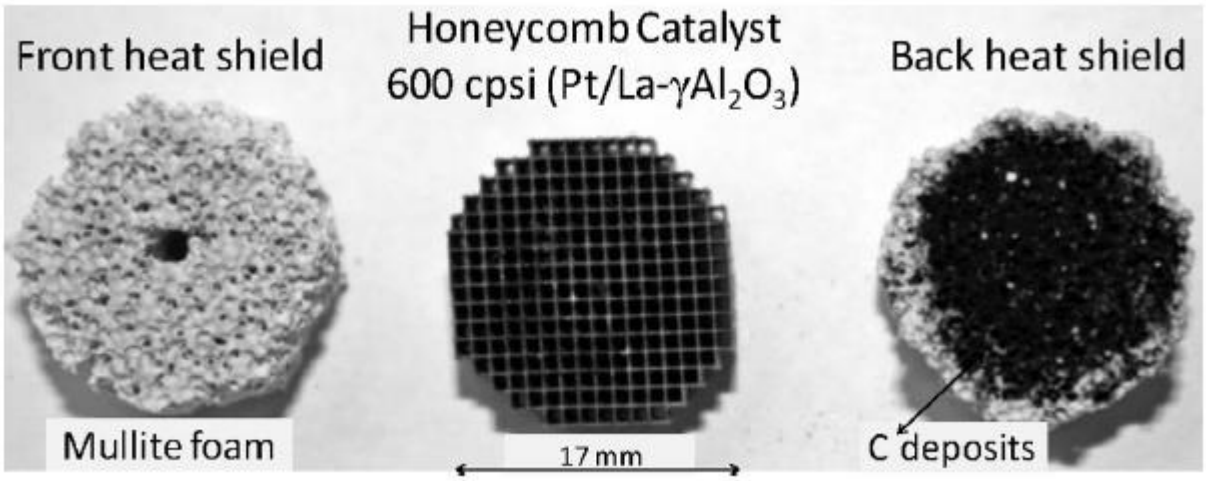

Figure 1. Pt-based honeycomb catalyst together with front and back heat radiation shields (mullite foams) after operation in the self-sustained ethane CPO at $C_2H_6/O_2=2$

Experimental results for the CPO of ethane with either Rh and Pt catalysts are presented and compared in Figure 2 and Table 2 in terms of fuel conversion and yields or flows of the main products.

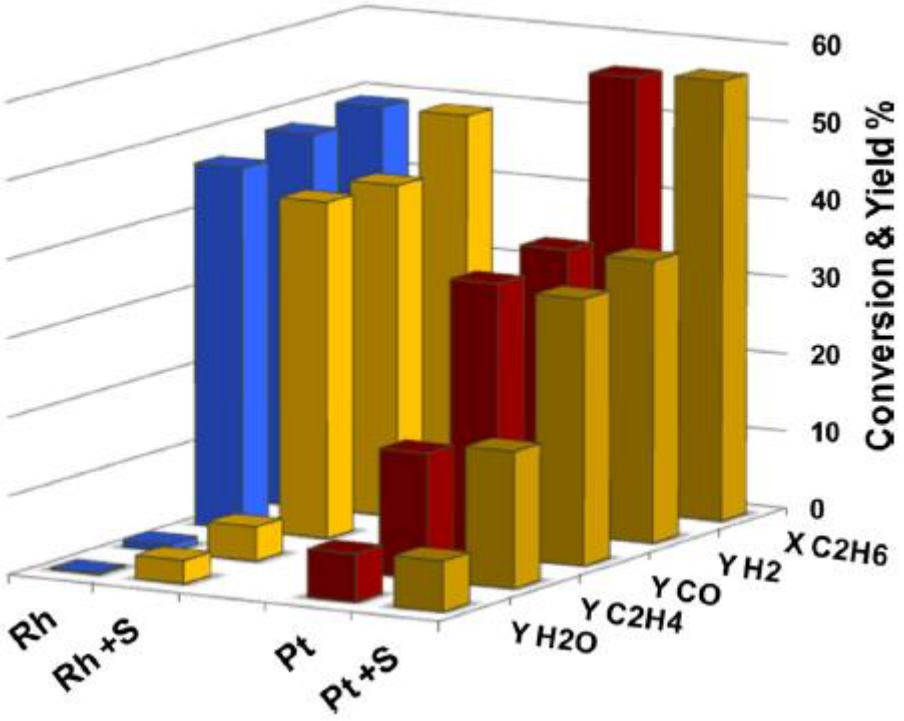

Figure 2. Integral reactor performance during the ethane CPO over Rh- and Pt-based honeycomb catalysts, under sulphur free conditions and with addition of 51 ppm SO_2 to the feed. $C_2H_6/O_2/N_2$ = 50/25/25 Sl/h, preheating 350°C.

Feed Composition	T_{cat}	X C_2H_6	CO	CO_2	CH_4	C_2H_4	C_2H_2	C_{3+}	H_2	H_2O
C_2H_6/O_2=50/25 (Sl/h)	°C	%	Sl/h							
S-free										
Pt	845	56.2	34.9	3.14	1.50	8.01	0.01	0.16	55.3	9.18
Rh	784	49.3	46.5	1.69	0.24	0.45	0.00	0.00	70.4	0.18
+ SO_2 51 ppmv										
Pt	851	56.7	34.0	3.14	1.53	8.70	0.01	0.18	54.7	9.60
Rh	821	49.2	43.1	1.28	0.41	2.17	0.00	0.00	62.0	4.32

Table 2. Product distribution from the ethane CPO reactor and catalyst temperature during steady state operation with Pt- and Rh- based honeycombs. Feed C_2H_6/O_2=50/25 Sl/h, preheating 350°C, eventual addition of 51 ppmv SO_2.

Under S-free conditions both catalysts showed a C_2H_6 conversion around 50%, while the Rh-based catalyst converted slightly less ethane than its Pt-counterpart (54% vs. 48%), and mainly formed CO and H_2 with high selectivities (94 % and 98 %, respectively), whereas the C- selectivity to ethylene was very low (below 1 %) and almost no water was found in the products. By contrast Pt

catalysts formed significant amounts of ethylene (with 29 % C-selectivity) and water, which was compensated by a lower process selectivity towards CO and H_2 (62 % and 65 %, respectively). Product distributions qualitatively agree with several previous reports in the literature, showing little ethylene formation on Rh catalysts, in contrast to Pt (and perovskite) based catalysts [6,7-9]. A closer examination reveals that relatively high selectivities to CO and H_2 were obtained with our Pt/γ-alumina honeycomb as opposed to Pt on bare monoliths [7-10]: in fact this corresponds to the effect of noble metal dispersion on a large surface area washcoat [11], which was shown to markedly lower ethylene selectivity in favour of syngas, while also reducing ethane conversion. Those observations point to a complex interaction between hetero-homogeneous reaction paths: ethylene is primarily formed by gas phase radical reactions (exemplified by eq. (5.1), (5.2)) driven by the heat of surface oxidations [7-8,12], and is eventually consumed by parallel or consecutive catalytic reactions mainly leading to syngas (eq.5.3, 5.4) [8], which are much faster than in the gas phase [13]. It follows that the reforming activity, which depends on type of metal and generally increases with metal dispersion, serves to distinguish catalysts for the C_2H_6 CPO [8].

$$C_2H_6 \leftrightarrow C_2H_4 + H_2, \qquad \Delta H_r^{298K} = +136 \text{ kJ/mol} \tag{5.1}$$

$$C_2H_6 + 0.5O_2 \rightarrow C_2H_4 + H_2O, \qquad \Delta H_r^{298K} = -136 \text{ kJ/mol} \tag{5.2}$$

$$C_2H_4 + 2H_2O \leftrightarrow 2CO + 4H_2, \qquad \Delta H_r^{298K} = +315 \text{ kJ/mol} \tag{5.3}$$

$$C_2H_6 + 2H_2O \leftrightarrow 2CO + 5H_2, \qquad \Delta H_r^{298K} = +347 \text{ kJ/mol} \tag{5.4}$$

$$CH_4 + H_2O \leftrightarrow CO + 3H_2, \qquad \Delta H_r^{298K} = +206 \text{ kJ/mol} \tag{5.5}$$

$$C_2H_6 + H_2 \leftrightarrow 2CH_4, \qquad \Delta H_r^{298K} = -65 \text{ kJ/mol} \tag{5.6}$$

Several authors have shown that Rh displays a significantly higher activity than Pt for surface oxidation reactions [8,14] as well as for steam reforming reactions [8,11,14-15]. Accordingly, Rh catalyst operated at a lower temperature level than its Pt counterpart (Table 2), at least in the second part of the CPO reactor, where the highly endothermic surface reforming chemistry prevails in the presence of Rh active sites [8,13-14], whereas exothermic oxidation reactions can still occur on Pt [8]. Indeed the almost complete lack of water observed in the effluent gas from our Rh CPO reactor (Table 2) confirms that H_2O was initially formed in the first oxidation part of the catalytic honeycomb, and then progressively consumed further downstream by reforming [8].

The lower ethane conversion measured for Rh with respect to Pt (Table 2) apparently contrasts with the higher activity of the former, as well as with the results reported in the previous chapter, during ethane CPO at lower feed ratio (C_2H_6/O_2=1) over identical catalysts. However, it can be argued that

the higher temperature level in the Pt-based honeycomb can support more effectively the homogeneous chemistry of ethane, which tends to prevail over surface reactions under oxygen deficient CPO conditions and with a less active catalyst. Indeed it was demonstrated by detailed spatial-profiles along Rh and Pt based ethane CPO reactors that ethylene formation occurred only when the (gas) temperature exceeded ca. 750°C and O_2 was still present in the gas [8].

The limited activity of Pt catalyst for the steam reforming of hydrocarbons (eq. 5.3-5.5) under CPO conditions can be the result of a self poisoning effect due to surface carbon coverage. This was recently demonstrated by Raman spectroscopy studies performed in situ on a Pt polycrystalline foil operated in the CPO of CH_4 [16] and after reaction, along a Pt/α-Al_2O_3 foam catalyst [17]: a substantial amount of carbonaceous deposits were found to block the majority of active Pt sites therefore inhibiting the reforming activity of the catalyst.

However, previous works on ethane CPO with Pt catalysts [7-8] found that the largest part of C_2H_4 was formed in the back heat shield, thus only after the catalyst, where ethylene consumption due to steam reforming is no more expected.

Additionally the Pt-based honeycomb yielded some small amounts of C3+ hydrocarbons and acetylene (Table 2), which were hardly measured (or not detected at all) for CPO on Rh. More methane was formed with Pt rather than with Rh (Tab.2), in contrast to the substantially higher catalytic activity of Rh for ethane hydrogenolysis (5.6) [15]. All those results could be interpreted in support of the hetero-homogeneous reaction scheme with homogeneous chemistry (oxy-cracking) prevailing within and after the Pt monolith. A further proof comes from the carbon deposits found on the back heat shield after the Pt monolith (Fig. 1), which were not found with the Rh honeycomb, in spite of the comparable temperatures and partial pressures of unconverted ethane.

5.3.2 Sulphur addition

Sulphur addition was studied in order to prove the contribution of some of the heterogeneous reactions to the overall performance of the ethane CPO reactor, taking advantage of the inhibiting effect of that poison, which selectively targets the noble metal and adversely affects steam reforming more than oxidation reactions [18-20], and should not impact on the gas phase chemistry.

The transient response to the addition and subsequent removal of 51 ppm of SO_2 to the feed of the CPO reactor operating at C_2H_6/O_2=2 is presented in Figure 3 in terms of temperature profiles for the catalytic honeycomb and for the exit gas.

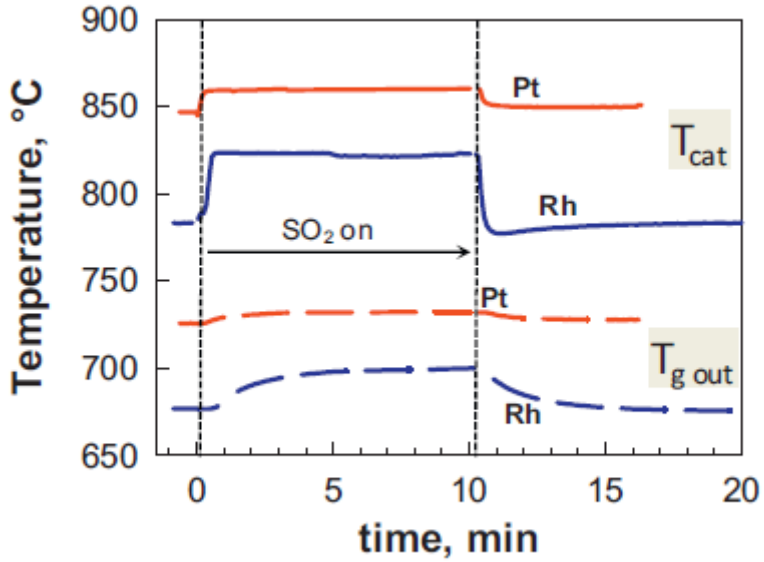

Figure 3. Transient response of the ethane CPO reactor to SO_2 addition (51ppm) and subsequent removal: temperatures measured in the centre of the Rh- and Pt- based catalytic honeycombs and in the gas leaving the reactor. Feed C_2H_6/O_2=50/25 Sl/h, preheating 350°C.

The temperature level rapidly increased over the Rh catalyst from ca. 780°C to ca. 820°C, and a new steady state was reached within 10 minutes. In analogy with results previous showed at lower feed ratio, the inhibiting effect of sulphur on Rh was reversible, as confirmed by the recovery of the original temperature levels, both inside the catalyst and in the product gas, within a similar time scale after the SO_2 flow was switched-off. A quite small and reversible effect was recorded for the Pt honeycomb, whose temperature increased by only 5 °C (Table 2). Prolonged operation of the Pt catalyst with sulphur appeared to induce a slow progressive increase in temperature which was accompanied by deposition of solid carbon, probably due to gradual loss of C_s gasification activity [16-17,21].

Figure 2 and Table 2 summarize the integral CPO reactor performance in the presence of sulphur. It can be observed that the addition of SO_2 only marginally impacted on the product distribution from the Pt catalyst. Ethane conversion was almost unchanged and ethylene yield increased slightly (+1.4%), which was accompanied by a decrease in the formation of CO and H_2, suggesting a small inhibiting effect of sulphur on the catalytic steam reforming of C_2H_4. On the other hand, ethylene formation on Rh catalysts increased by as much as 5 times due to sulphur addition to the feed, whereas ethane conversion remained unchanged.

A careful comparison of the variation in the molar flows of products induced by sulphur addition (Table 2) indicated that roughly 2 moles of CO and almost 5 moles of H_2 disappeared, and 2 more moles of H_2O were produced for every additional mole of C_2H_4 formed. The overall stoichiometry,

as well as the heat effect induced by sulphur are compatible with the inhibition of the endothermic steam reforming of ethane or ethylene. However, no direct conclusion can be drawn on whether the ethylene already formed was not consumed anymore by catalytic reforming, or some additional ethane was dehydrogenated to ethylene instead of being reformed away. A combination of the two effects can be inferred considering that: i) the temperature increase in the second half of the catalyst (above 750 °C) could speed-up the homogeneous ethane dehydrogenation, ii) the steam reforming of C_2H_6 or C_2H_4 occur at comparable rates on Rh [15] and S poisoning is expected to slow down both reactions without altering the relative reactivity.

During the self sustained CPO of ethane to produce syngas the inhibiting effect of sulphur on the activity of Rh appeared to saturate above 30-50ppm (depending on inlet conditions) [see chapter 4], even if the steam reforming activity was never completely shut down [20,22]. The observation that markedly larger amounts of ethylene and water were obtained with the Pt catalyst (respectively 4x and 2x, Table 2), even when the rate of steam reforming reactions on Rh was severely diminished by S-poisoning, confirms a faster production of C_2H_4. This is related to the lower rate of O_2 consumption by surface reactions on Pt, which leaves oxygen available in the gas phase throughout the CPO reactor (and even after it), as opposed to Rh catalyst, which consumes all of the O_2 in a short section close to its entrance [8,14]. Therefore, in the Pt-based CPO reactor the gas phase formation of ethylene can proceed via the oxidative dehydrogenation path (5.2) that is significantly faster than the ethane thermal cracking route (5.1) [8,22], the main available route with the Rh catalyst.

5.3.3 Sulphur addition with sacrificial H_2

To further probe the differences between Pt and Rh the effect of sulphur addition during the CPO of ethane with H_2 co-fed as sacrificial fuel was also studied, as H_2 was proved to significantly enhance ethylene yield [6,10,23-24]. H_2 rather than C_2H_6 is preferentially oxidized on Pt based catalysts with the molecular oxygen [10,24], so that: i) more ethane is free to react to form C_2H_4, and ii) more heat is produced for each mole of oxygen consumed [12], thus increasing the temperature and boosting the homogeneous dehydrogenation reactions from the very beginning of the catalytic monolith [8]. Figure 4 and Figure 5 report the exit flow rates of the main species form Pt and Rh catalysts and the corresponding temperatures in the catalytic honeycomb as a function of SO_2 content in the feed.

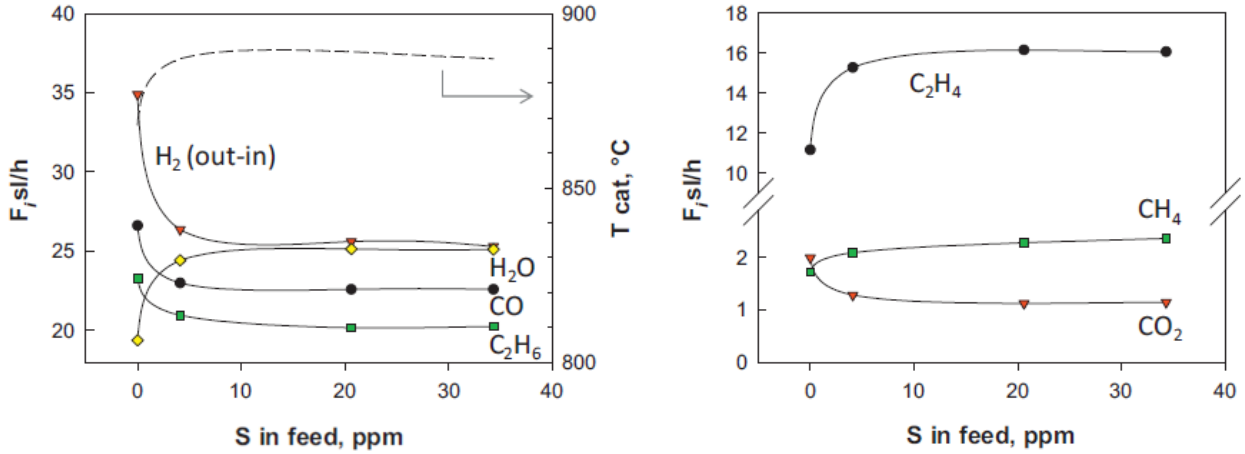

Fig. 4. Effect of SO_2addition on the flow rates of the main products and on catalyst temperature during the CPO of ethane with H_2 added as sacrificial fuel over the Pt-based honeycomb. Feed $C_2H_6/O_2/H_2$= 50/25/50 Sl/h, preheating 295°C.

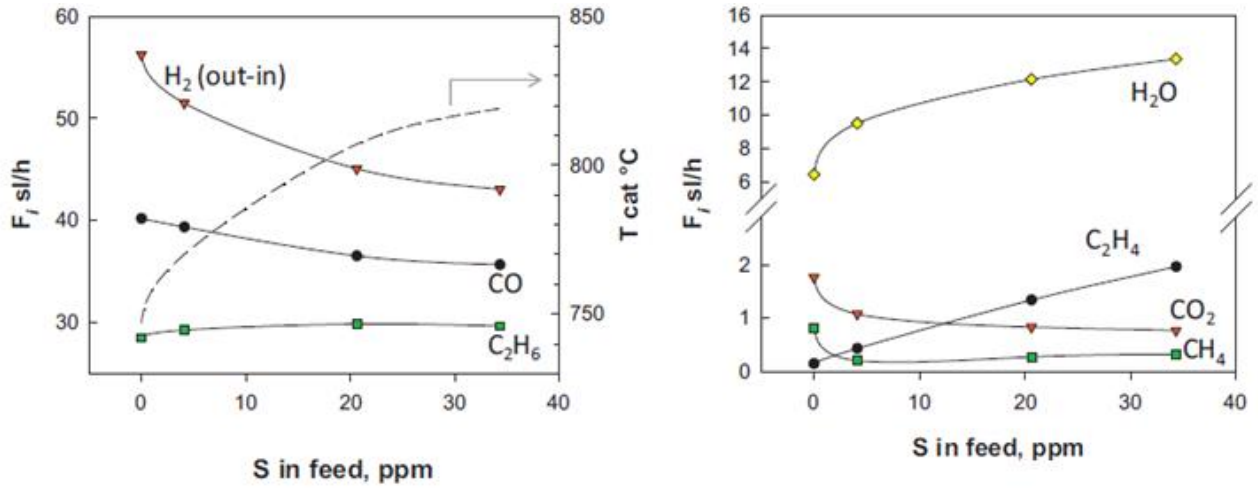

Fig. 5: Effect of SO_2addition on the flow rates of the main products and on catalyst temperature during the CPO of ethane with H_2 added as sacrificial fuel over the Rh-based honeycomb. Feed $C_2H_6/O_2/H_2$= 50/25/50 Sl/h, preheating 295°C.

The same results are conveniently reported in Table 3 in terms of variations registered when passing from 0 to 34 ppm of SO_2 in the feed to the CPO reactor.

Feed Composition (Sl/h) $C_2H_6/O_2/H_2$=50/25/50	Δ (SO_2 34ppm – 0ppm)							
	ΔT_{cat}	ΔC_2H_6	ΔCO	ΔCO_2	ΔCH_4	ΔC_2H_4	ΔH_2	ΔH_2O
	°C	Sl/h						
Pt	+19	-3.1	-4.0	-0.9	+0.6	+5.0	-9.5	+5.8
Rh	+72	+0.9	-4.4	-1.0	-0.3	+1.8	-13.4	+6.3

Table 3. Variation in the flow rate of the main products induced by S poisoning with 34 ppm of SO_2 during the ethane CPO with H_2 co-fed as sacrificial fuel over Pt- and Rh- based honeycombs. Feed $C_2H_6/O_2/H_2$=50/25/50 Sl/h, preheating 295°C.

As expected, under S-free conditions, the H_2 addition produced an increase in the ethylene yield on Pt at the expense of CO_x (Table 2 and Figure 4). This was not the case with the Rh monolith (Figure 5), whose performances were hardly modified by H_2 in the feed.

The addition of increasing quantities of sulphur induced a reduction in H_2 and CO formation over both catalysts with the simultaneous increase in water and temperature levels. The inhibiting effect on syngas formation levelled-off on Pt for relatively low S levels, whereas it was more progressive on Rh catalyst (Figures 4 and 5). At the maximum SO_2 concentration in the feed, the drop of CO production was similar for the two catalysts; the variations in the flows of H_2 were correspondingly larger by a factor 2.4 for Pt and 3 for Rh (Table 3). A temperature increase of ca. 20°C was measured on the Pt catalyst, whereas it was almost 4 times larger for Rh.

An important difference between the two catalyst regards the conversion of ethane, that increased for Pt in the presence of sulphur (from ca. 53 % to ca. 60 %), whereas it slightly decreased for Rh (from 43 % to 40.5 %).

More ethylene was formed with both catalysts in the presence of sulphur. The positive effect was larger for Pt which displayed an increase in ethylene flow by 5 Sl/h (Table 3) corresponding to as much as 10 % points of yield. It is observed from Table 3 that the surplus C_2H_4 formed on Pt largely exceeded the extra amount of ethane that was converted; on the other hand C_2H_4 and unconverted C_2H_6 increased together with S addition to the Rh catalyst.

In general it appears that S-poisoning impacted more on ethane conversion and ethylene formation when H_2 was co-fed as sacrificial fuel to the CPO reactor. This is especially true if one considers that, for equivalent S levels in the feed, the higher partial pressure of H_2 should lower the equilibrium S-coverage of the metal active sites [19]. For both catalysts a new effect of sulphur can be argued that is related to the clear shift in oxygen utilization towards H_2O rather than CO_x, suggested by the simultaneous drop of CO_2 and CO flows (Figs. 4 and 5, Tab. 3). Indeed S-

poisoning seems to favour the selective oxidation of H_2 by slowing down the catalytic oxidation of ethane: in turn this would explain the temperature rise [12] measured also for Pt in contrast to the results found on the same catalyst when operated without any sacrificial fuel. Having a higher temperature and more C_2H_6 free to react, larger quantities of ethylene can be formed via the homogeneous (oxidative) dehydrogenation.

The poisoning effect on the catalytic steam reforming was still predominant for Rh and increased progressively with sulphur concentration, as indicated by the increasing trends of C_2H_4, C_2H_6 and H_2O and temperature (Fig. 5), whereas it was still rather limited on Pt.

Finally, sulphur poisoning on Pt catalyst slightly enhanced the formation of methane as well as of other minor species such as C_2H_2 and C3+. Since pre-sulphidation was shown to significantly reduce the hydrogenolysis activity of Pt/Al_2O_3 catalysts [25], it can be argued that CH_4 formation occurred mainly in the gas phase and increased following the rise in temperature and process severity [6,26]. In contrast, almost no acetylene or C3+ were detected in the case of Rh catalyst regardless the addition of sulphur. The exit CH_4 flow on Rh, which was lower than on Pt under S free conditions, dropped further for the first addition of sulphur. According to the previous results (Chapter 4), this could to be related to a strong sulphur poisoning effect on the ethane hydrogenolysis (5.6) [25], which proceeds at a much higher rate on supported Rh rather than on Pt catalysts [14]. The slight recovery of CH_4 formation on Rh catalyst for higher S levels might derive from the gas phase chemistry and/or a stronger inhibition of its consumption by catalytic steam reforming (eq. 5) [18-20].

5.4 Conclusions

Transient and steady state ethane CPO tests were run under self-sustained high temperature conditions over Rh and Pt honeycomb catalysts in order to investigate the impact of sulphur poisoning on ethylene production by addition/removal of ppm levels of SO_2 to the feed at $C_2H_6/O_2=2$ .The addition of SO_2 only marginally impacted on the product distribution and temperature of the Pt catalyst, confirming that ethylene was mainly formed in the gas phase and possibly downstream of the catalyst. In contrast ethylene formation increased by as much as 5 times on Rh with sulphur added to the feed, which was accompanied by a significant temperature increase on the catalyst, whereas ethane conversion was unaltered. The effect of sulphur was compatible with the selective inhibition of the undesired steam reforming of ethane/ethylene, which was thus probed to significantly limit the yield to olefin for the Rh catalyst. Nevertheless, even when the rate of steam reforming reactions on Rh was severely diminished by S-poisoning, markedly larger amounts of ethylene and water were obtained with the Pt catalyst, thus confirming a faster

production of C_2H_4 in the gas phase. Regardless of sulphur addition, Pt displays a lower catalytic consumption rate of O_2 which in turn boosts ethylene formation in the CPO reactor via homogeneous oxidative dehydrogenation of ethane, that is significantly faster than its thermal cracking, the main available path with a Rh catalyst.

When H_2 was co-fed as a sacrificial fuel, sulphur addition induced stronger effects on the CPO reactor performance either for Rh and also for Pt honeycombs, showing a larger increase in ethylene formation and catalyst temperature. In this case an additional positive feature of the S-poisoning was inferred that is related to an enhancement in the selectivity of the catalytic oxidation of the sacrificial H_2 rather than ethane feed. The lower consumption of ethane/ethylene obtained by sulphur addition through the direct inhibition of their catalytic partial oxidation and steam reforming, combined with the consequent increase in the temperature level of the CPO reactor, remarkably enhanced ethylene yield with the Pt catalyst, at the expense of a somehow larger coke formation. Under those tested conditions, methane formation appeared to occur mainly via thermal cracking for the Pt honeycomb, whereas a contribution from ethane hydrogenolysis was probed for Rh, which was substantially stopped by sulphur poisoning.

References

1) Eng C., Tallman M., Hydrocarbon Processing, 87 (4), 2008, pp. 95–101
2) F. Cavani, N. Ballarini, A. Cericola, Catal. Today 127 (2007) 113–131.
3) Basini L.E., Guarinoni A., Ind. Eng. Chem. Res., 52 (2013) 17023−17037
4) Chemsystems Nexant, Production of Olefins Via Oxidative Dehydrogenation of Light Paraffins At Short Contact Times, in: PERP Report 03/04S2, 2004.
5) Bodke A, Olschki D, Schmidt LD, Ranzi E.; Science 1999; 285: 712-715.
6) Lange JP, Schoonebeek RJ, Mercera PDL, Van Breukelen FW.; Appl. Catal. A 2005; 283: 243-253
7) D.A. Henning, L.D. Schmidt, Chem. Eng. Sci. 57 (2002) 2615–2625.
8) Michael BC, Nare DN, Schmidt LD. Chem Eng Sci 2010; 65: 3893-3902.
9) F. Donsì, S. Cimino, A. Di Benedetto, R. Pirone, G. Russo, Catal. Today 105 (2005)551–559.
10) F. Donsì, S. Cimino, R. Pirone, G. Russo, Ind. Eng. Chem. Res. 44 (2005)285–295
11) A. Bodke, S. Bharadwaj, L. Schmidt, J. Catal. 179 (1998) 138–149.
12) Cimino S., Donsì F., Russo G., Sanfilippo D.; Catal. Today 2010; 157: 310-314.
13) Donazzi A, Livio D, Maestri M, Beretta A, Groppi G, Tronconi E, Forzatti P.; Angew Chem Int Ed 2011; 50: 3943-3946.
14) Horn R., Williams K.A., Degenstein N.J., Bitsch-Larsen A., Dalle Nogare D.,Tupy S.A., Schmidt L.D. J. of Catal. 249 (2007) 380–393
15) Graf P, Mojet B, Van Ommen J., Lefferts L.; Appl. Catal. A 2007; 332: 310-317.
16) O. Korup, R. Schlogl, R. Horn, Catal. Today 181 (2012) 177–183.
17) O. Korup, C. Goldsmith, G. Weinberg, M. Geske, T. Kandemir, R. Schlogl, R. Horn,J. Catal. 297 (2013) 1–16.
18) Bitsch-Larsen A., Degenstein N.J., Schmidt L.D.; Appl. Catal. B. 78 (2008) 364-370
19) Cimino S. , Torbati R., Lisi L., Russo G.; Appl. Catal. A. 360 (2009) 43–49
20) Cimino S., Lisi L., Russo G., Torbati R.; Catal. Today 154 (2010) 283–292
21) Xie C., Chen Y., Li Y., Wang X., Song C., Appl. Catal. A 390 (2010) 210–218
22) Beretta A, Ranzi E, Forzatti P.; Chem Eng Sci 2001; 56: 779-787.
23) Cimino S, Donsì F, Russo G, Sanfilippo D.; Catal Lett 2008; 122: 228-237.
24) A. Bodke, D. Henning, L. Schmidt, S. Bharadwaj, J. Maj, J. Siddall, J. Catal. 191(2000) 62–74.
25) Rice R, Keptner D. Appl Catal A 262 (2004) 233-239.
26) L. Basini, S. Cimino, A. Guarinoni, G. Russo, V. Arca, Chem. Eng. J 207–208 (2012)473–480.

Overall conclusions

The investigation of sulphur tolerance of a novel monolith catalyst based on Rhodium supported on Alumina and doped with phosphorous during the CPO of methane has demonstrated the superiority of this active phase over its undoped counterpart. Indeed, a good interaction obtained between Rh and Phosphorous has resulted in a metallic surface with higher CO chemisorption capacity than the reference catalyst and improved dispersion, leading to an enhancement of the specific steam reforming reaction rate. During CPO operations in presence of sulphur, P doped Rh catalyst was more S-tolerant, preserving an higher residual steam reforming activity than the reference catalyst, correlated to the metal sites capable to strongly bond CO.

The beneficial effect of P-doping has also been demonstrated during the dry reforming tests carried out at Technical University of Munich. Indeed, also in this reaction, the enhanced dispersion relative to phosphorous addition resulted in high activity and excellent stability of the catalyst, without any deactivation due to coke formation, on the contrary of previous results reported in literature on detrimental effect on steam reforming activity of ethane for P doped systems.

The impact of sulphur poisoning has also been studied during the CPO of ethane to syngas over Rh- and Pt-based honeycomb catalysts. Accordingly to the results obtained for CPO of CH_4, although the adverse impact of sulphur was more limited due to the higher reforming reactivity of ethane in comparison to methane, the addition of up to 58 ppm of SO_2 to the feed resulted in a rapid, completely reversible, directly dependant on S-concentration, leading to a new steady state characterised by a higher surface temperature of the catalyst and a correlated drop in fuel conversion and yield to syngas. The two catalysts examined showed a different behaviour, in fact Rh catalyst which is more active than Pt with S-free feed, was affected in a higher extent by Sulphur addition than Pt. Three effects related to sulphur poisoning on Rh catalyst were found: inhibition of hydrogenolysis, steam reforming of ethane and ethylene and WGS, even if the latter was observed only for operation with Rh at temperatures below 750 °C. Finally, it was shown that sulphur poisoning significantly increases the net production of ethylene particularly over Rh catalyst, but also over Pt, discovering the role of heterogeneous reactions consuming both the reactant (ethane) and the product (ethylene) of the gas phase dehydrogenation chemistry.

The addition of Sulphur to the ethane feed during CPO preformed at $C_2H_6/O_2=2$ to obtain ethylene over Rh and Pt honeycombs, confirmed that ethylene was mainly formed in the gas phase, as the

impact of sulphur on the olefin production over Pt catalyst was only marginal. On the other hand, the ethylene production increased by as much as 5 times on Rh with sulphur added to the feed, and this effect was explained through the selective inhibition of the undesired steam reforming of ethane/ethylene. The effects of sulphur on the CPO performance over both the catalysts were larger in the presence of H_2 as a sacrificial fuel. Firstly, the selectivity of the catalytic oxidation of the sacrificial H_2 rather than ethane feed was enhanced. Moreover, the sulphur poisoning of steam reforming pathways of both the reactant and desired product, coupled to the increase in the temperature level of the CPO reactor, remarkably enhanced ethylene yield with the Pt catalyst, at the expense of a somehow larger coke formation.